Dec 1973

11

FOSTER-MILLER ASSOCIATES INC.
ENGINEERS
135 SECOND AVE.
WALTHAM, MA 02154
617 890-3200

DESIGN AND DEVELOPMENT OF A CONICAL BORING DEVICE TO ENLARGE A PILOT HOLE THROUGH ROCK

Final Technical Report
Covering the period
1 May 1972 through 1 June 1973

Sponsored by
Advanced Research Projects Agency
ARPA Order No. 1579, Amend. 3
Program Code No. 2F10

This research was supported by the Advanced Research Projects Agency of the Department of Defense and was monitored by Bureau of Mines under Contract No. H0220076

Contractor: Foster-Miller Associates, Inc.
135 Second Avenue
Waltham, Massachusetts 02154

Project Engineer: Paul Wurlitzer (617) 890-3200
Program Manager: Hans A. Hug (617) 890-3200

Effective Date of Contract: 13 June 1972
Contract Expiration Date: 13 July 1973
Amount of Contract: $148,620.00

TABLE OF CONTENTS

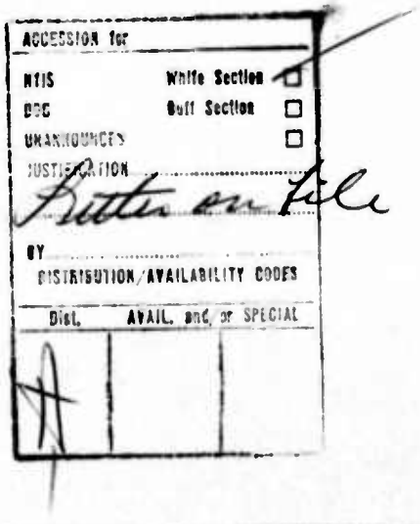

LIST OF FIGURES

1. Summary

This report summarizes Foster-Miller Associates effort completed during the second year of a multi-year program to design and develop a conical, self-advancing and self-rotating boring machine. The conical borer will use a proven and energy effective mechanical fragmentation system -- roller cutters -- and will operate as a reaming device to enlarge an existing 8 3/4 inch pilot hole to a final 39 inch bore.

This effort has been a continuation of development work begun under Contract H021044 during which a prototype single stage conical borer was fabricated and "proof" tested.[1]*

The current program has been divided into four phases:

Phase I - Test and Cutter Refinement;
Phase II - Final Design of the Conical Borer;
Phase III - Mucking Studies; and
Phase IV - Investigation of Surface Hardware Requirements.

During Phase I, detailed testing and refinement of the cutting structure of the prototype borer was completed. As a result of this research, a marked reduction in the values of the thrust loads which were obtained during the first year proof tests was achieved. Thrust loads of approximately 10 percent of that required for a conventional tri-cone bit were observed. The specific energy required (inch-pounds per cubic inch of rock removed) was only 13 percent higher than that of a comparable tri-cone bit. This is considered very good in view of the extensive development history of tri-cone cutters.

*Numbers in parentheses refer to the list of references at the end of this report.

The detailed design of the borer (Phase II) has been completed, using the results of the Phase I and Phase III testing. Design layouts have been prepared and are presented in this report. A complete set of fabrication drawings has been prepared.

During Phase III air flow passages through and around the borer were designed. Analyses of the pressure-vacuum system were made to develop design parameters for the pressurized air supply and the vacuum discharge system. The transport of the cuttings is critical in several areas, particularly in the vicinity of the conical cutters and at the joints between the stages of the overall borer. Solutions to overcome these potential transport problems were generated and tested experimentally to determine the most efficient system.

A mucking test unit, consisting of a half-scale, two stage model of the borer encased in a plexiglass shell were designed and fabricated. The model was rotatable to ensure close simulation of the flow of air and cuttings around the actual conical borer. Simulated cuttings of sand, fish gravel, and cuttings obtained during Phase I were introduced into the test model and their flow characteristics were photographically recorded. The design analyses were verified during these tests.

Investigation and determination of the required ground support equipment (Phase IV) was completed during the last part of the year. This is the auxiliary equipment that will be required for full scale field testing of the borer.

The major conclusions and results of this program are as follows:

1. The experimental program confirmed again the main advantage claimed for the conical borer; i.e., that it will require significantly reduced thrust loads (less than 10 percent) than conventional roller cutter bits of the same diameter and at the same penetration rate.

2. The cutter refinement conducted under this effort successfully reduced the required borer thrust loads below those obtained in previous testing.

3. The specific energy required for rock fragmentation was reduced to a level only 13 percent greater than for highly developed tri-cone cutters.

4. A practical mucking system was designed and successfully tested. In addition, parametric design relations for predicting the performance of any borer were developed and experimentally verified (Appendix B).

5. Design of the borer was completed. A complete drawing package for fabrication was prepared. The structural integrity and bearing life was analyzed and found to be satisfactory (Appendices C and D).

6. The ground equipment required for field testing was delineated and investigated. The most expensive item required will be the hydraulic lines, their carrier reels, and the diesel driven hydraulic power supply.

2. Introduction and Background

The U. S. Government, acting through the Advanced Research Project Agency, ARPA, and its agent, the Bureau of Mines, Department of the Interior, is seeking improvements in all elements of underground rock excavation through its Program for Rock Mechanics and Rapid Excavation. Rock disintegration has been singled out as a key element of this program.

A great many novel rock disintegration processes have been or are being proposed and studied, and it can be expected that this research will produce one or more processes that will ultimately be simpler, more reliable, more flexible, and more economical than the presently available tried and proven mechanical fragmentation methods. It can be expected that some of these more "exotic" methods will move from the laboratory to the field by 1980. In the meantime, every effort should be made to improve on the existing state-of-the-art boring and drilling methods so that the expected benefits can be practically realized in the field in the next two to three years. To accomplish this, Foster-Miller Associates formulated a comprehensive program for the development of a new boring machine utilizing a proven principle of mechanical fragmentation involving roller cutters. The unique feature of this machine is that it utilizes the cutter action to generate all the thrust and reaction forces required for fragmentation. The need to supply these forces currently limits the performance and reliability of hard rock tunneling and boring machines. In addition, this new device, termed a conical borer, promises significant additional advantages. Much greater bearing capacity is available, and, by "locking" the cutter elements into the rock, the impact loads that currently limit the penetration rate and life of conventional roller cone bits are eliminated. Furthermore, its particular shape promises to considerably improve the removal of cuttings from the working face, a major problem in the construction of large diameter shafts and tunnels.

During the first year of this program a prototype single stage of the proposed three stage experimental unit was designed, fabricated and run in granite test samples, successfully demonstrating the basic concept. This work is described in detail in Reference 2. In the following report the work of the second year which culminated in the complete design is presented.

The specific objectives of the program are to prove out the basic concept for a simple single stage unit and then to design, fabricate and test a versatile multistage powered experimental unit which could be used to investigate full scale performance. A pictorial description of the proposed multistage unit is presented in Figure 1. It is designed to ream an 8 3/4 inch hole to 39 inches in hard rock at rates of 10 feet per hour. All necessary forces are generated by the borer's weight, hydraulic motors, and the roller cutters.

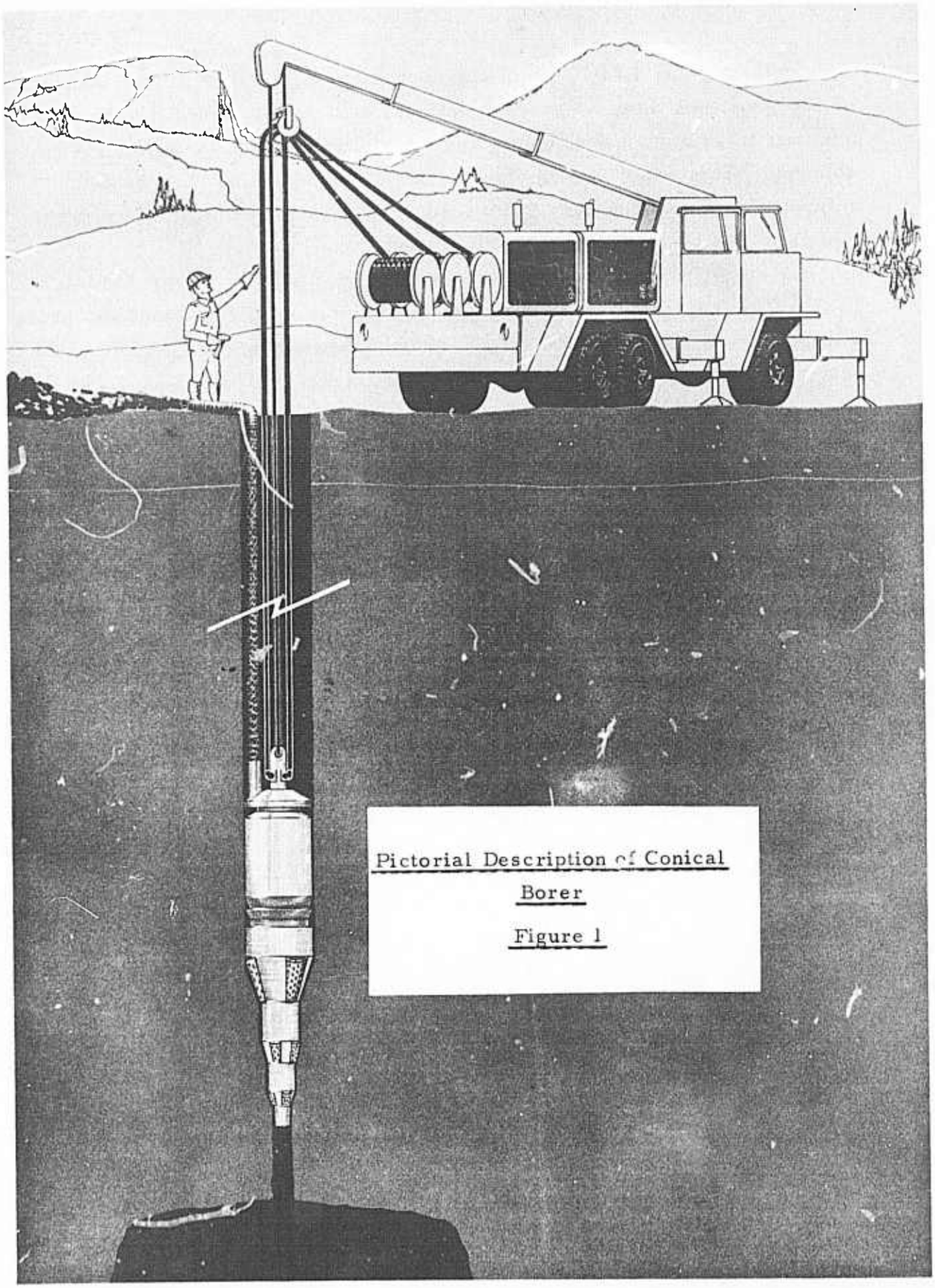

Pictorial Description of Conical Borer

Figure 1

3. Objectives and Plan of Research

Effort under this contract has been devoted to the detailed design and development of the conical boring device. This is a continuation of research conducted during Contract H021044, where a preliminary design of the device was completed (Figure 2). The conical borer will operate as a reaming device to enlarge an 8 3/4 inch pilot hole to a 39 inch bore at penetration rates equal to or greater than those obtainable with existing boring devices, but with substantially lower thrust load requirements. A pneumatic mucking system will be used to clean the cutting area and transport cuttings to the surface.

The research has been divided into four phases as specified in Section 1.1 of the subject contract. These phases are as follow:

Phase I: Testing of the nose section of the conical borer developed under Contract H021044 to optimize its cutting performance and establish basic torque and thrust load requirements.

Phase II: Final design of the conical borer.

Phase III: Performance of mucking studies required in the pneumatic flushing and transport system, including design, analysis and model testing.

Phase IV: Investigation of surface equipment requirements.

Progress under each of these phases of effort is discussed in the following sections. The experimental data generation phases (I and III) are discussed first, followed by a presentation of the final design and the surface equipment requirements.

4. Cutter Development and Testing - Phase I

During the Phase I effort, as described in Section 1.2.1 of the subject contract, a prototype nose section of the conical borer developed under Contract H021044 was revised and tested to optimize its cutting performance and to establish its performance characteristics. The tasks of this effort were as follow:

(a) Further study of the previous test data (Contract H021044) and closer examination of the prototype nose section.

(b) Rebuilding of the cutters including redistribution of teeth and changing of the tooth density.

(c) Testing, modification, and retesting of the prototype nose section.

(d) Data reduction, analysis and establishment of performance characteristics.

A detailed discussion of the research conducted during Phase I is given in our Phase I Test Report dated 23 August 1972.[2] A summary of that research with important data and results is presented in the following sections.

4.1 Description of the Prototype Borer Nose Section

Figure 3 is a photograph of the assembled nose test section. It is designed to ream an 8 3/4 inch hole to 14 inches. The hole-bottom half-angle is 18^c and the cutter skew angle is 4^c.

The nose frame is a weldment of five pieces: the lower cylinder or bearing housing; the three struts; and the upper cylinder or bearing housing. The upper portion of the upper cylinder shown in the

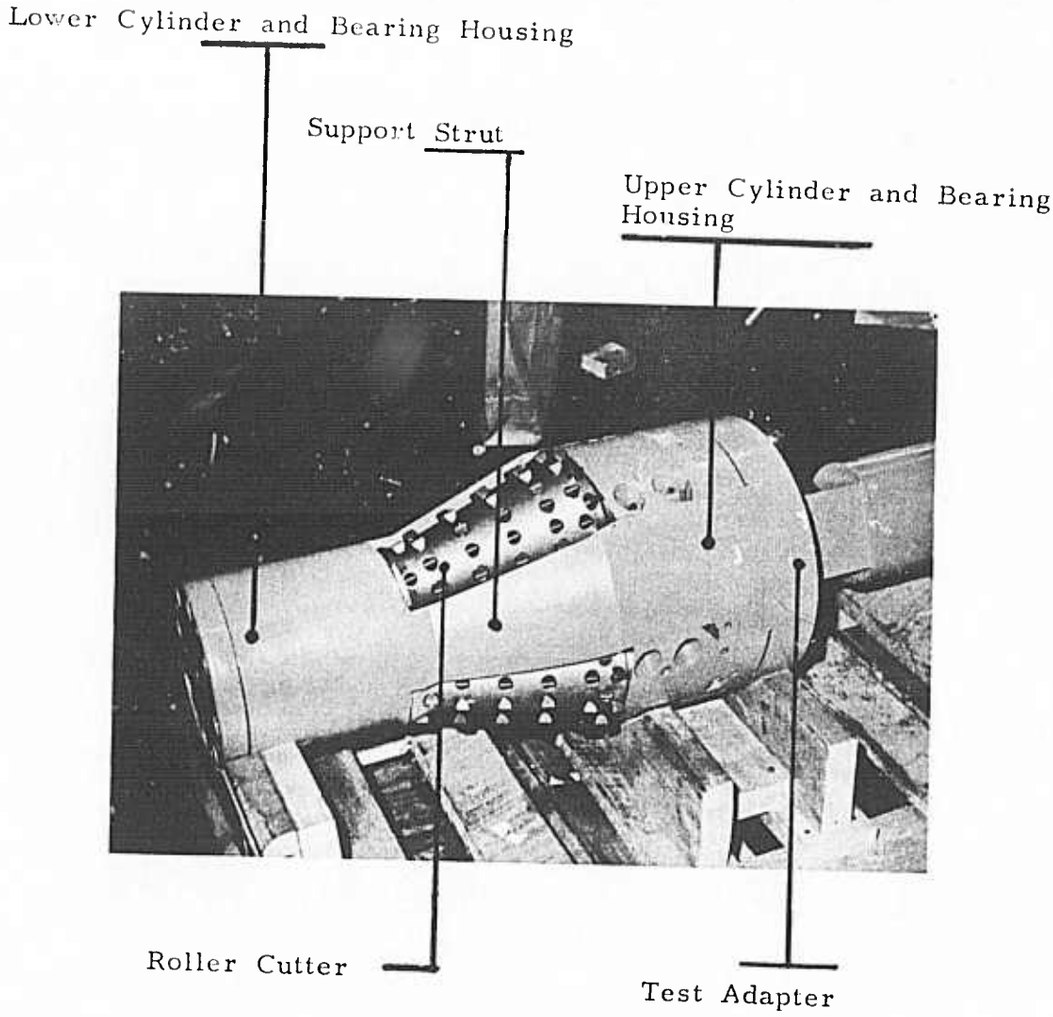

Photograph of Nose Section

Figure 3

photograph is an adapter (not a separate piece in the mock-up) connected to the test facility for testing of the nose section. This adapter is bolted to the nose frame through a face spline. The same bolting arrangement and face spline connects the nose section to the complete borer main frame.

In an attempt to provide maximum bearing capacity in the cramped lower cylinder, a non-standard bearing assembly method was designed so that the cones served as the inner race of the bearing. Lower end bearings, both radial and thrust, contained in three separate cartridges, with the cartridges serving as outer races for the three radial bearings. These bearing cartridge assemblies are inserted axially into the frame from the lower end, thus avoiding split bearing caps in the lower cylinder.

The upper bearings are also contained in fully enclosed (i.e., not split) blocks which fit within essentially rectangular seats in the upper cylinder. The four retaining bolts which can be seen in Fig. (3) are for retention only; they carry no loads imposed by boring.

Assembly of cutters is a three-step procedure:

(a) Each upper bearing assembly and block is slipped over the stub shaft extending from the upper cutter end;

(b) With lower bearing cartridges not in place, each cutter and upper bearing combination is inserted in the frame, with the lower cutter stub shaft fitting easily within the large lower bearing cartridge bore; and

(c) Each lower bearing cartridge is then pushed over the lower stub shaft within its bore in the lower cylinder.

The three lower bearing cartridges are retained axially by a single cover bolted within the end of the lower cylinder.

The three struts connecting upper and lower cylindrical frame sections are roughly triangular in cross section to fully utilize the space available between cutters. A one-inch hole extends through each strut to carry flushing fluid to the lower end of the borer. This fluid will issue upwardly from the sides of the lower cylinder.

The frame also contains a lubricant reservoir connected to all of the bearings to provide long-term lubricant capacity. This reservoir is provided with an external fitting for convenient replenishment, and it is pressurized by the flushing fluid (acting through a rolling diaphram) to provide positive lubricant pressure. Long-term lubricant capacity was of course not necessary for the nose section tests, but it will be necessary in anticipated testing of the complete borer.

Figure 4 shows the three cutters with their carbide cutter teeth. The teeth are General Electric Tungsten Carbide Grade No. 268. They are nominally 0.6275 inches in diameter with a 70° chisel point.

4.2 Test Facilities, Equipment and Procedures

All testing was done at the laboratory facilities of the Hughes Tool Company in Houston, Texas. The rock drilled was pink granite with approximately 30,000 psi compressive strength. It was delivered to and used in the test facility in approximately four foot cubes.

An 8 3/4 inch pilot hole was drilled in the granite with a conventional Hughes W7R rock bit. After the pilot hole was drilled it was reamed with the conical borer to an approximate diameter of 14 1/8". All tests were run at 40 rpm and water was used to flush

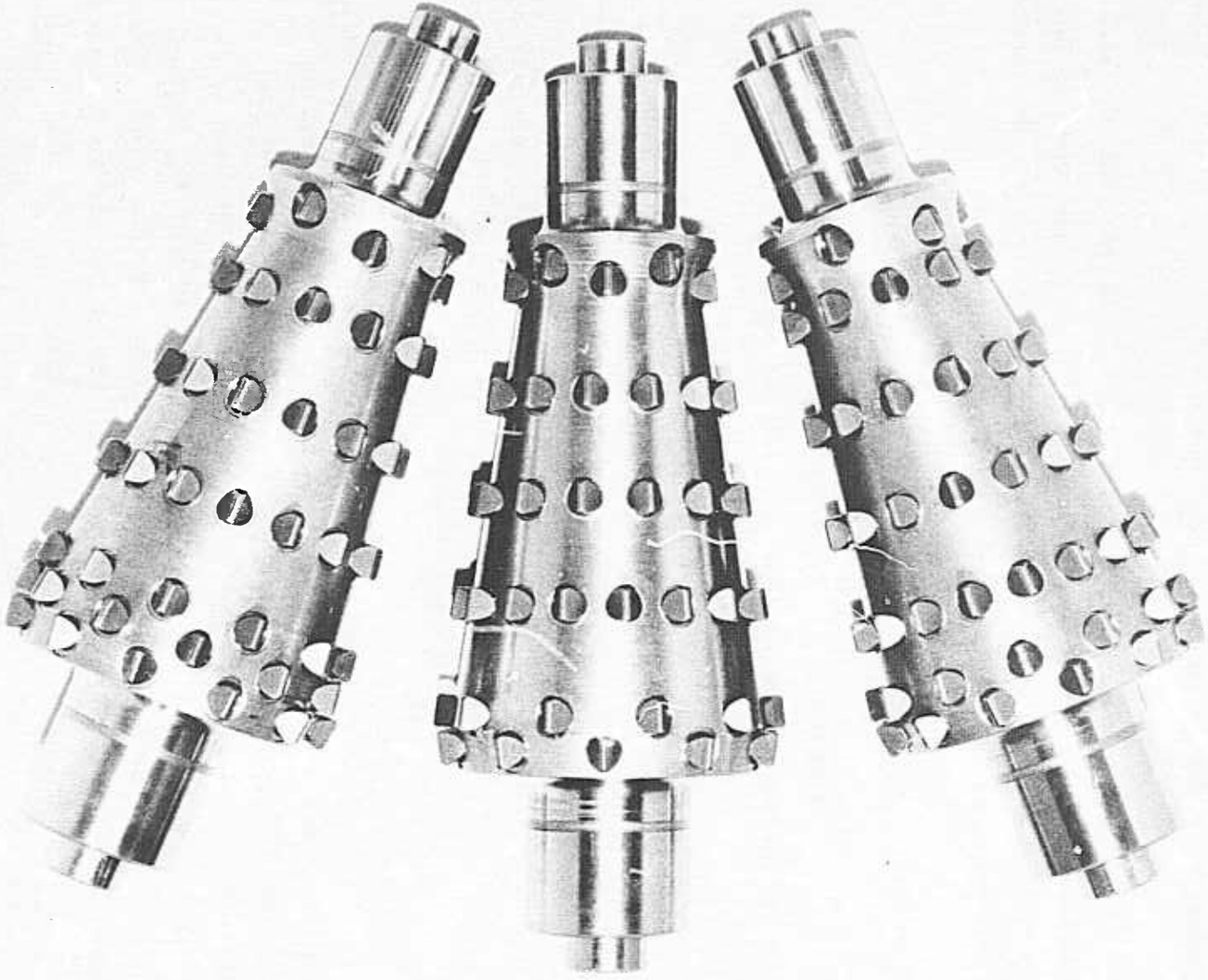

Completed Roller Cutters

Figure 4

the cuttings out of the hole. The load was varied from 2,000 pounds to approximately 14,000 pounds and the penetration rate and torque were measured.

Figure 5 is a photograph of the conical borer, the test equipment, and the granite specimen.

For comparison, a 13 3/4 inch W7R rock bit was used to ream the same size hole in the same rock. The drill rates of this bit were held constant at 3, 6, 9 and 12 feet per hour while the torque and load required to maintain these rates were measured.

4.3 Review of Previous Data

Further study of the first year data and closer examination of the prototype nose section revealed two areas of concern:

(a) at the higher drilling rates the rate did not remain constant over any significant depth interval; and

(b) the cutter cone-bodies were rolling and scraping on the rock due to a "rock-gear" formation on the hole-bottom, shown in Figure 6.

A detailed review of the drilling data indicated that at a constant load the rate usually continued to decrease with increasing penetration. This implied that most of the excess load (above the original design value) may have been attributable to cutter-body contact on a developing rock-gear hole-bottom. Discussions with the observers of the tests at Hughes Tool Company indicated that the rock-gearing was observed at several intervals during the drilling of the one rock sample.

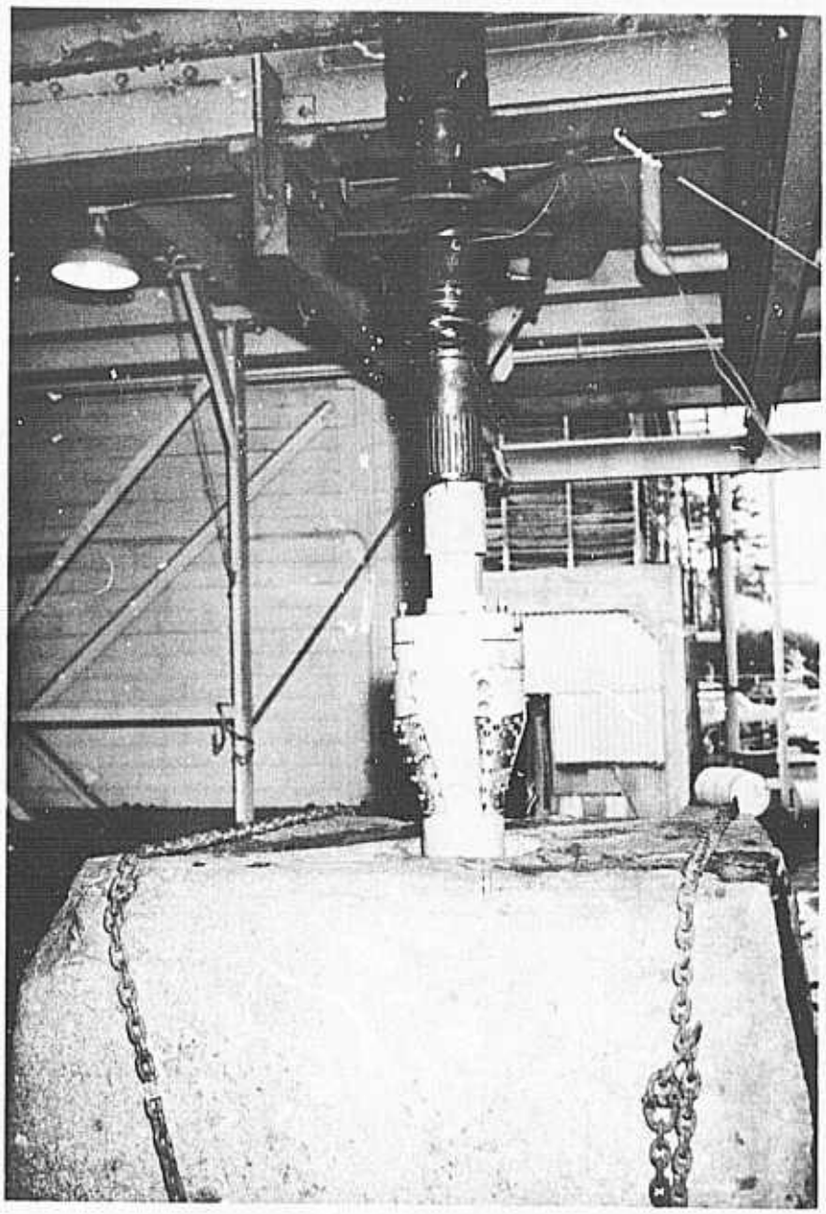

The Conical Borer and Test Equipment

Figure 5

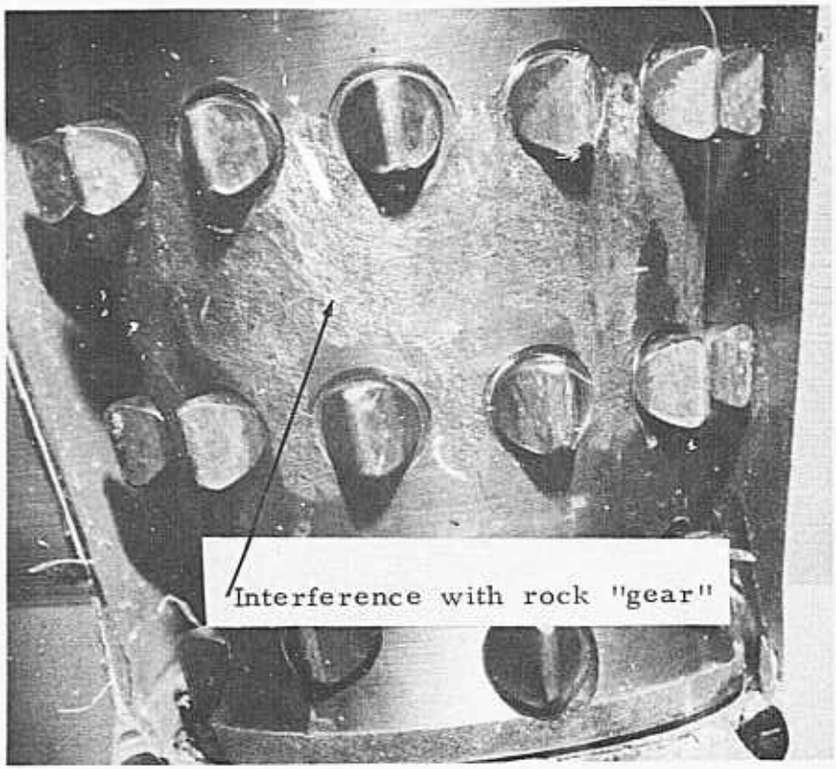

Prototype Cutter Cone After Tests

(a)

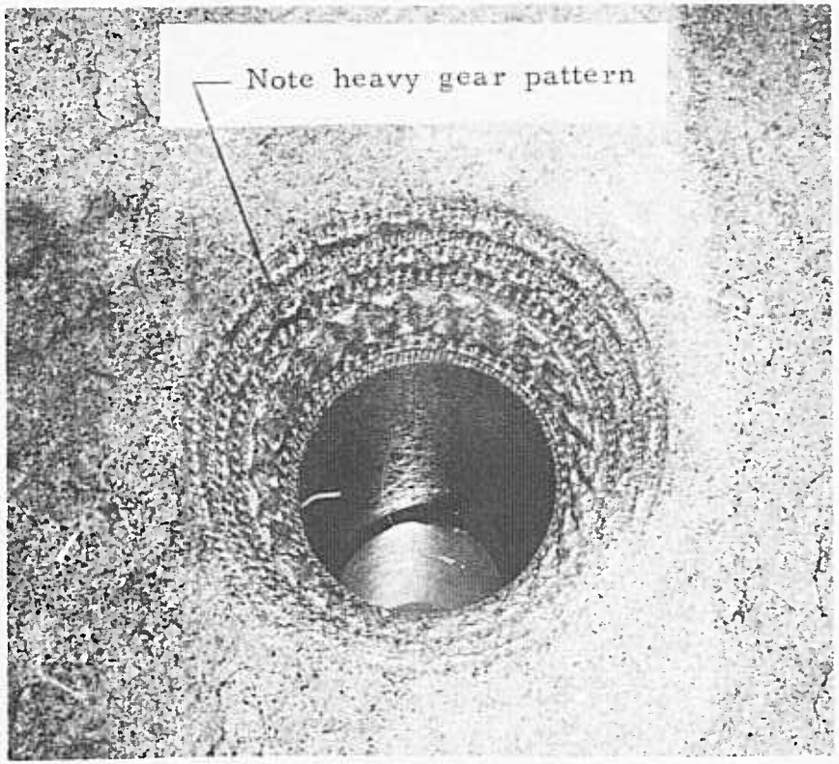

Hole Bottom Configuration

(b)

Photographs of Cutter Cone and Hole Bottom to Show the Effect of "Gearing" During the Tests of 14 March 1972

Figure 6

The appearance of the cutter cone-bodies and pictures of the hole-bottom showed that rock-gearing was only occurring within the span of 3 or 4 tooth rows that had nearly equal tooth spacing and which comprised the lower third of the conical cutters. This probably caused the cutter teeth to fall "into step" at an integral number of revolutions per borer rotation. This phenomenon is unique with the conical borer in that one row of teeth on one cutter can advance into the pattern of a lower row on another cutter.

4.4 Modifications to the Borer

From the review of previous data it was concluded that further optimization of the borer performance would first require elimination of the rock-gearing. Then the number of teeth could be reduced as originally planned in pursuit of the desired relationship between load and drilling rate. It seemed inadvisable to remove any teeth before a good rock bottom-hole pattern was observed in test.

The design approach used for modifying the cutters to avoid rock-gearing was as follows:

(a) Each tooth row was drawn to show the nearest integral number pattern in one bit revolution; i.e., the likeliest rock-gear pattern for that tooth row;

(b) A few teeth added above each particular tooth row, arranged to fall so that during the passage of a few bit revolutions they would "knock-out" any rock-gear;

(c) Where possible, the spacing of teeth added on one cutter was made to be out of step with teeth on the other cutters near the same axial position;

(d) The axial circumferential, and cutter-to-cutter distribution of teeth was balanced closely to minimize vibrational loads on the bit.

The total number of teeth on the bit was increased by only 14 percent to accomplish the plan just described.

The cutters were modified by inserting tungsten carbide teeth in the same manner as for the original construction. In order to optimize the use of our time at the Hughes test facility in Houston, dummy blocks with carbide inserts were constructed to test the planned deletion of teeth. An electric carbon arc, air-jet, reverse polarity, 250 amp. welder was quite effective for melting the teeth without excessive heating. This procedure was used to delete the teeth during the tests at Houston.

The deletion of specific teeth was planned prior to testing. Teeth were to be selectively deleted from clusters or dense regions, but not from the gage rows or from the group of teeth that were correctively added.

4.5 Results from the Second Test Sequence

Three rock samples were drilled as described in Section 4.2. Of these, two were drilled with the cutters which had the added teeth to eliminate rock-gearing while the last sample was drilled with cutters from which approximately 8 percent of the teeth were discriminantly deleted.

Data was monitored automatically on a Visicorder for load, torque, speed, and time. Load and torque were measured in a strain-gage "sub" immediately above the bit. Net zeros were established before and after drilling, and penetration marks were manually noted on the chart record. The signals were filtered out above 10 Hz. A sample of the record is given in Figure 7.

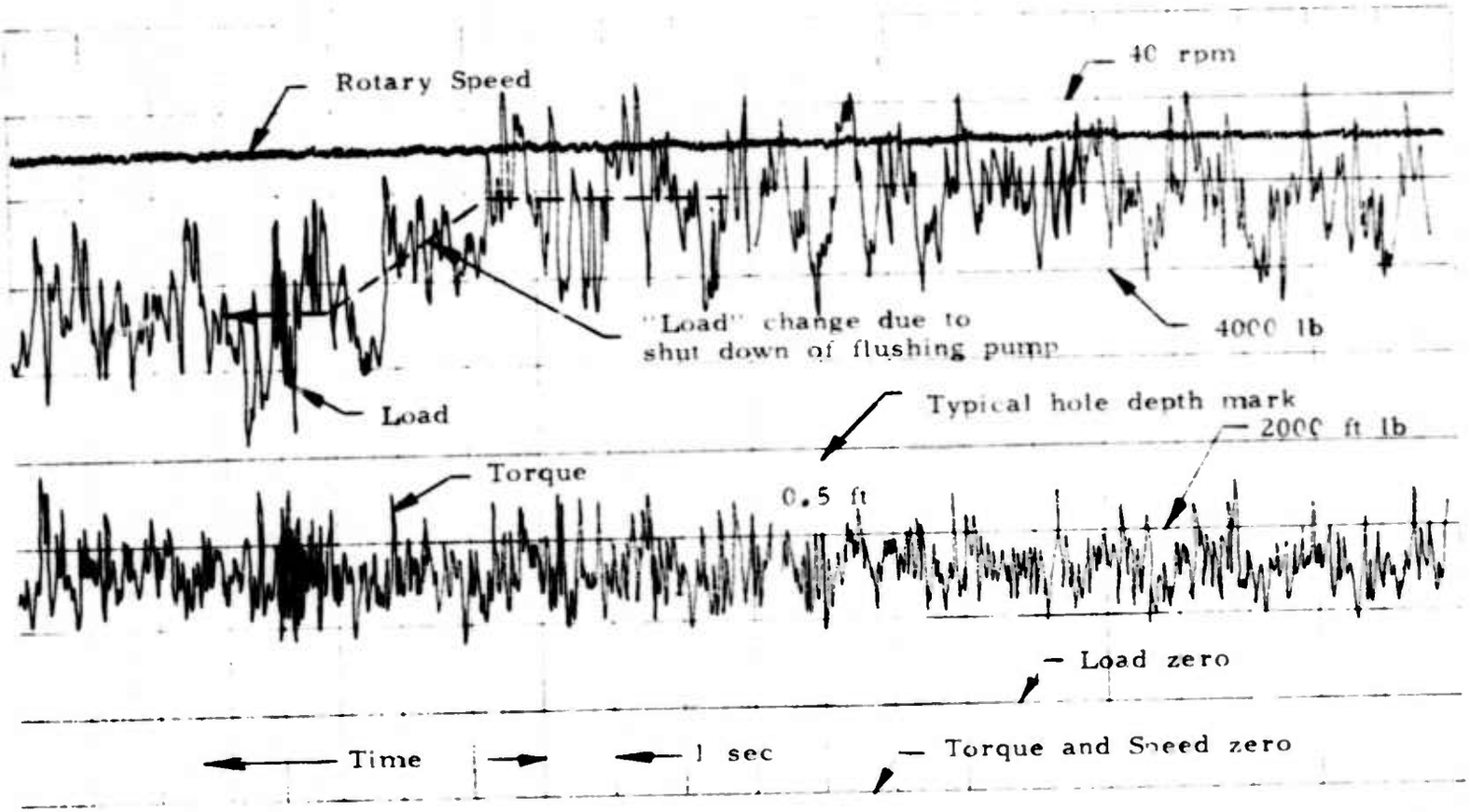

Sample of Visicorder Record of Drilling Data

Figure 7

From the test records, average levels of drilling parameters were estimated for those drilling intervals in which performance was constant for more than about 0.3 ft. Only these data values were used in establishing the average bit performance shown in Figures 8, 9 and 10. Figure 8 shows the penetration rate at 40 rpm achieved as a function of total thrust on the rock surface by the bit cutting structure (i.e., thrust equal to drill stem and bit weight plus all external forces). Figure 9 shows the bit torques required to achieve the drilling rates.

Both Figures 8 and 9 show that the performance of the bit with deleted teeth was about the same as that of the borer with the teeth added to eliminate rock-gearing. In both cases the thrust load required at a given penetration rate was about 1/10th that of a comparable tri-cone bit, while the required torque was about 20 percent greater.

More precisely determined from rock volume rate and input power, the specific energies of rock removal are compared in Figure 10. The conical borer consumed only 13 percent more power than the flat bottomed tri-cone bit at the usual drilling rate, and both bits appeared to behave the same parametrically.

Several subjective observations made during testing are worth mentioning since there seemed to be agreement between personnel from Hughes Tool Co., the Bureau of Mines, and Foster-Miller Associates.

The conical bit seemed to be "quiet" running, better than comparable flat-bottom bits. It behaved well during a difficult run-in when the pilot hole entry was broken away asymmetrically. Reference to Figure 7 shows that although the relative variation of load and torque are large, their absolute variation is not. Records show the absolute variation to be comparable to or less than that of the pilot bit.

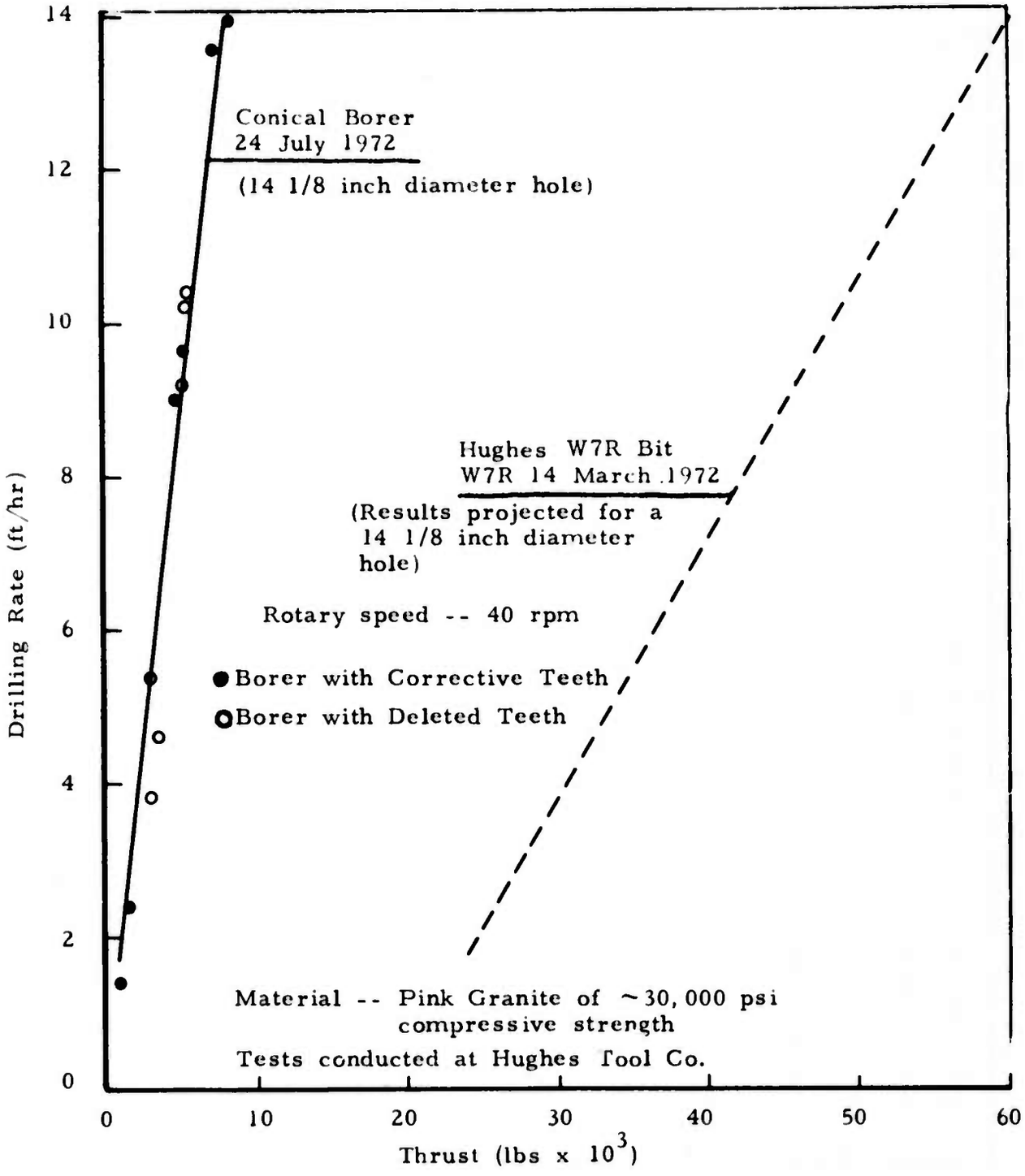

Figure 8

Thrust vs. Drilling Rate for the Nose Section Prototype Conical Borer

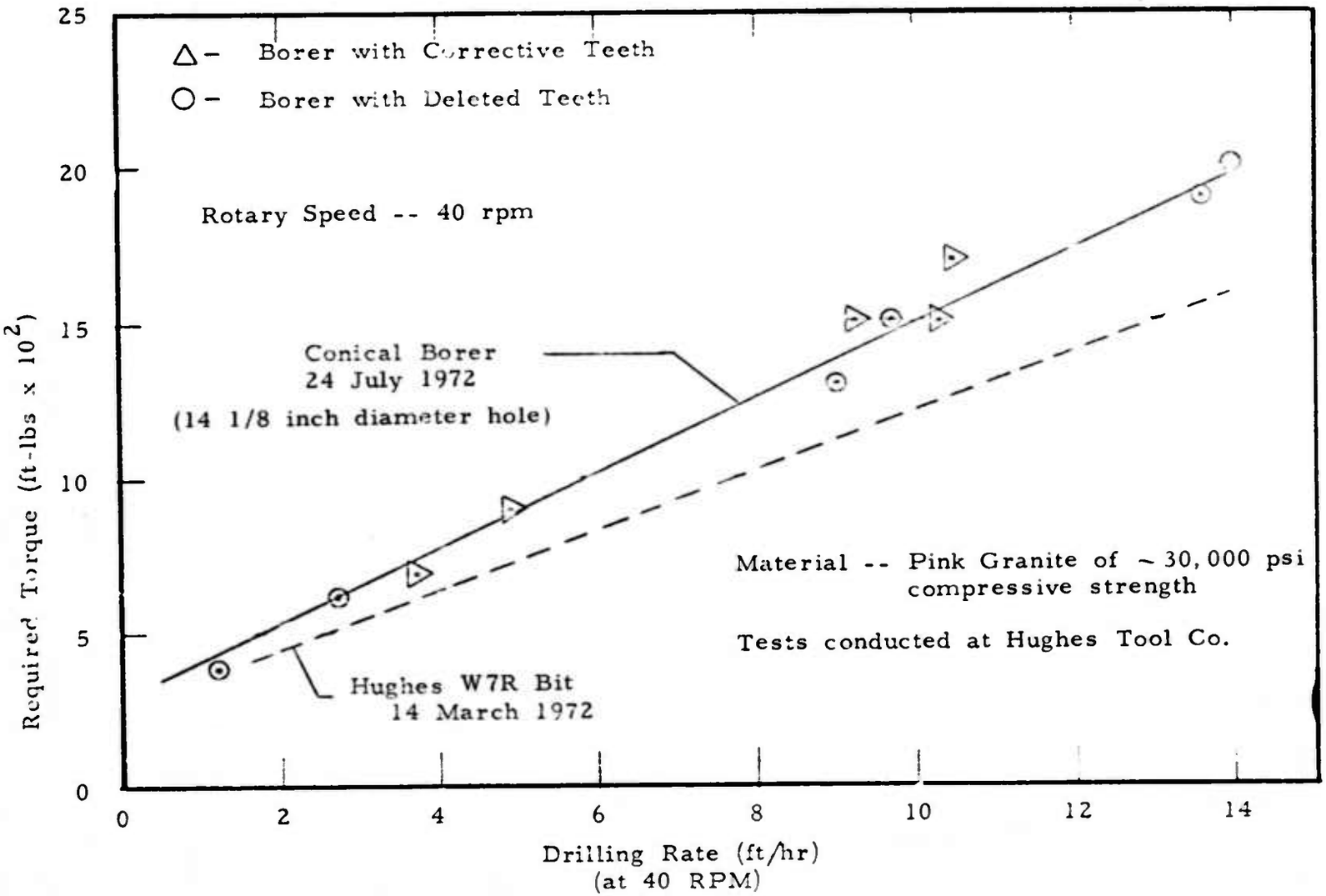

Torque vs. Drilling Rate for the Nose Section Prototype Conical Borer

Figure 9

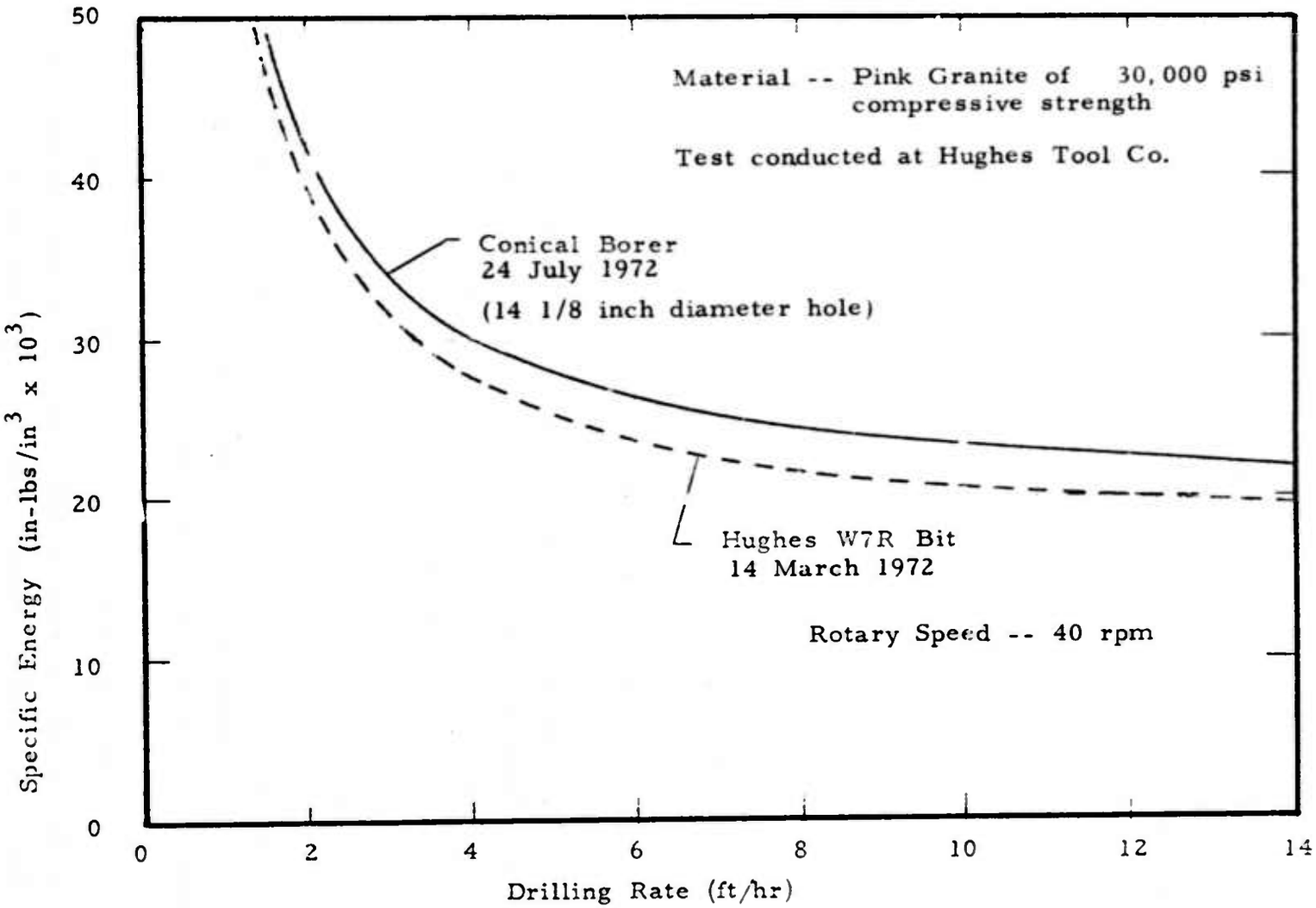

Specific Energy vs. Drilling Rate for the Nose Section Conical Borer Prototype

Figure 10

The bottom-hole pattern (actually side-hole pattern) showed the surface to be randomly lumpy (generally considered to indicate efficient rock cutting). Figure 11 shows typical bottom hole patterns made by the conical borer. The bored hole shows some gage rifling and a slight rock-gear pattern at the top of the hole where the entry of the pilot hole was broken away asymmetrically. This was an extreme case; all other observations showed no gearing or rifling.

The chips made by the conical borer were similar to those made by usual bits. There was some milled dust, a predominance of coarse rock grains, and a noticeable fraction of penny size and larger chips. Figure 12 compares sample cuttings from conical borer and pilot holes. During hand sifting of the dried cuttings, those from the borer feel coarser, with less mill dust present. The cuttings made with the conical borer after teeth were deleted were not apparently different from those made before.

4.6 Conclusions on Phase I Efforts

The conical borer operated quite successfully, proving once again the thrust-reducing capabilities of the concept. With the cutter refinements it was possible to reduce the load to less than 1/10 that required by a conventional bit operating at the same conditions.

During the tests there was no damage to the borer external structure. No tooth breakage or wear occurred, and no further scraping of the cones was apparent. As predicted, the addition of a few teeth, judiciously placed, corrected the problem of rock-gearing observed in the original proof test.

Disassembly of the borer revealed three cracked needle bearings and minor race damage on one cone. It is believed that this can be attributed to a misalignment of the bearing surfaces during machining. As a result of this data, a self-aligning bearing structure was provided in the three-stage unit design (see Sec. 6.1).

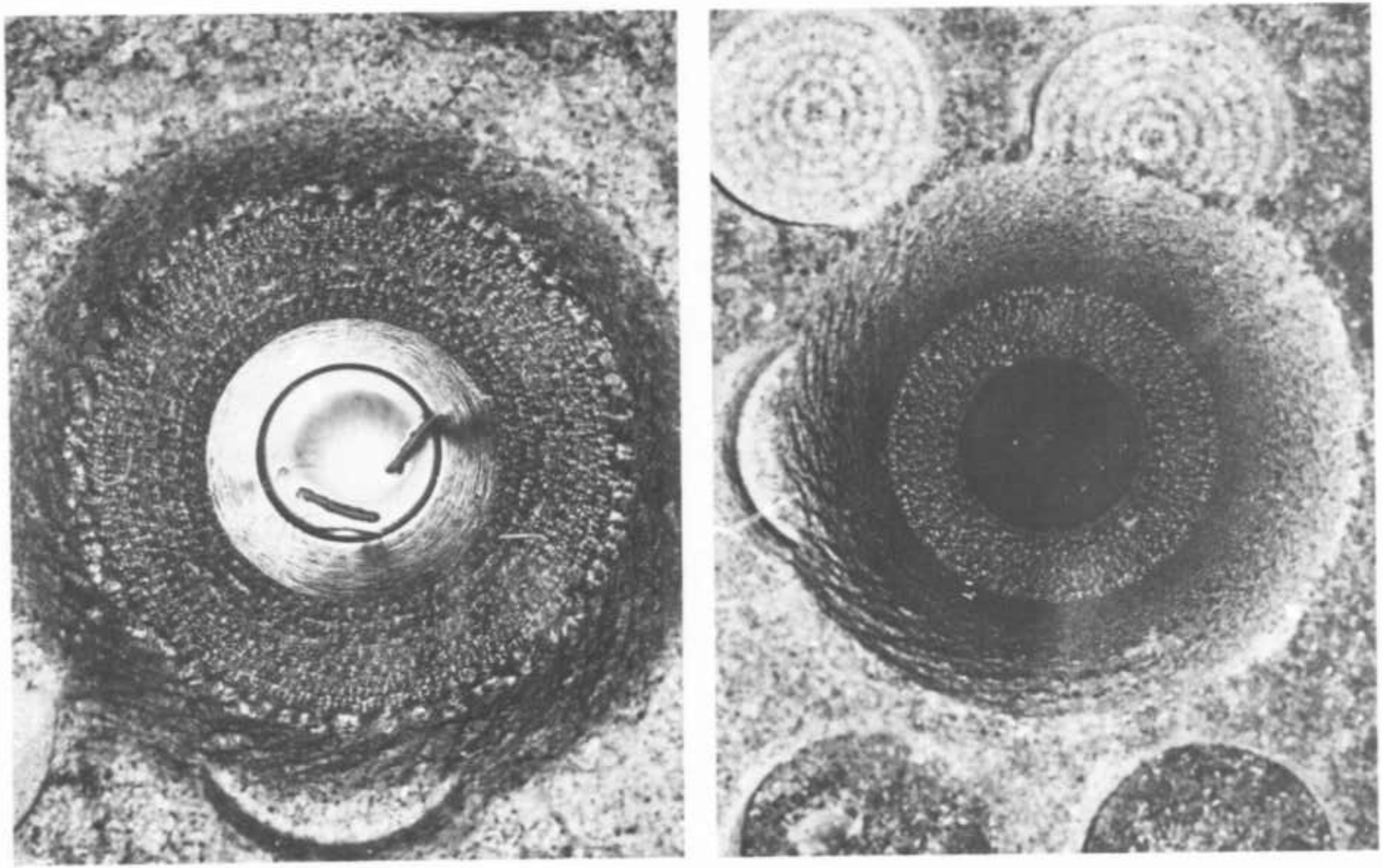

Typical Bottom Hole Patterns Made by the Conical Borer
During Tests of 24 July 1972

Figure 11

Rock No. 1 Conical Borer

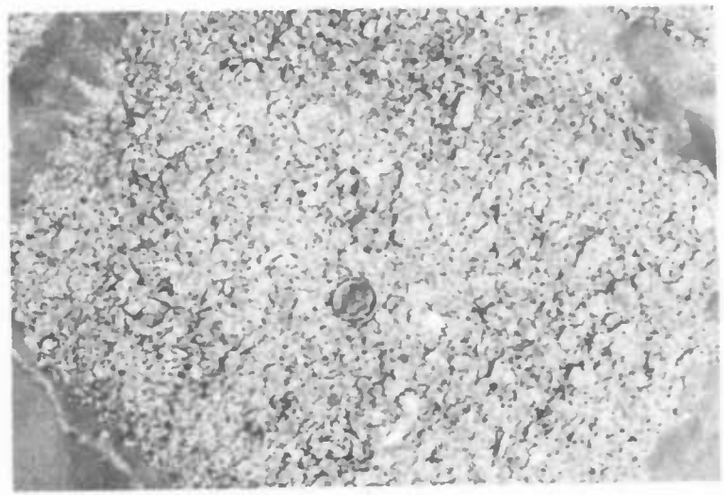

Rock No. 3 Conical Borer

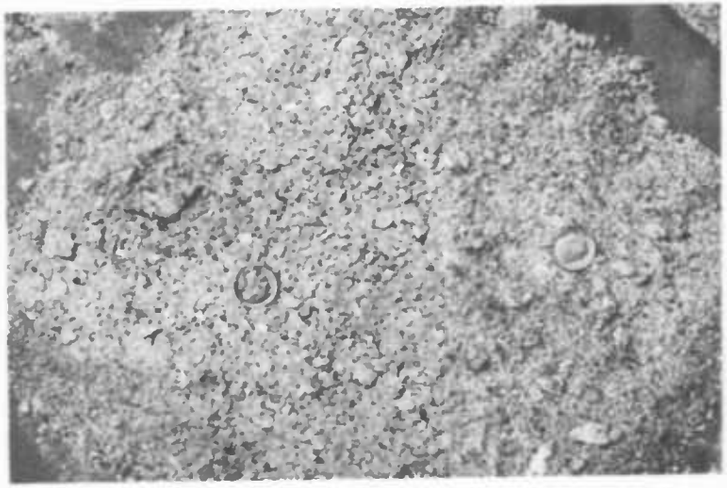

Rock No. 1 Pilot Hole Bit

Rock No. 3 Pilot Hole Bit

A Pictorial Comparison of Rock Chips Generated During
The Drilling Tests of 24 July 1972

Figure 12

Except that it required significantly less thrust load, the borer behaved similarly to a normal, flat-bottomed roller bit; it produced a good pattern of cutting and drilled smoothly up to 14 ft/hr at 40 rpm, indicating that higher speeds and penetration rates are possible. The load-penetration characteristic of the borer was approximately linear, similar to other bits (except that the load level was an order of magnitude less). Furthermore, comparatively less load was required to drive the borer past the "threshold" of low penetration that is characteristic of other hard rock bits.

The deletion of a modest number of teeth had very little effect on the drilling characteristics. It was concluded that the tooth density was sufficiently close to optimum for the purposes of this research.

5. Mucking System Studies - Phase III

5.1 Introduction

The conical borer is to incorporate a unique pneumatic mucking system to flush chips away from its cutting faces and transport them out of the bore hole to the surface. During the program various concepts for this system were generated and analyzed to determine their operating parameters and requirements. (Appendix B.) Concepts utilizing vacuum and/or pressurized air in combination with various jet locations, baffles, collectors, scrolls, seals and rotary union designs were studied. Design requirements for the most promising concepts were reviewed and the solution was worked into the overall borer layouts.

The final overall system concept chosen will incorporate a combination of pressurized air and vacuum. This concept system, as shown in Figure 13, will utilize compressed air fed through a hose from the surface, through the rotary union and directed to nozzles in the struts of the borer main frame. The high velocity air jets will "scrub" the surface of the cutter cones and agitate and propel the chips upward. Air and chips will be directed to the discharge pipe and carried to the surface by the vacuum transport system. The flow rate induced by the vacuum system will be maintained slightly higher than that of the pressurized air. The additional air volume will come from above and around the upper section of the borer housing.

This system has a number of distinct advantages over pure vacuum or pressure systems. For this reason it was decided to build a model of the borer and its hole and to experimentally test potential mucking systems. This testing was successfully completed during this year. It revealed that our design was conservative and that mucking problems appear unlikely. Details of this testing are presented in the following paragraphs.

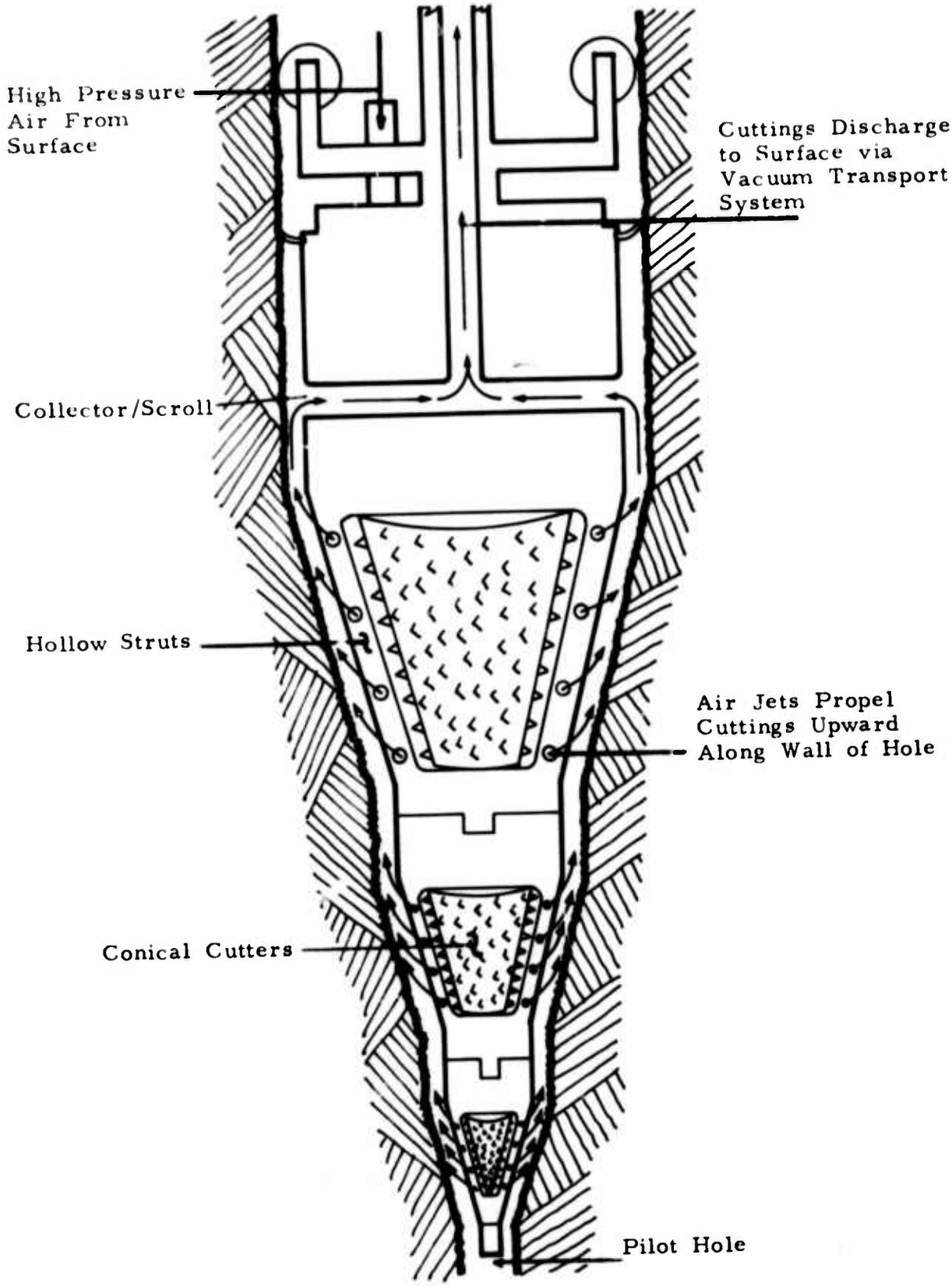

Overall Mucking System Concept

Figure 13

5.2 Description of Potential Mucking Problems and Solutions

It was anticipated that the major technical problems in the mucking system design would occur due to velocity discontinuities encountered in the vicinity of the conical cutter sections of the borer. These discontinuities are created by abrupt changes in the air-cuttings flow paths between cutter stages and by the very large area at the top of the powered cutter stage. The areas available for vertical air flow were obtained from the current design layouts and are shown in Figure 14. The typical configuration of these flow paths in the area of the conical cutters is shown in Figure 15. The flow configuration in the area of the interstage couplings and power section housing are simply annular rings between the borer and the hole wall.

Several potential problems became apparent after studying these flow paths:

(a) The divergent areas along the cutter sections could result in decreasing air velocities and possible subsequent particle separation.

(b) The abrupt change in area at the couplings implies rapid changes in air-particle direction and velocity which could result in excessive pressure drops and abrasive wear on local members.

(c) Flow around and between the cutters could be largely affected by the cutting teeth. Although there might be little restriction to air flow, considerable particle interference with the teeth could reduce the transport efficiency.

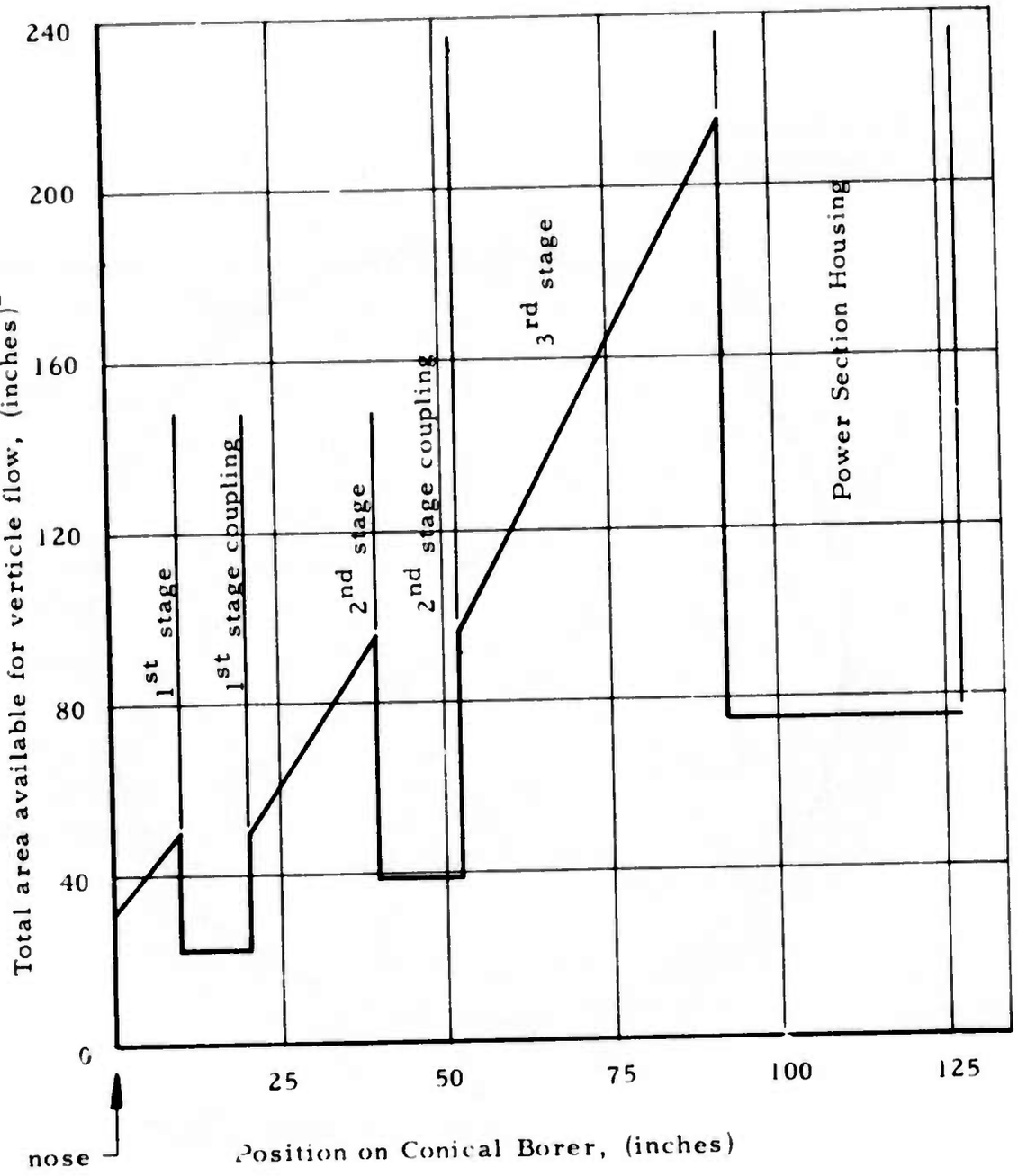

Total Projected Area Available for Vertical Air Flow at Various Positions on the Conical Borer

Figure 14

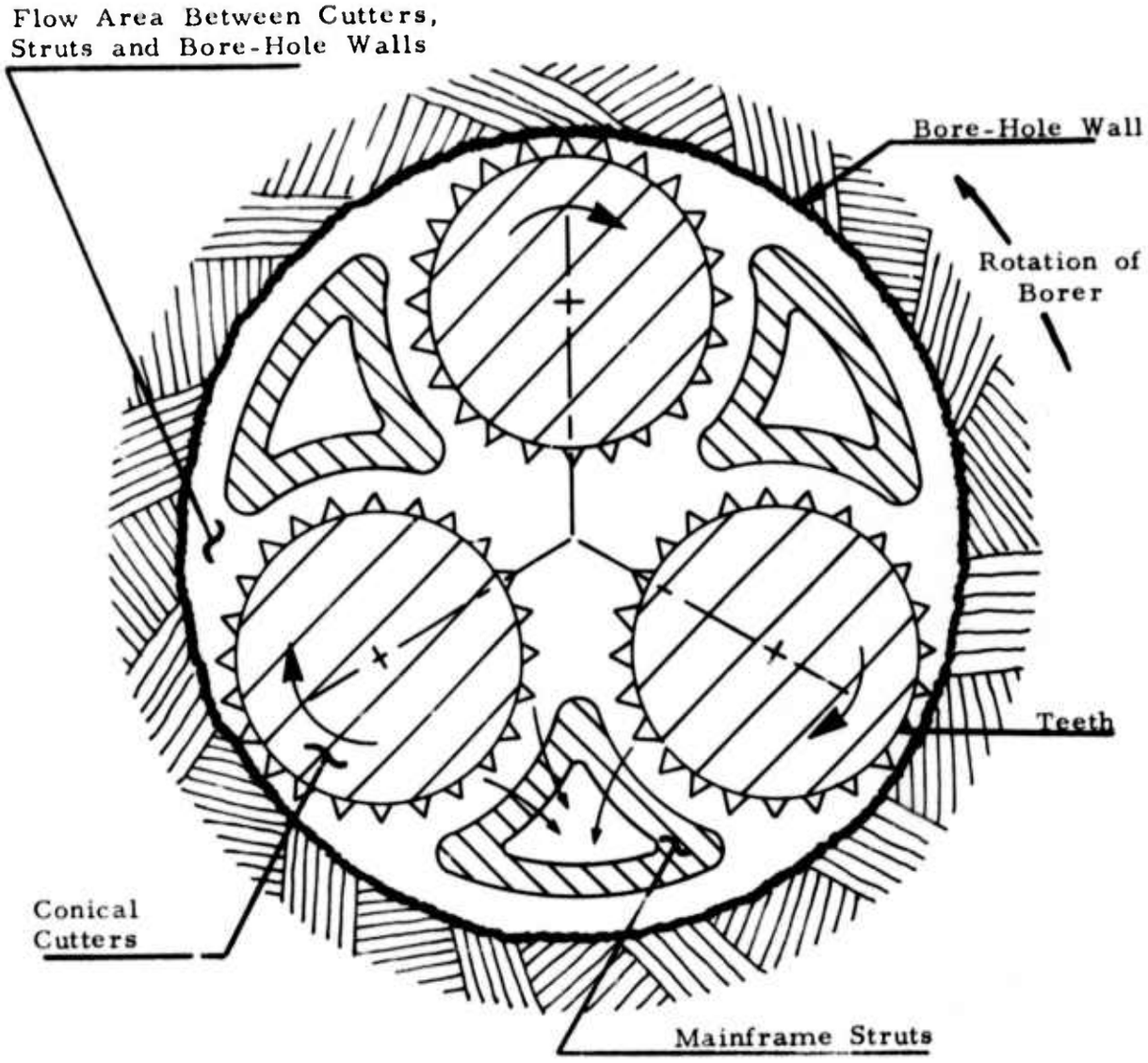

Typical Configuration of Flow Paths
in the Area of the Conical Cutters

Figure 15

(d) Particle transport in the area of the interstage couplings could be inhibited by the rough bore hole wall.

Several conceptual solutions to the above problems were generated and are discussed below:

1) The problems associated with the divergent areas along the cutters could be overcome by distributing the incoming air through nozzles along the length of the borer struts as shown in Figure 16 (Concept #1). The volume of air induced at each level would be proportioned to maintain uniform air velocity along the cutters. The high velocity jets, in this concept, would be directed upward and spaced properly to create a high velocity upward stream between the borer and the rock wall. It was assumed that the relatively close clearances between the cutter teeth and the struts would provide a sufficient flow barrier to prevent diffusion of the stream and recirculation of the cuttings. The total volume of flow would, therefore, be confined to the outer regions of the cutter stages and be more consistent with the discharge pipe requirements.

2) Mucking Concept #2 is shown in Figure 17. A relatively large, downward pointed air jet would be incorporated above the center of each cutter stage in addition to the upward pointed jets along the main frame struts. The large jet would be designed to diffuse in such a way as to prevent upward flow between the cutters and to result in a net radial outward flow between the cutters and

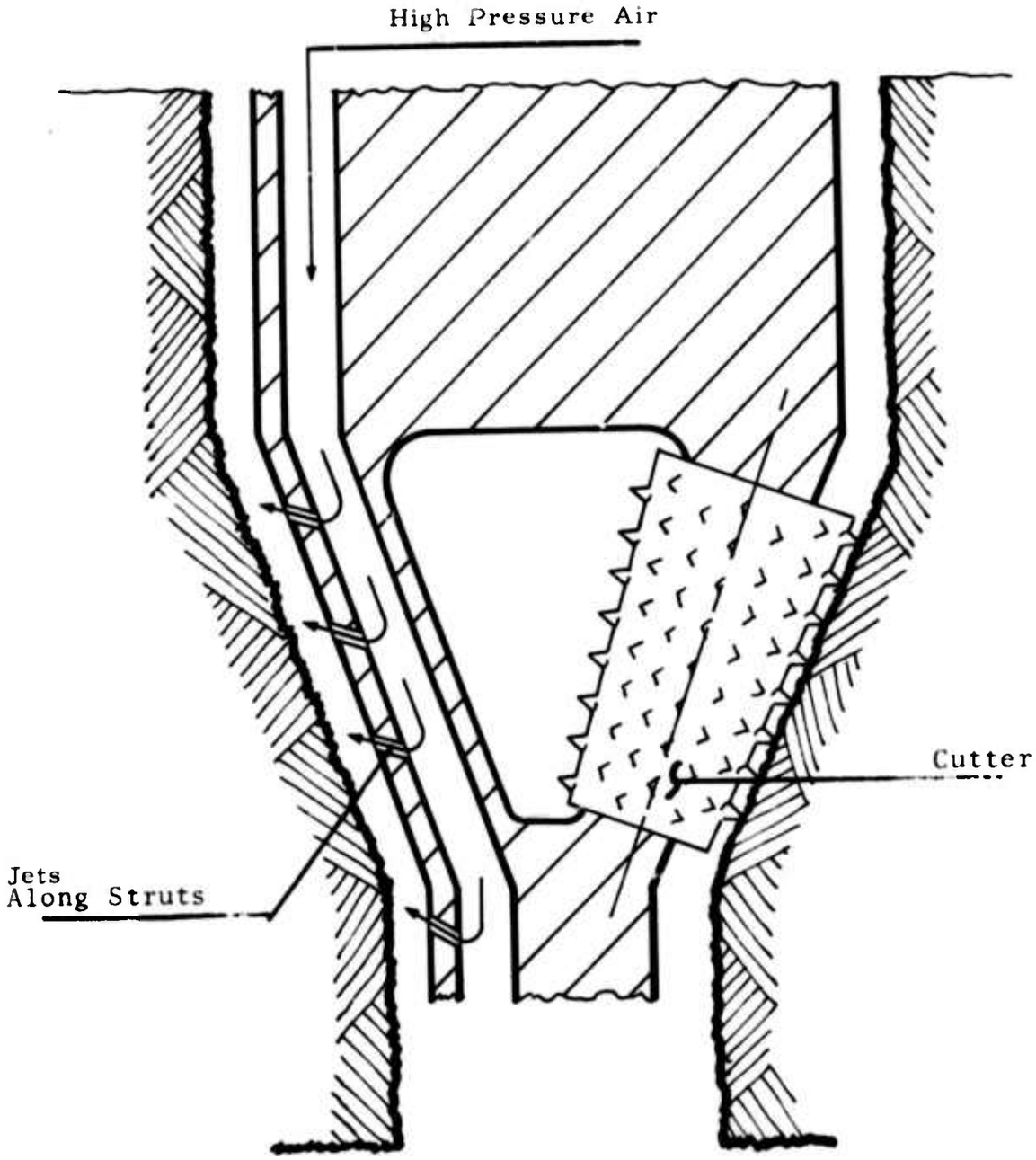

Mucking
Concept #1

Figure 16

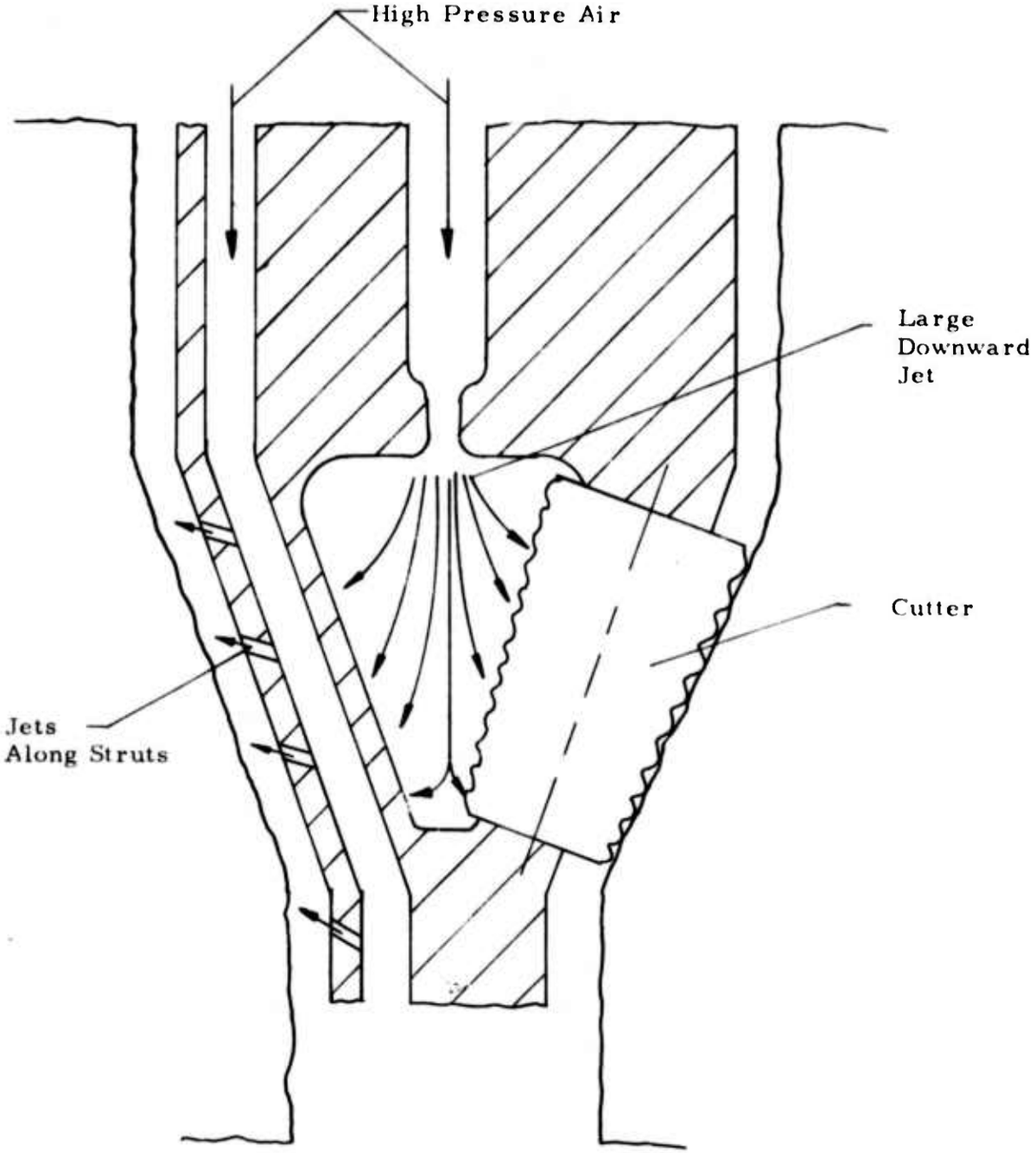

Mucking Concept #2

Downward Jet Concept for Transport
in the Area of the Conical Cutters

Figure 17

the struts. The total air volume would be sufficient to carry the cuttings upward along the hole wall since inward flow would be blocked by the outflow of air from the large jet.

3) A third concept would incorporate a suction pipe above the center of each cutter stage as shown in Figure 18. Suction at the top of the idler cutter stages would be generated by ejectors which would be powered by the high pressure air supply for upward pointed jets at the bottom of each cutter stage. The jets would propel the cuttings upward along the hole wall where they would be drawn into the center of the stage by the cutter rotation and the vacuum pipe air stream. The central air stream would be continuous from stage to stage and pass through the rotary union and discharge pipe to the surface vacuum system. Flexible baffles as shown in Figure 19 would control the air stream and prevent major recirculation and regrinding of the cuttings. The advantage of this concept is that the air and cuttings would be immediately collected in a confined cylindrical, smooth pipe between the stages, which would afford efficient and smooth transfer from stage to stage and up through the rotary union to the discharge pipe.

Each of the concepts described above has significant advantages and disadvantages which could not be quantitatively compared by simple analytical means. A mockup system therefore was built to test the various concepts and establish the most promising method which best satisfies the overall system requirements. A detailed discussion of the mock up model follows.

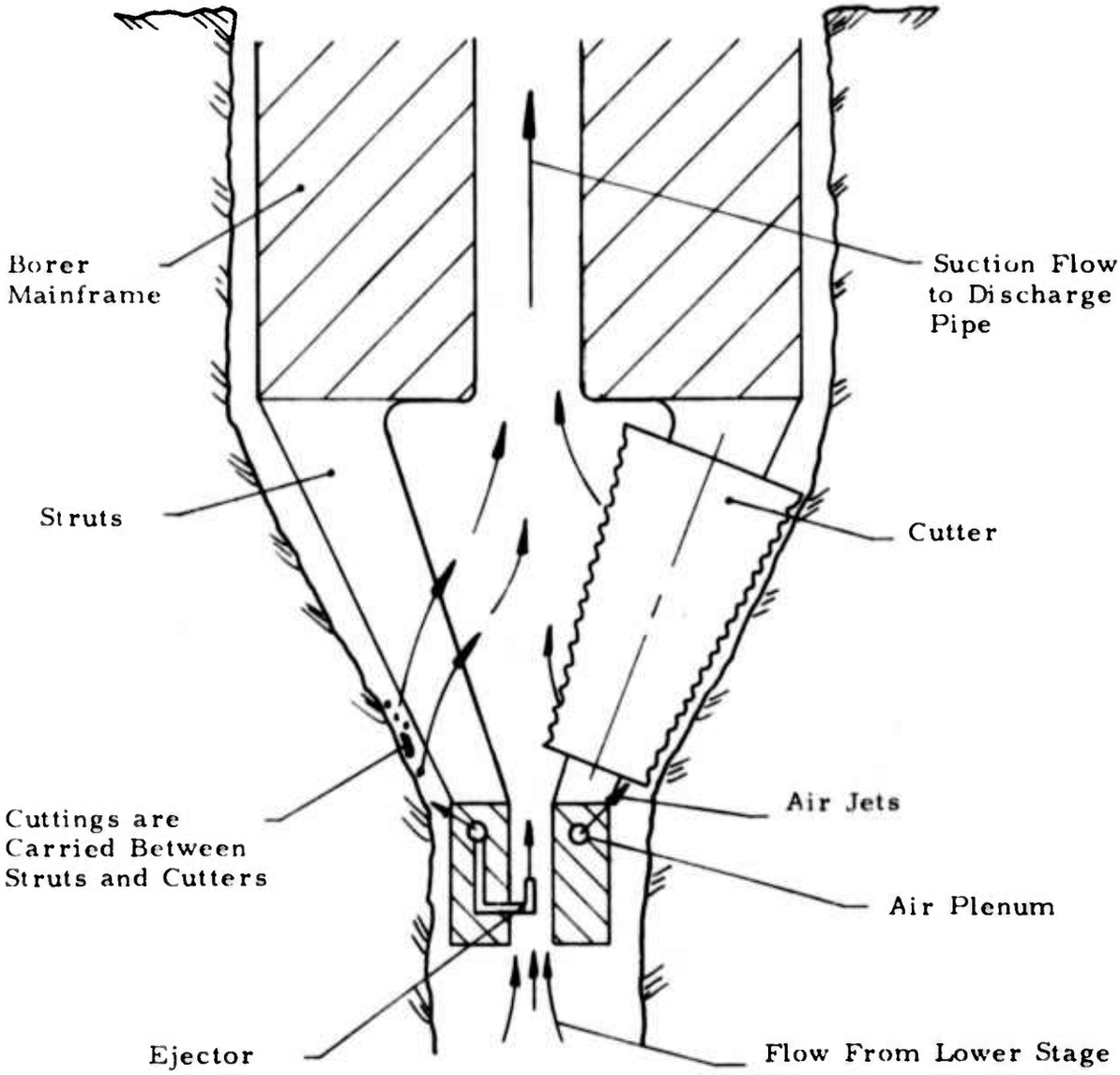

Mucking Concept #3

Suction Pipe Concept for Transport in the Area of the Conical Cutters

Figure 18

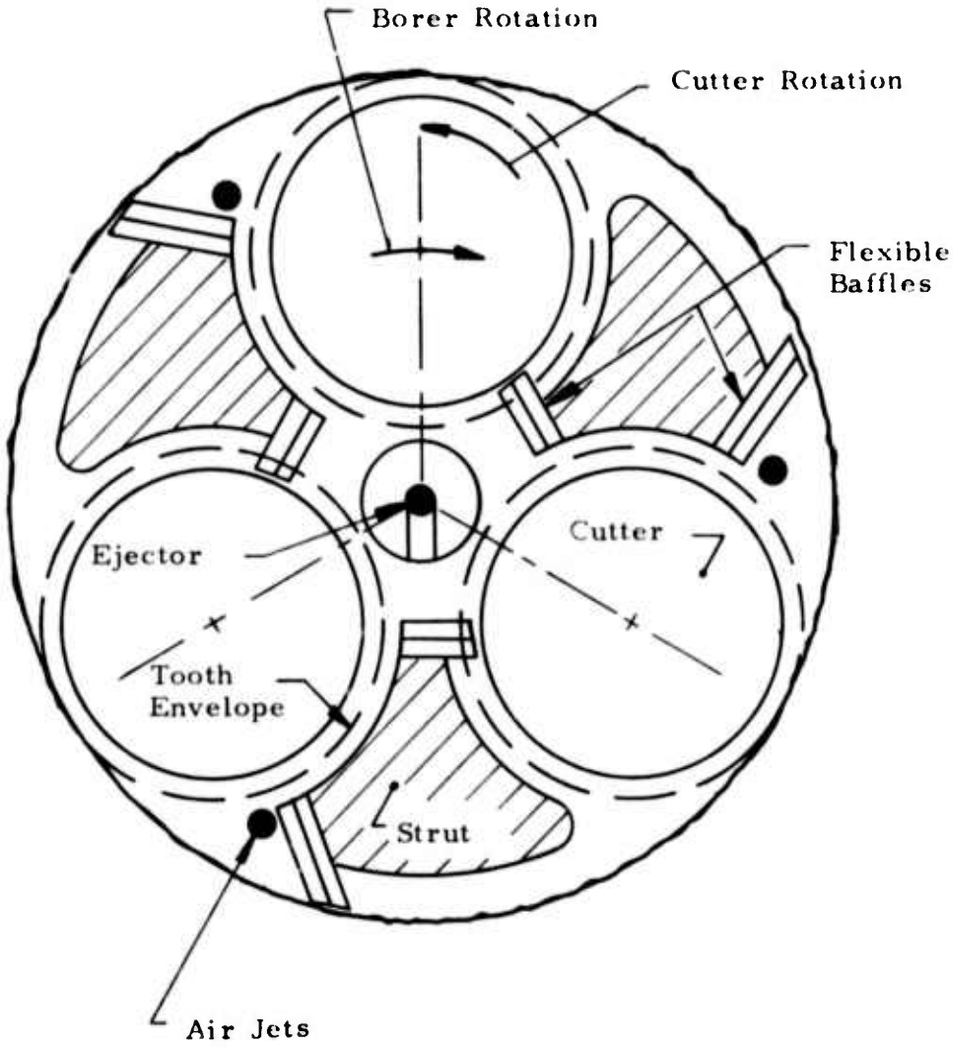

Cut-away of a Typical Stage to Show Baffles and Air Jet Locations for the Suction Pipe Concept

Figure 19

5.3 Mucking-System Model

The test model consisted of a two stage, half scale, mock-up of the borer encased in a plexiglass shell which simulated the bore-hole. The model was rotatable within the shell. Provisions were made for the pressurized air supply, for feeding cuttings from within simulated cutters, and for air-cuttings discharge and separation.

This model represented a departure from the contract statement* but was considered necessary to resolve the potential problems in the area of the conical cutters. The transfer of cuttings around the borer is dependent upon the design and position of local air jets. It was believed necessary, therefore, to allow the jets to sweep over the bore hole surface (as they would in the real case) in order to establish their true working behavior and their proper angular relationship.

A schematic description of the mock-up model is shown in Figure 20. Compressed air is fed through a rotary union and pipes to the struts of both stages. The struts were fabricated of aluminum to provide a thick wall for the drilling of positively directed air jets and to withstand the high pressure of the supply air. Cuttings were stored and collected above the upper stage and flowed down through the simulated cutter cones in both stages. Holes in the outer surface of the cones allowed cuttings to flow out at a prescribed rate. The conical sections of the plexiglass shell were of two piece construction which allowed convenient access to the model borer for modifications or examination. The model borer was suspended on bearings and was rotated at controlled speed by a variable speed rotary drive. Figure 21 shows the unit.

The model was designed half scale with two stages to minimize costs and complexity. The two stages allowed careful study of the interstage transition. It is believed that the data obtained from the half

*COR approval was obtained.

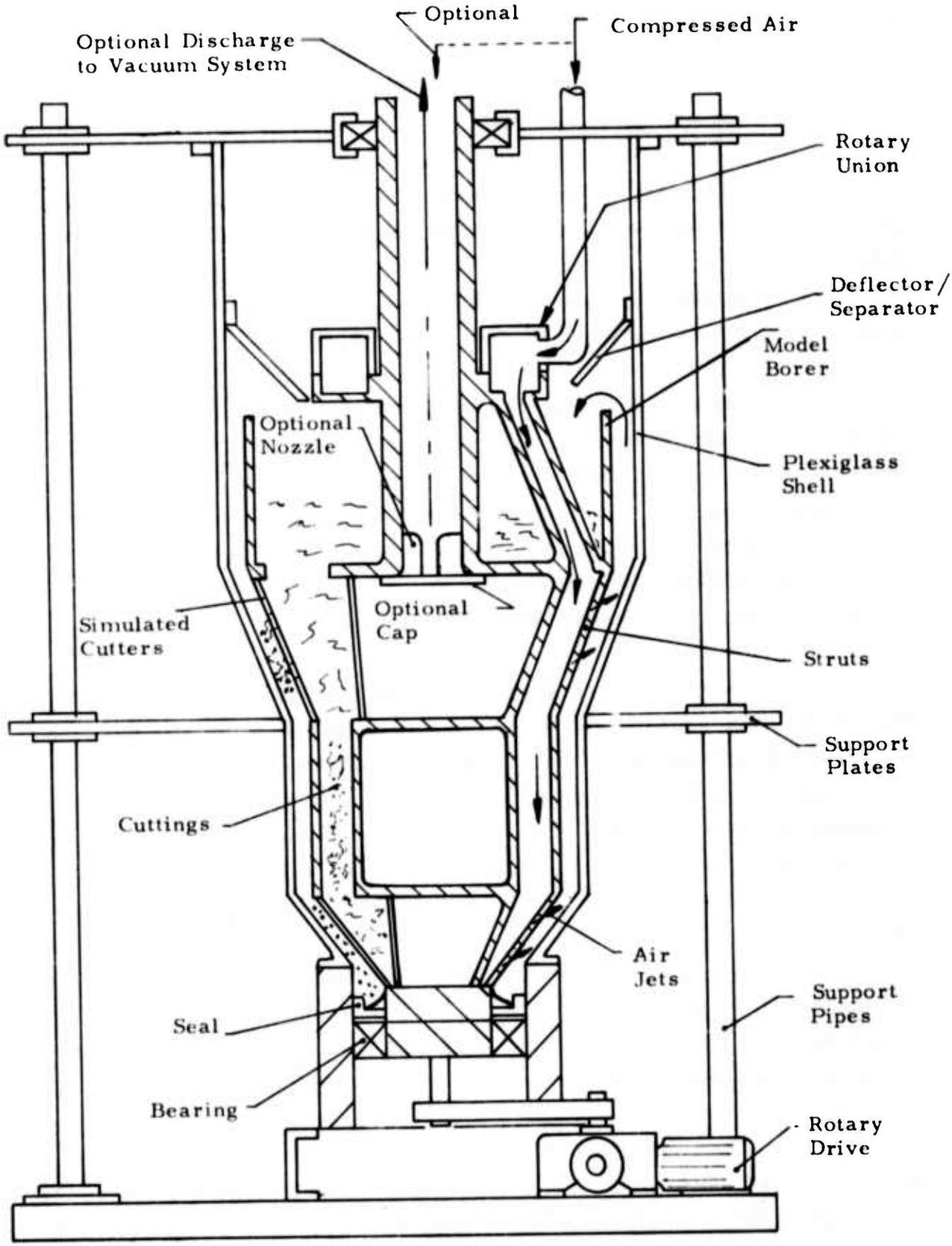

Schematic of Mucking System Model

Figure 20

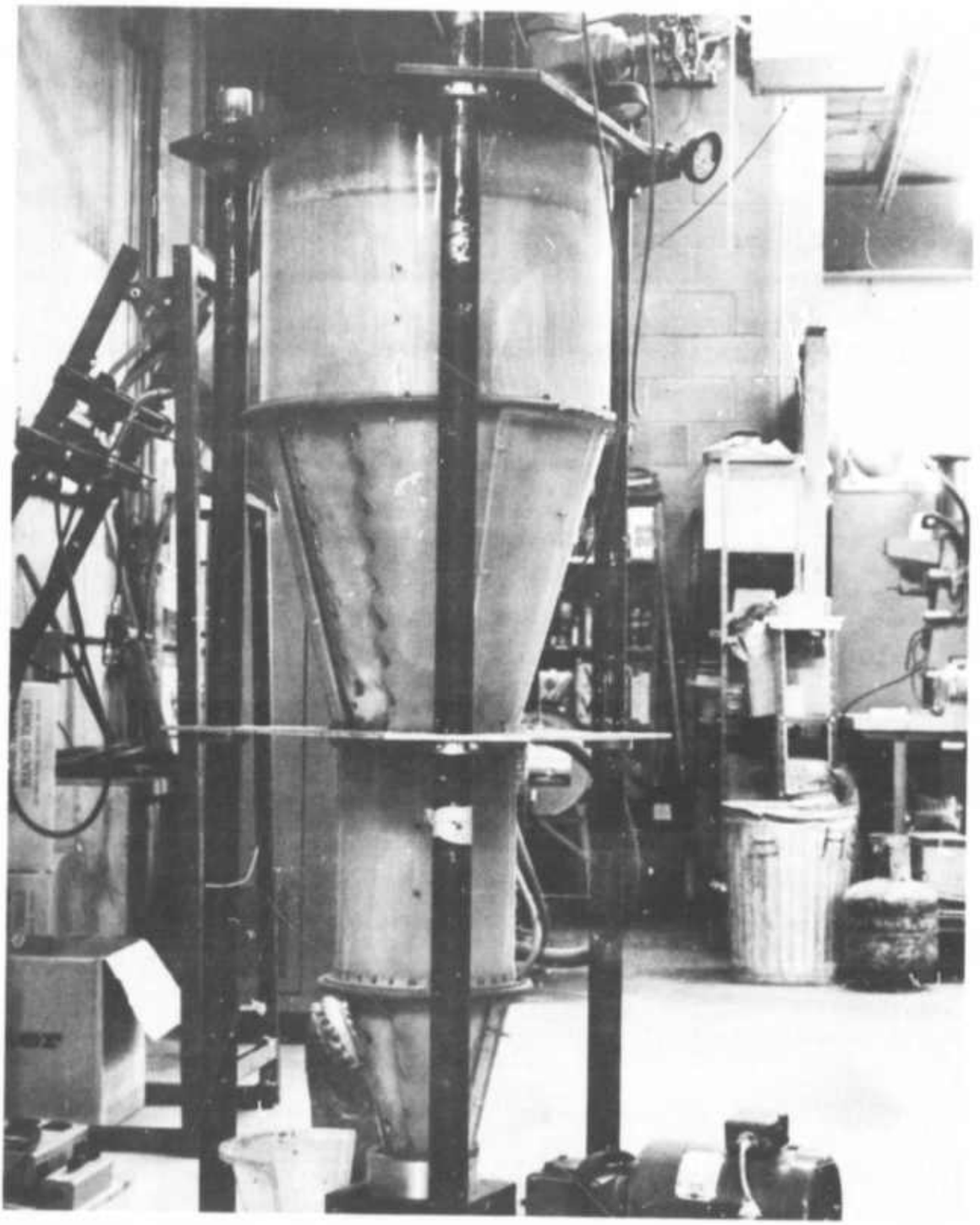

Photograph of Mucking System Model

Figure 21

scale model testing can be confidently used in the design of the full scale system and that the need for closer simulation of the actual cutter area transport far outweighed the discrepancies in half size scaling.

On the borer struts, a total of 72 tapped holes were put in as possible locations for air jets. In the second (upper) stage, threaded plugs were made with a 0.150 diameter hole through at 15^{o} to the plug axis. This angle allowed jet position variation simply by rotating the plug. Solid plugs were also used so that the number of jets and jet direction were controllable. Due to the smaller area in the first (lower) stage, jet direction was assumed to not be as important, therefore, plugs with 0.150 diameter holes straight through and solid plugs were used.

To test Mucking Concept #3, a vacuum supply was necessary. This was obtained by fabricating an eductor which utilized pressurized air to create a vacuum with a capacity of 1000 SCFM at 8 inches of mercury. The eductor is shown in Figure 22.

Air flow was monitored during testing by using an orifice plate in conjunction with a differential pressure gauge. Air velocities were monitored at four positions; the two cutter zones and the two cylindrical portions on top of the cutters. This monitoring was accomplished using pitot probes and an inclined manometer. Four static pressure taps were also designed into the plexiglass shell for both safety and monitoring purposes.

5.4 Experimental Procedures and Results

5.4.1 Concept #1: Air Flow Out Jets with Cuttings Propelled to Annullus Area

Every other jet in the second stage was plugged (24 of 48 closed). The remaining second stage jets were then aimed as closely as possible at the point of cuttings generation. In the first stage, 6 of the 24 jets were plugged -- two in each strut.

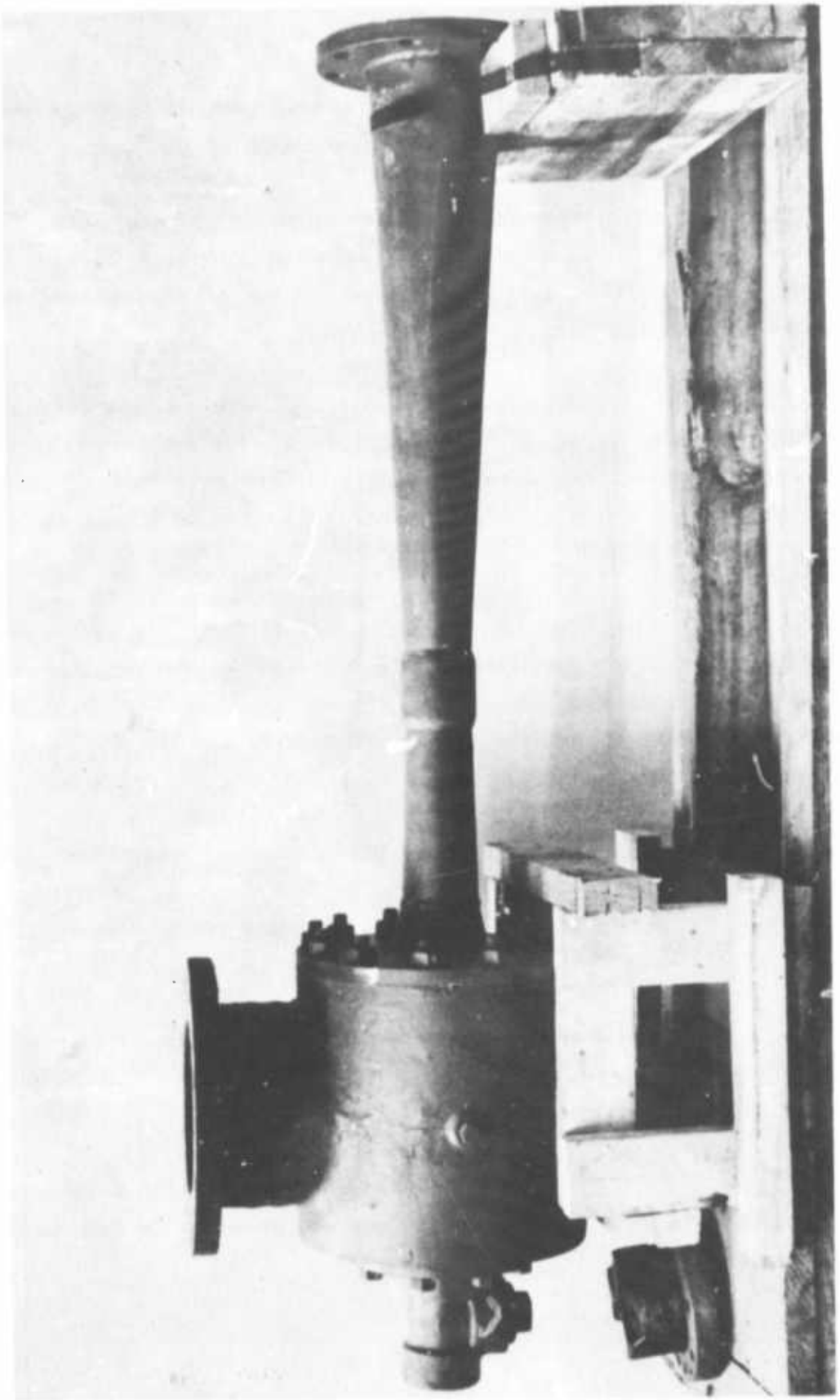

Photograph of Eductor

Figure 22

The air flow was started with the cuttings generation system off. This permitted data accumulation on the flow of air only.

With the plexiglass shields removed, pressure readings were taken to ascertain any pressure drop through borers' passage ways. The shields were then replaced and the circumferential velocity distribution measured.

After recording this data, the cuttings generation system was actuated and sand was ejected through the mock cutters at positions and in quantities similar to the actual full scale borer. The flow characteristics of the sand/air mixture were then observed while the volume of air was varied.

Upon completing this test, the procedure was repeated in a series of experiments. The variable factors in this series consisted of jet positioning, number of jets involved, surface obstacles on the cutters, surface obstacles on the plexiglass, and the use of coarse fish gravel and actual cuttings.

The cuttings exhibited a strong tendency to follow the annulus flow with little material build-up in the cutter. Air flow rates between 300 to 500 SCFM did a very adequate job of removing the cuttings.

Early in the testing it became evident that jet positioning was not extremely critical as the cuttings were successfully removed in all jet positions.

The only time performance degraded seriously was when 50% or more of the jets were plugged or when the jets in one area were all plugged.

In an effort to cause a more turbulent passage for the cuttings and approximate the surface roughness of a bore hole, 1/8" thick x 1/2" wide x 1" long, rubber patches were placed both on the inside of the plexiglass shield and the outside of the borer cutters. While diverting the flow of cuttings somewhat, these patches had no major effect on performance.

As a further test of the system's effectiveness, fish gravel particles of approximately 1/8" diameter were used instead of sand. These particles were fed in at a rate well over 30 pounds/minute almost exclusively through the first stage. Here again the system handled them very well. This fact is quite impressive when it is considered that the desired (scaled) material removal rate is 30 pounds/minute (1/4 of full scale) total for both stages.

5.4.2 Concept #2: Air Flow Out Jets and through Center of Second Stage with Cuttings Propelled to Annullus Area

The basic test procedure remained the same, with air flow analysis followed by cuttings admission and combined cuttings/air flow observation. An added variable in these tests was, as the title implies, air through the center of the second stage cutters. This air was controlled by a 2" gate valve and injected through a 1/2" diameter orifice.

Utilizing the jet positioning data obtained in segment #1 of this study, variation of jet position was much more limited in this series.

In Concept 2 there were some localized zones of low velocity which initially would fill with the cuttings, but since these zones were bordered by higher velocity streamlines, they soon would reach a steady state condition where the net rate of mass transfer went

to zero. These small zones existed near the top of the struts and lower portion of the cylindrical sections somewhat triangular in shape. When air was admitted through the center jet these zones disappeared and the variations of the circumferential velocity were reduced in the cylindrical positions of the borer. This addition of 50 to 100 SCFM in the center jet produced a less turbulent flow with better cleaning characteristics.

5.4.3 Concept #3: Air Flow Out Jets and Cuttings Propelled Out through Center of Cutter Stages

In this final battery of tests, the central air jet passage way was now converted into a cuttings removal pipe. The vacuum eductor was connected into the system and the same basic procedure as in Concepts 1 and 2 was followed.

One difference in this test was that the cuttings generation system was a closed loop recycle system. The cuttings were recirculated after filtering them from the air. Cuttings passing through the vacuum removal system were pneumatically conveyed to an outside holding facility making continuous reloading of cuttings necessary during operation. The unique variable in this portion of our testing wa the vacuum used to evacuate the cuttings. It was controlled by a 2" gate valve on the motive air input to the eductor.

Due to the strong tendency of the cuttings to travel in the annulus area, the vacuum system did not work quite as effectively as concepts of 1 or 2. While the cuttings were removed, there was a build-up of material in the cutter area.

5.5 Conclusions of the Mucking Study

The data obtained in these tests were very encouraging. Many of the problem areas that were anticipated proved to be easily correctable.

One major concern, that of jet aiming and locating, does not now appear to be that difficult a task. By the lack of significant response to changes in the second stage jet positioning, it can be assumed that a fairly wide range of jet angles exist that will provide adequate system performance.

A broad range of acceptable jet locations also exists. During the testing, a wide range of jet locations were used all with equally good results.

With such good flow characteristics up the annulus of the borer, Concept #3 of cuttings removal through the center of the stages seems to be an unnecessarily complex and difficult system to utilize.

Concept #2 using strut and center jets is the most effective. With a 20-25% increase in SCFM (50-100 SCFM) a much more defined flow path is created. However, incorporating this system into the final borer design would probably cause more difficulty than its advantages are worth. This is especially true since Concept #1 of air out of the jets in the struts alone was entirely adequate in the tests. Concept #1 was therefore selected for use in the final design.

Figure 23 schematically shows the recommended mucking concept. High pressure air (85 psi) is ducted through the borer structure and discharged through jets mounted in the struts. Typical expected operating pressures and flow rates are indicated on the figure. Details of the passages are shown in the layouts of Section 6.

Although the results of the mucking study were very optimistic, one factor that is still of concern is the water content and cohesiveness of the cuttings. This was one area where test capabilities were extremely limited. Obviously this characteristic will vary from formation to formation. Extensive field testing will be required before this question can be answered.

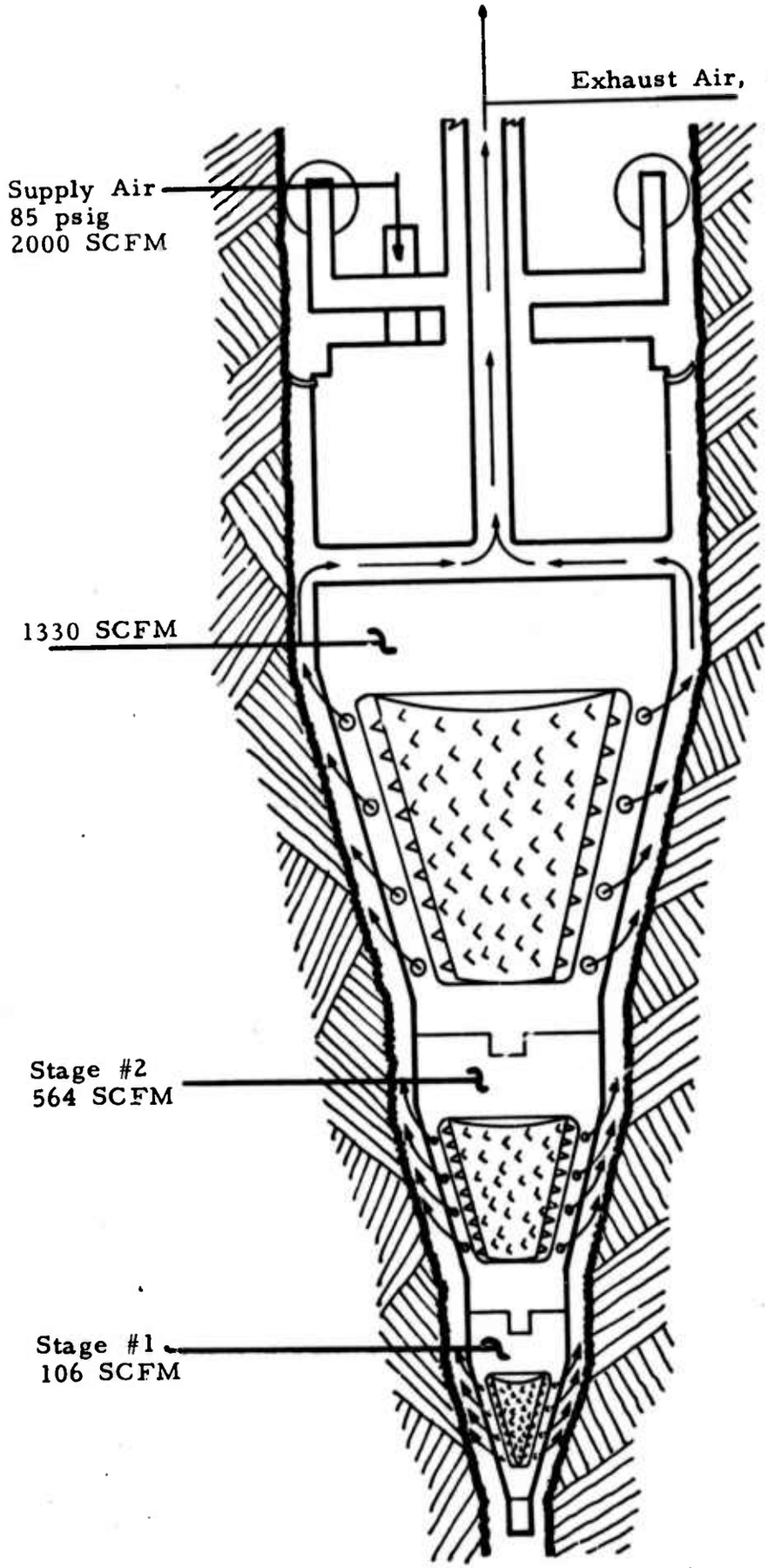

Note: All conditions based on a penetration rate of 10 ft/hr.

Recommended Mucking System

Figure 23

6. Description of the Borer Design

The overall unit will be approximately 18 feet long and will weigh 16,000 - 18,000 pounds, not including external components such as hoses and lift cables. Based on the data presented in Section 4, a cone angle of 18° and a skew angle of 4° were chosen. Descriptions of the major subassemblies follow.

6.1 Description of the First Cutting Stage

The first stage (Fig. 24) will enlarge the 8 3/4 inch pilot hole to approximately 14 inches. It is an idler stage (the cutters are not individually powered), driven by the torque transmitted through the adjacent second stage.

A removable nose plug with a protected grease fitting is provided. This will allow addition of an adaptor section and a pilot bit if desired.

The flushing air is carried through passages in the frame struts. The air passages are continued through the nose end of this stage so that flushing air could be easily provided to an optional pilot bit.

The three cutter cones are mounted in heavy duty spherical roller bearings. These bearings are typically used in such heavy duty applications as rock crushers and ball mills. The calculated life expectancy of the most heavily loaded bearing is approximately 2,500 hours. (See Appendix C.)

Double seals are provided for all the bearings. The primary seals are Cartriseal units, used in many earth-moving equipment applications. Secondary O-ring backup seals are also employed.

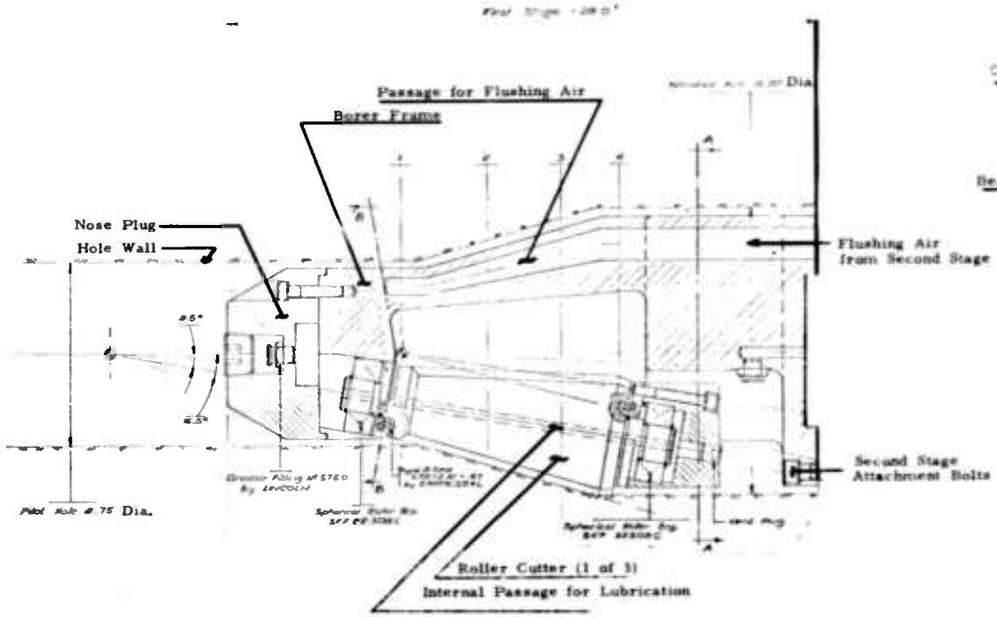

First Cutter Stage
Figure 24

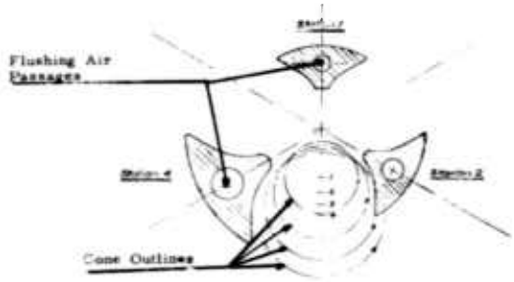

Station Sections

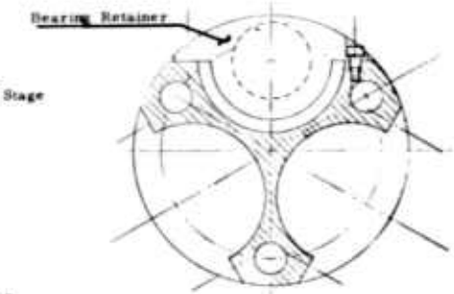

Section A-A

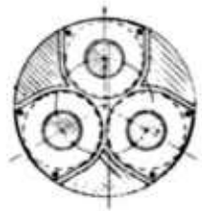

Section B-B

Bearing lubrication is provided through the fitting in the nose plug. The vent hole through the cutter and the vent plug at the cutter top end allow lubrication of all bearings in the stage from a single fitting.

The cutters will be equipped with 0.625 inch diameter 120° carbide compacts. The bearing mounting structure allows for easy replacement of the cutter cones. It is anticipated that the compact life of any stage will not be more than 300 hours. Consequently, the roller cutters as well as the bearings will be replaced at that time.

The first stage is joined to the second stage by high-tensile socket head cap screws. Driving torque is transmitted through the interlocked first and second stage frames and not through the screws.

6.2 Description of the Second Cutting Stage

The second cutting stage (Fig. 25) is also an idler stage. It is similar in design to the first stage and will enlarge the 14 inch first stage hole to 24 inches.

6.3 Description of the Third Cutting and Drive Stages

The third cutting stage (Figs. 26 and 27) is physically like the first and second cutting stages in the method used to retain the three cones and in the air passages. The cones are driven by means of Schmidt couplings directly from Vickers hydraulic motors.* Power to these motors goes through a flow dividing system that compensates for the variation in the surface condition of the borer hole. This prevents loss of traction to any cone and overspeeding and burnout of these motors.

The drive portion of this stage is enclosed by a metal shroud that attaches to the bottom of the flushing manifold. This prevents contamination from surface material and also serves to contain the normal

*The power requirement and motor specifications were calculated from the data shown in Figs. 9 and 10 plus Vickers' data sheet i-32 (Model MHT-150-R1-12).

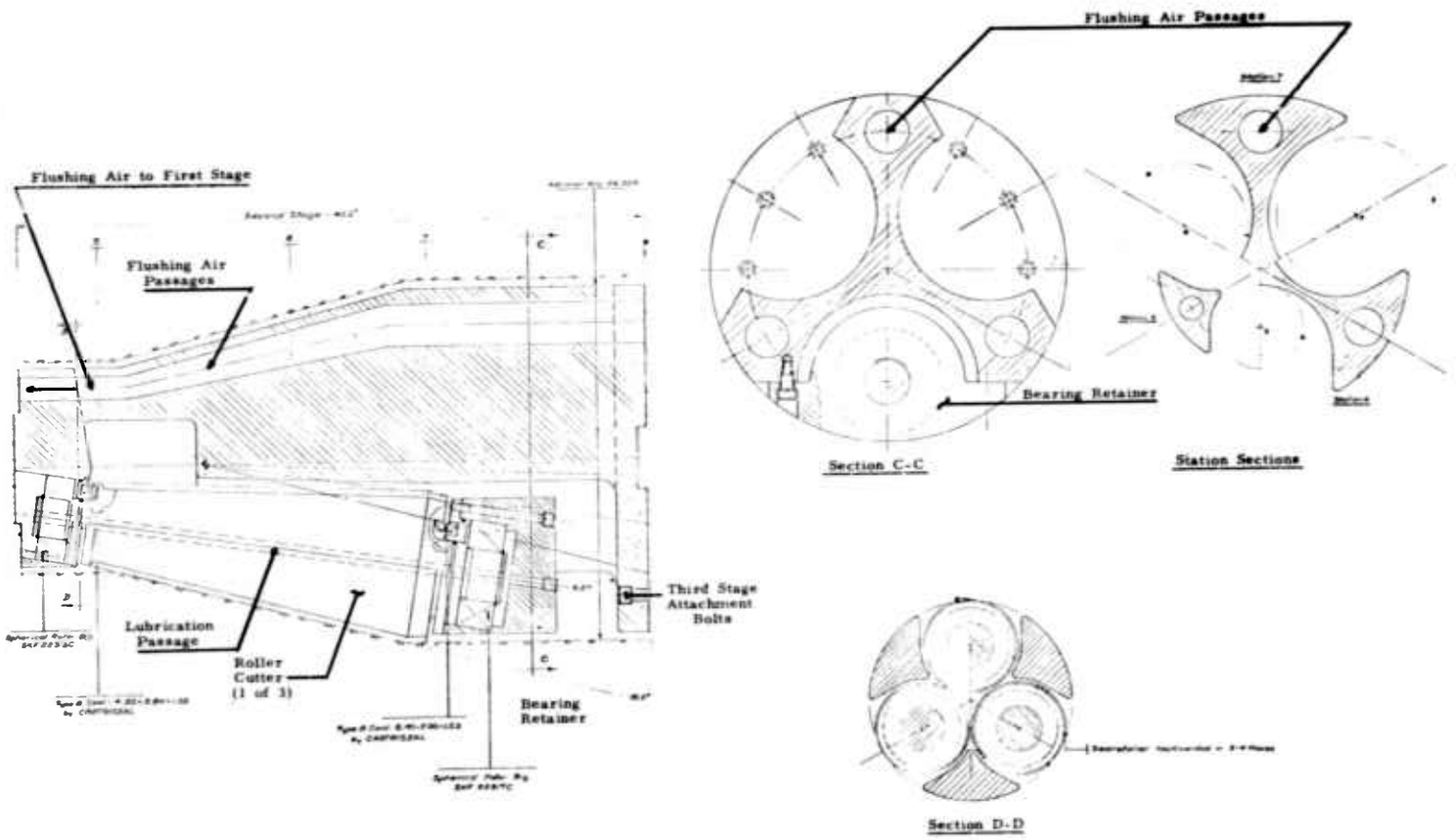

Second Cutter Stage

Figure 25

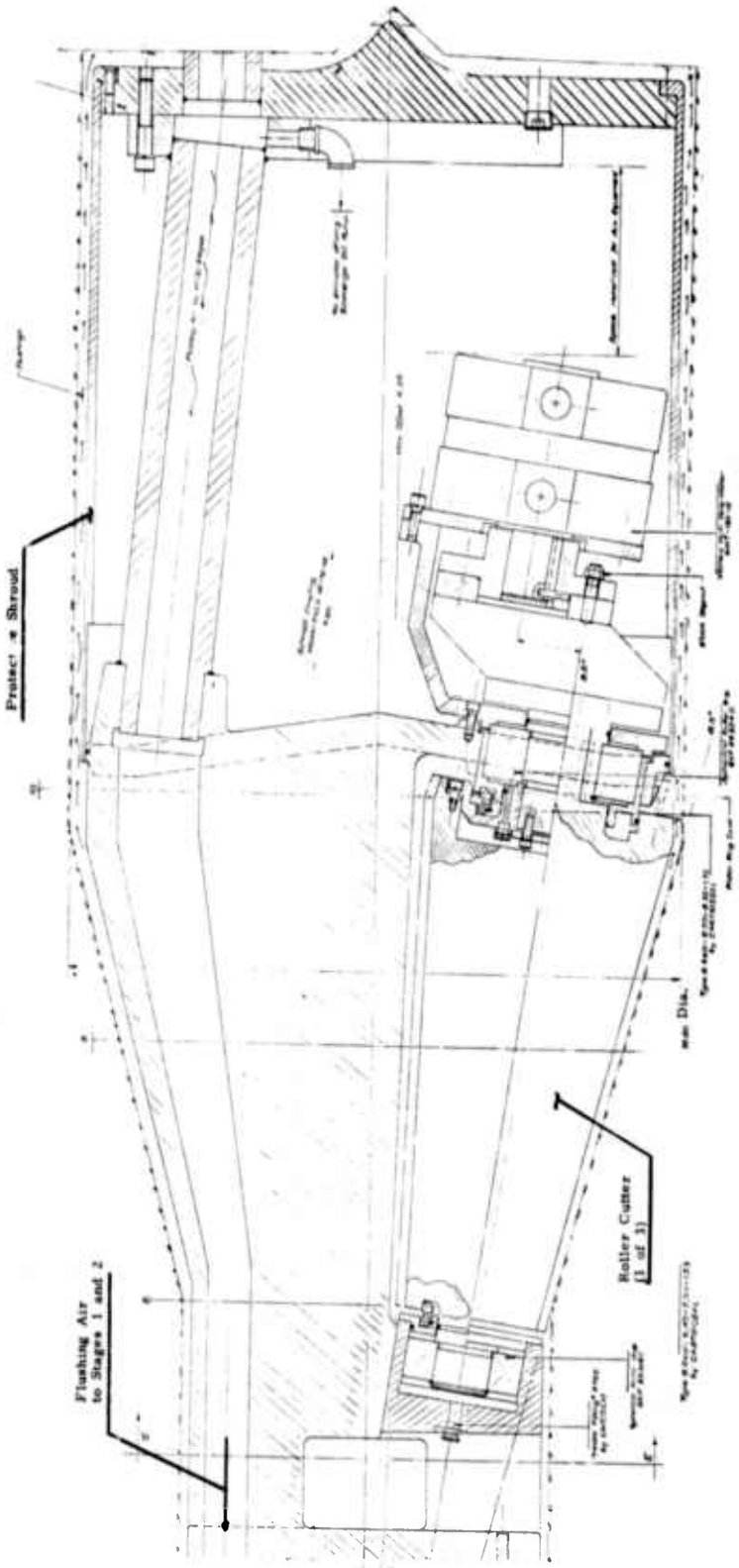

Third Cutter Stage

Figure 26

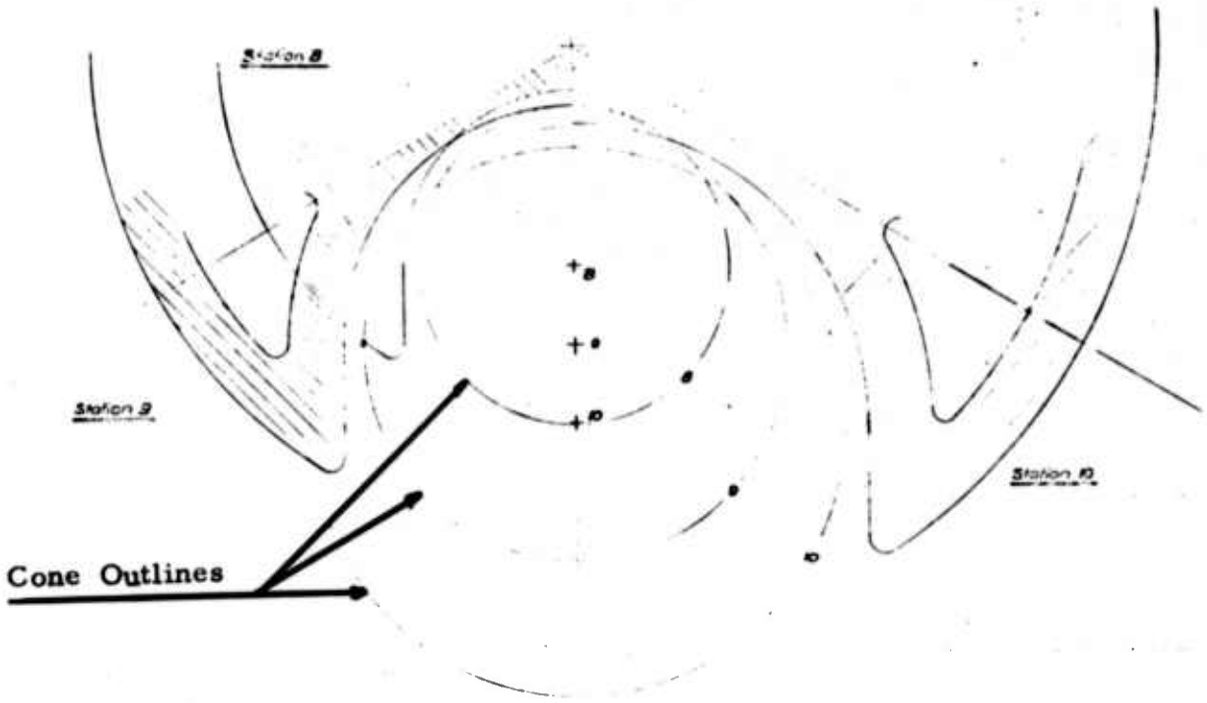

Station Sections

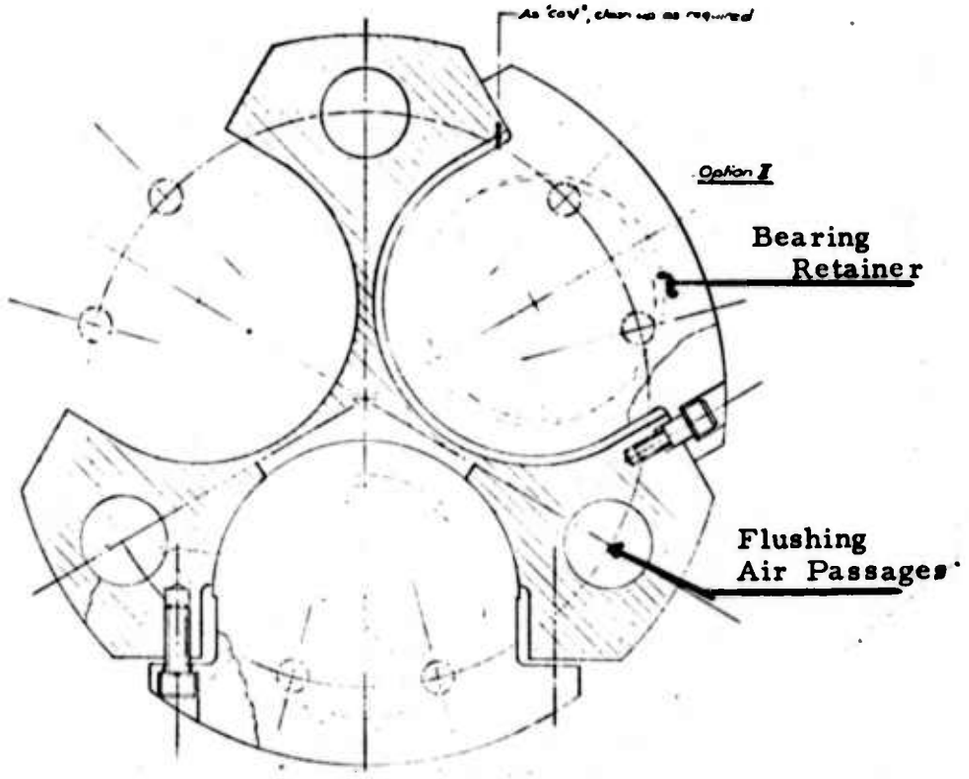

Section E-E

Sections of Third Stage

Figure 27

oil leakage from the hydraulic motors. A scavenger pump, located within this portion, is capable of removing the oil faster than the worst leakage rate of 6 gpm.

6.4 Description of the Rotary Union

The rotary union (Fig. 28) portion of the borer is positioned between the top portion of the flushing manifold and the anti rotation stage. This section provides the manifolding to take the high pressure inlet oil, the flushing air and the return oil from their stationing flexible hoses and to transmit them with minimum leakage to the rotating borer. It also provides the passages to carry the cuttings from the annular region in which they are generated and transported to a stationary control exhaust line.

The outer portion of this unit remains non-rotating as the borer advances. High pressure inlet oil is ducted to an annular groove on the outside surface of the stationary center portion. This groove is axially seated by rotating high pressure seals and communicates directly with a mating groove on the inside surface of the rotating outer protion. Individual flow passages lead from this outer groove to the flow dividers and the three hydraulic motors. Return oil and flushing air is handled in much the same manner.

A large turntable bearing ring at the top of this unit provides axial and diametral support. Additional axial support is provided by needle bearings at the bottom of the unit.

Cuttings are carried from the annular region to the center of this unit and up an exhaust line. A flexible seal is provided at the top of the unit between the unit and the hole wall to minimize air leakage. Conveyor belting was chosen for the seal material because of its durability and low cost.

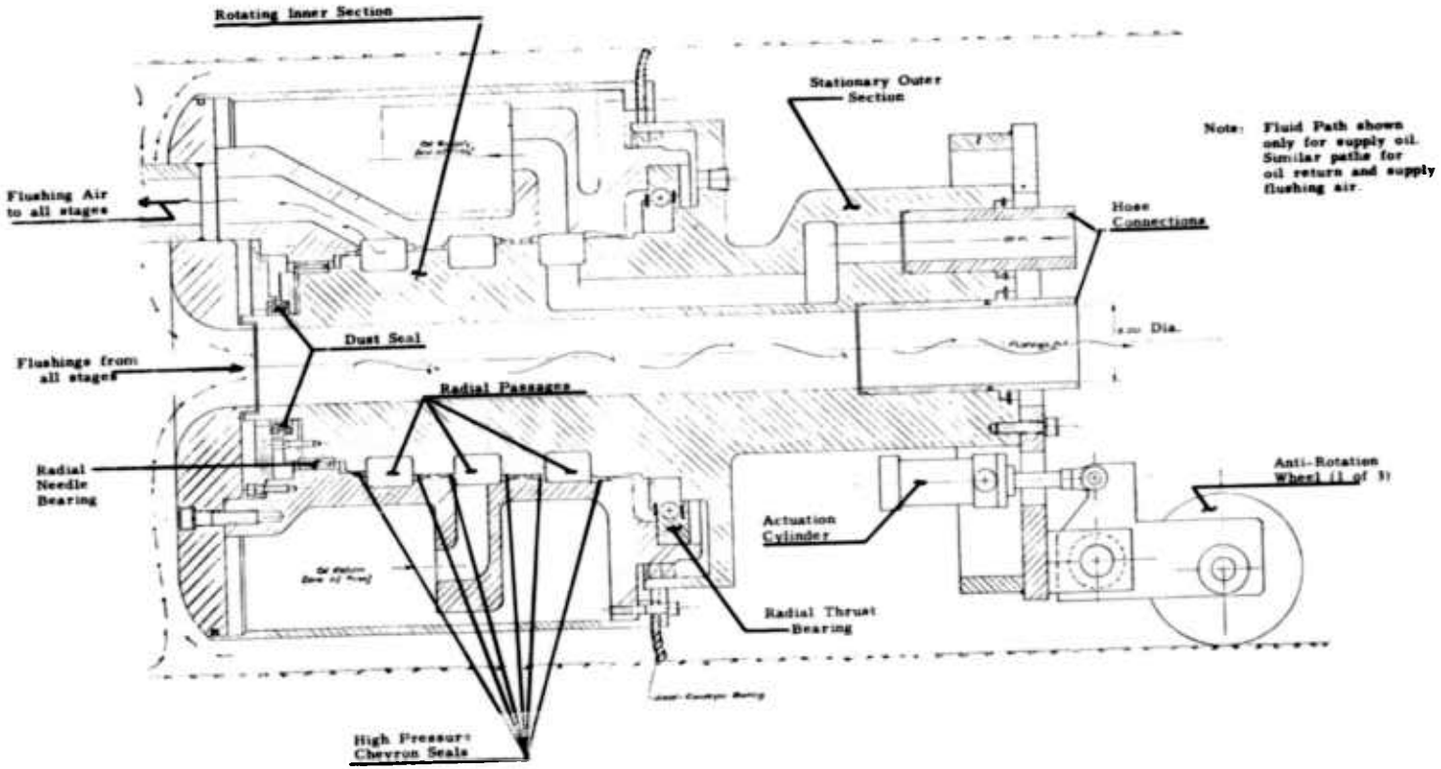

Rotary Union Stage

Figure 28

6.5 Description of the Anti-Rotational Assembly

The assembly (Fig. 28) provides clamping to the wall of the bored hole to prevent the oil supply and exhaust hoses from rotating. It consists of three cylinders with wheeled contact arms. This allows the borer to advance while preventing the rotation of the stationary housing of the rotary union.

6.6 Structural Calculations

The borer structural calculations are summarized in Appendix D. Based on these calculations, no structural problems are anticipated.

6.7 Material of Fabrication

As a result of the structural calculations, it was decided to cast the main frame of Mechanite type SP80. The cutters will be constructed of AISI 4140 and heat treated to hardness of Rockwell 30.

6.8 Parts List

A complete parts list showing all special and off-the-shelf components and their specifications has been prepared.

6.9 Cutter Detail

Detail of the cutter compact is shown in Figure 29.

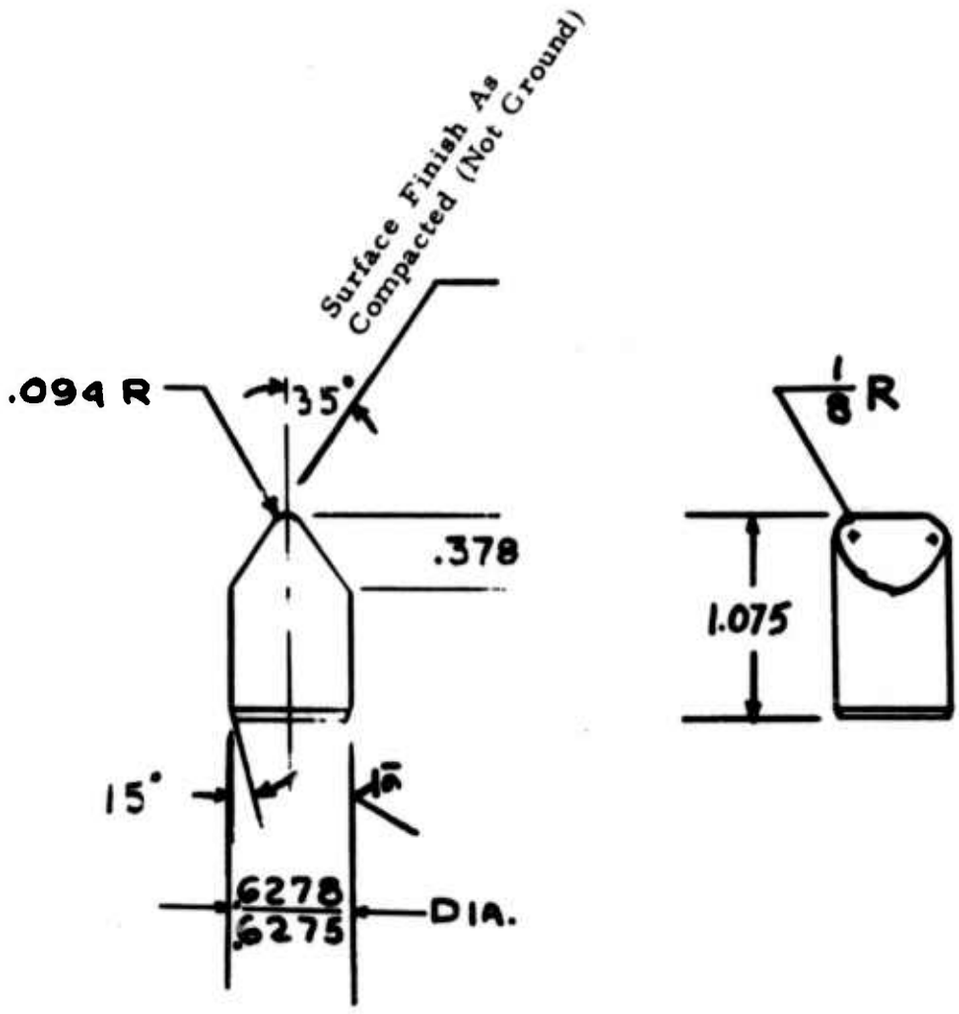

Third Stage

Detail of Cutter Compact

Figure 29

7. Determination of Required Field Support Equipment - Phase IV

The following major pieces of equipment will be required to conduct the field tests:

a) Hydraulic power supply
b) Hydraulic lines
c) Hose reels (3)
d) High pressure air compressor (2)
e) Vacuum blower and dust separator
f) Flexible exhaust line for cuttings
g) Motorized crane or derrick
h) 500-1000 gallon fuel tank for diesel oil.

It has been assumed that the test site will be located in a remote area and that electric power of 400 to 600 kw will not be readily available. Therefore, all major prime movers will be diesel engines, fueled from a single tank of 500 to 1000 gallons capacity. The following additional assumptions have also been made:

a) The depth of hole to be bored is 500 feet.
b) The rocks to be bored will be a granite of approximately 30,000 psi compressive strength.
c) The hole will be dry.
d) The rock will be sufficiently competent that no casing will be required.

Detailed descriptions of the other equipment are presented in the following sections. Specific manufacturers' names are presented only to illustrate the type of equipment required.

7.1 Hydraulic Power Supply

The required hydraulic power can be provided by a 460 hp Detroit Diesel complete with matching transfer gearbox driving a pressure

compensated Vickers piston pump. The hydraulic oil should be stored in an enclosed 600 gallon reservoir complete with sight gauges, breather assembly, magnetic drain plugs, air to oil heat exchangers, filters, etc. All equipment can be mounted on a skid-type subframe, 6.5 ft. wide x 6.5 ft. high and 16 feet long. It will weigh approximately 10,000 lbs.

The piston pump (Vickers or equivalent) should be capable of delivering 220-250 gpm at 3,000 psi continuously and 4,000 psi intermittently.

7.2 Hydraulic Lines

In order to withstand the high working pressures (up to 4,000 psi) and severe environment produced by a vertical application, hoses that meet "AP/Grade C" specifications were specified. To carry the volume of hydraulic fluid necessary at a sufficiently low velocity, a 2.5" I.D. hose is required. Such a hose is manufactured by Hewitt Robbins (Hewitt MC 750) and several other companies. The MC 750 hose has a 2.5" I.D. and a 5.25" O.D. It weighs 13#/ft. and comes in 75 foot lengths with integral 3" API male threads on the ends and weighs 138#/length. Total weight of the hydraulic hoses is approximately 15,600 pounds.

7.3 Hose Reels

To assure uninterrupted borer advance, all service hoses must be fed into the hole without interruption. This is best accomplished by using (3) powered hose reels with integral rotary unions capable of handling the required flow and pressure. Reel rotation for hose payout and retrieval is accomplished by means of directly coupled hydraulic torque motors.

Total vertical height of individual reels including reel chassis must be kept under 11 feet; for ease of movement, they will be loaded on a low-bed trailer. Total overall height cannot exceed the Federal Highway Specification of 13' 6". (Figure 30.)

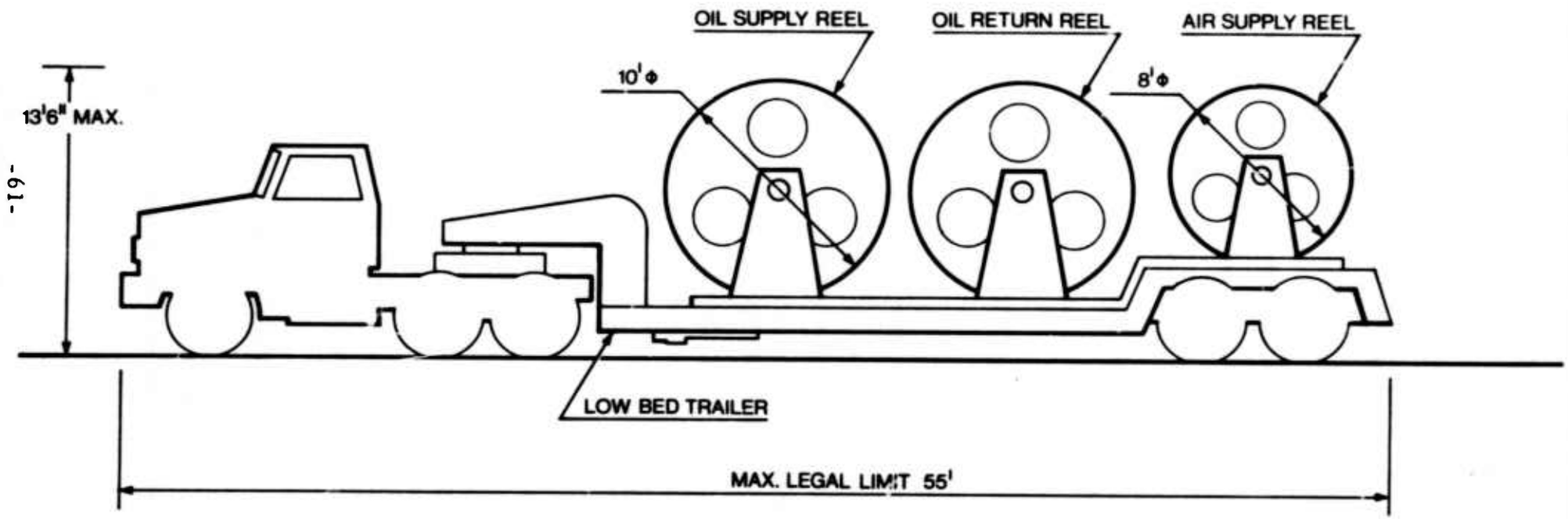

Hose Reel System

Figure 30

Both oil supply and oil return reels will be identical since either must be capable of operating at a pressure of approximately 3,000-4,000 psi and a temperature of 175°F.

The third hose reel will convey the compressed air to the borer at 100 psi and 150°F. Due to the smaller hose diameter of 3.5 inches, the vertical dimensions of the reel will be somewhat smaller.

The estimated total weight of the three reels and reel drive units is 16,000 pounds.

7.4 High Pressure Air Supply

Based on the mucking flow tests, it was determined that approximately 2,000 SCFM of air at a pressure of 100 psi will be required. This flow requirement can be satisfied either by a single Diesel driven portable compressor system or dual positive displacement compressors manifolded together. The most common portable Diesel compressors are 900 SCFM and 1200 SCFM units, manufactured by Chicago Pneumatic, Ingersol-Rand, Joy, and others. It is expected that these compressors with the specified air delivery can be rented at the test location with little difficulty.

7.5 Flexible Exhaust Line for Cuttings

The exhaust line carrying the cutting to the surface will be in 50 foot lengths that are threaded together. This should eliminate the need for any takeup reels and provides more flexibility. An abrasion resistant hose similar to the 6 inch I.D. Hewitt Crete King hose with swagged on end fittings will be required.

7.6 Vacuum Blower and Dust Separator

A Diesel driven rotary blower equivalent to a series #3200 Sutorbuilt model can be used to power the vacuum system. In addition,

a cyclone type separator like those made for the AEC will be required to remove the drill cuttings and dust particles before the incoming air reaches the blow intake. Blower models of similar performance (300 CFM at 22 inches of mercury) and in various stages of repair are available from equipment storage yards belonging to the Atomic Energy Commission and the U. S. Bureau of Mines. In all probability, this equipment could be made available on a Government-furnished basis. During the next program phase a study of available Government equipment should be made. A considerable reduction in testing costs could be made if a suitable piece of equipment could be obtained from the Government.

7.7 Derrick Lifting System

A lifting unit is needed to place the conical borer over the intended hole location and to retrieve it for inspection and servicing. This unit must have a clear vertical span of at least 30 feet, measured from the top most position on the load hook. Means for guiding the borer along the vertical tower must also be provided. (Figure 31.)

The winching system must allow for controlled lowering and hoisting of a 30,000 lb. load (borer + hose + cable) at speeds up to approximately 200 to 300 ft/min. All service lines, such as oil in, oil out, air in and vacuum air return should be vertically supported by the wire rope via star-shaped, quick disconnect clamps spaced every 50 feet.

For operating convenience the derrick together with the cable winch and hoisting system should be mounted on a four-axle truck chassis. Outrigger jacks will provide the necessary stability. It appears the commercially available units, such as Warner Swasey 8425 would be suitable for this requirement.

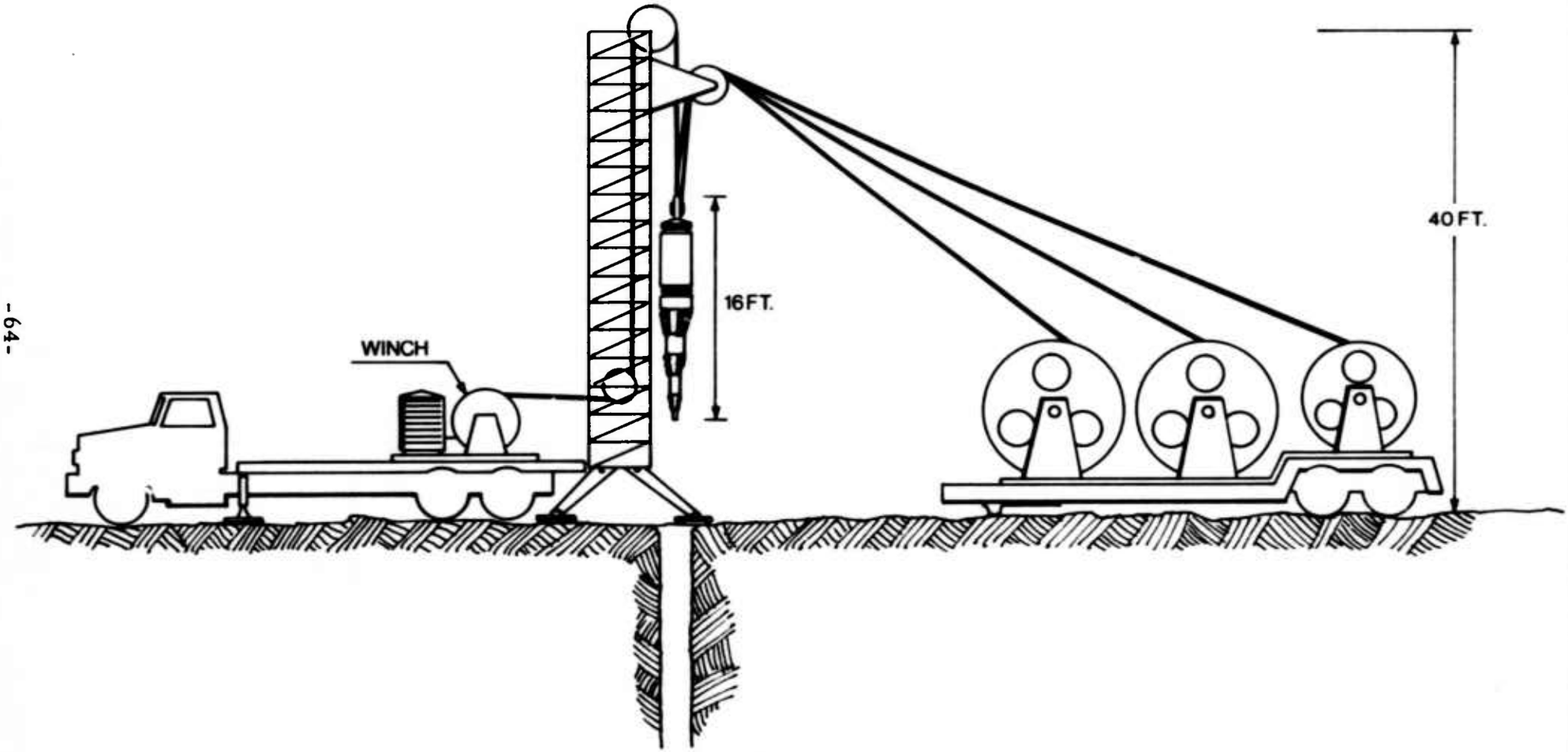

Derrick Lifting System

Figure 31

7.8 Equipment for Drilling Pilot Hole

The unit requires an 8 3/4" pilot hole. A mobile drill unit, similar in capability to a Bucyrus-Erie 40-R or 45-R will be satisfactory.

7.9 Starting Procedure

In order to start the borer, the pilot hole will be reamed to a diameter of 30 inches to a depth of 9 feet. The borer can then be lowered into the hole and the third stage powered cutters engaged.

7.10 In Summary

In summary it should be noted that the operational depth of the borer is currently limited only the the length (and cost) of the hydraulic lines. Obviously, at some greater depth it will be necessary to provide more hydraulic capacity and more mucking system air power to overcome frictional losses in the lines. No other apparent physical factors appear to limit the maximum hole depth (or hole diameter for that matter) possible with a conical borer.

8. Conclusions and Recommendations

The major conclusions and results of this program are as follow:

1. The experimental program confirmed again the main advantage claimed for the conical borer; i.e., that it will require significantly reduced thrust loads (less than 10 percent) than conventional roller cutter bits of the same diameter and at the same penetration rate.

2. The cutter refinement conducted under this effort successfully reduced the required borer thrust loads below those obtained in previous testing.

3. The specific energy required for rock fragmentation was reduced to a level only 13 percent greater than for highly developed tri-cone cutters.

4. A practical mucking system was designed and successfully tested. In addition, parametric design relations for predicting the performance of any borer were developed and experimentally verified.

5. Design of the borer was completed. A complete drawing package for fabrication was prepared. The structural integrity and bearing life was analyzed and found to be satisfactory.

6. The ground equipment required for field testing was delineated and investigated. The most expensive item required will be the hydraulic lines and their carrier reels.

Based on these results, it is recommended that a program be undertaken to fabricate and test the unit designed in this program.

To most efficiently accomplish this effort, it is further recommended that efforts be undertaken to

a) Locate and arrange for the use of available Government equipment for the test program.

b) Delineate and evaluate possible test sites.

A judicious selection of the surface support equipment and the test site could result in a significant reduction in the cost of the test program.

BIBLIOGRAPHY

1. Foster-Miller Associates, Inc., "Design, Fabricate and Test A Conical Borer," Final Technical Report on Contract HO210044. Available from National Technical Information Service, Springfield, Virginia, AD-744989, March 1972, 55 pp.

2. DerMarderosian, Dikrum and Hug, Hans A., "Design and Development of a Conical Boring Device to Enlarge a Pilot Hole Through Rock," Semiannual Technical Report on Contract H)220076. Available from National Technical Information Service, Springfield, Virginia, AD-751565, September 1972, 81 pp.

APPENDIX A

THE CONICAL BORER PRINCIPLE

A.1 Simple Conical Geometry

The operating principle of the conical borer is best illustrated in terms of a simple conical roller-cone bit. It must be noted that such a bit would not be practical, at least in a self-advancing form, but this has no bearing on the principle of operation. Let us compare a conventional bit that cuts a flat bottom hole with a bit of the same diameter that cuts a conical hole.

The conventional bit, shown in Figure A-1a, experiences a distributed line load, F_n' pounds per inch, along the rolling contact of each cone. Load distribution is assumed constant along the line length for convenience in illustration only. Since there are three rollers, the total roller length is $\frac{3}{2}d$, and the thrust required to generate the loading is simply

$$T_{90} = \frac{3}{2} d \; F_n' \qquad (A-1)$$

where the subscript 90 signifies a 90° hole-bottom half angle (flat bottom).

Consider next the three-roller conical bit of Figure A-1b, loaded to the same line load F_n', and having the same tooth geometry but at a half angle α. Simple statics indicates that, whatever the angle α, the thrust to generate this load remains

$$T_\alpha = \frac{3}{2} d \; F_n' \qquad (A-2)$$

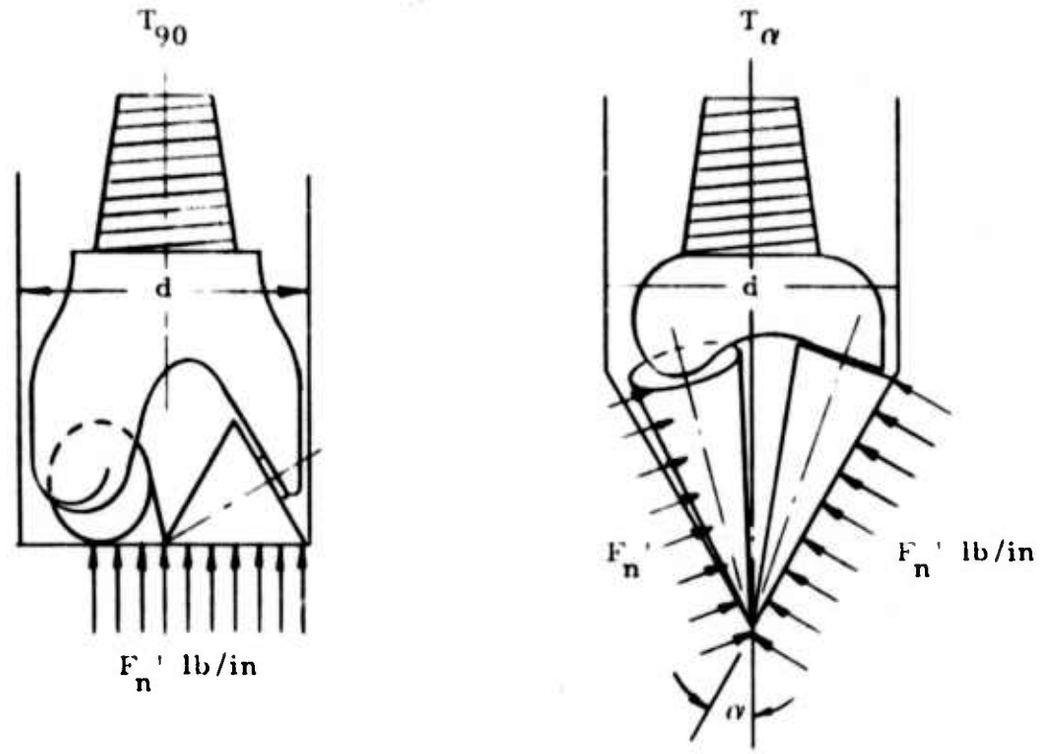

(a) Flat-bottomed (90 deg) Bit (b) Conical (α) Bit

Flat and Conical Bit Comparison

Figure A-1

Thus there has been no thrust reduction. However, if we examine a representative unit length of cutter at the same bore radius on each of the bits, they are essentially identical, with the same tooth geometry and load. The slight rock surface curvature of the conical bit should have no influence on fragmentation behavior except, perhaps, very near the tip. Hence, in one revolution, a unit length of conical bit roller should fragment the same quantity of rock as a unit length at the same mean radius on the conventional bit. But the conical bit contains more cutter length, in the ratio $\frac{1}{\sin \alpha}$, and hence will advance faster in this same ratio. Conversely, if we wish to advance at the same rate as the conventional bit, the required load can be reduced. With the usual assumption that, with good cleaning, penetration per revolution is proportional to cutter load per inch, the thrust can be reduced in inverse proportion to the ratio of cutter lengths. Thus, in comparing the performance of conventional and conical bits run at the same speed, we can write the following relationships for advance rate, R, and thrust, T:

$$R_\alpha = \frac{1}{\sin \alpha} R_{90} \quad \text{at constant T} \tag{A-3}$$

$$T_\alpha = \sin \alpha \; T_{90} \quad \text{at constant R} \tag{A-4}$$

In passing we note that Figure A-1b illustrates the impracticality of simple conical bits, i.e., the impossible bearing and stress situation presented by long, thin, cantilever-mounted rollers. This is certainly true for smallα as would be required for self advancement (see Section A. 3), but it is possible that, with sufficient development, simple bits could be constructed to approximately halve the thrust required by conventional bits. Thus the self-advancing borer, the subject of this effort, is presently

considered as a reaming device.

A.2 The Helical Cutter Path

The simple description of Section A.1 is based upon an examination of a normal force at the cutter-rock interface. There is, in addition, a rolling force which requires the application of torque to rotate the bit and through which energy is transmitted to fragment the rock. In addition to these well-known forces, there may be a side force on the cutter, depending upon whether the cutter is or is not in pure rolling contact with the rock.

For simplicity, let us consider the motion of a single row of cutter teeth on one roller, as shown in Figure A-2. As the bit rotates and advances, the locus of the cutter-rock contact point is not a simple circle but is a helix as shown for greatly exaggerated advance per revolution. If the roller is to follow this helix in pure rolling contact, clearly it must be tilted or skewed forward to the helix angle, β_o. If the cutter is not skewed, the axial component of its motion will be accomplished by skidding, and accompanied by a side force on the cutter, as shown in Figure A-3a. This side force has an axial component which would be undesirable in that it would require the application of additional thrust to cause bit advance. Skewed to β_o, the cutter would experience pure rolling and the simple situation of Figure A-2, shown again in Figure A-3b would prevail. If, now, the cutter can be skewed beyond the advance helix angle β_o, as shown by Figure A-3c, the cutter teeth will experience a rearward skidding motion as they contact the rock.

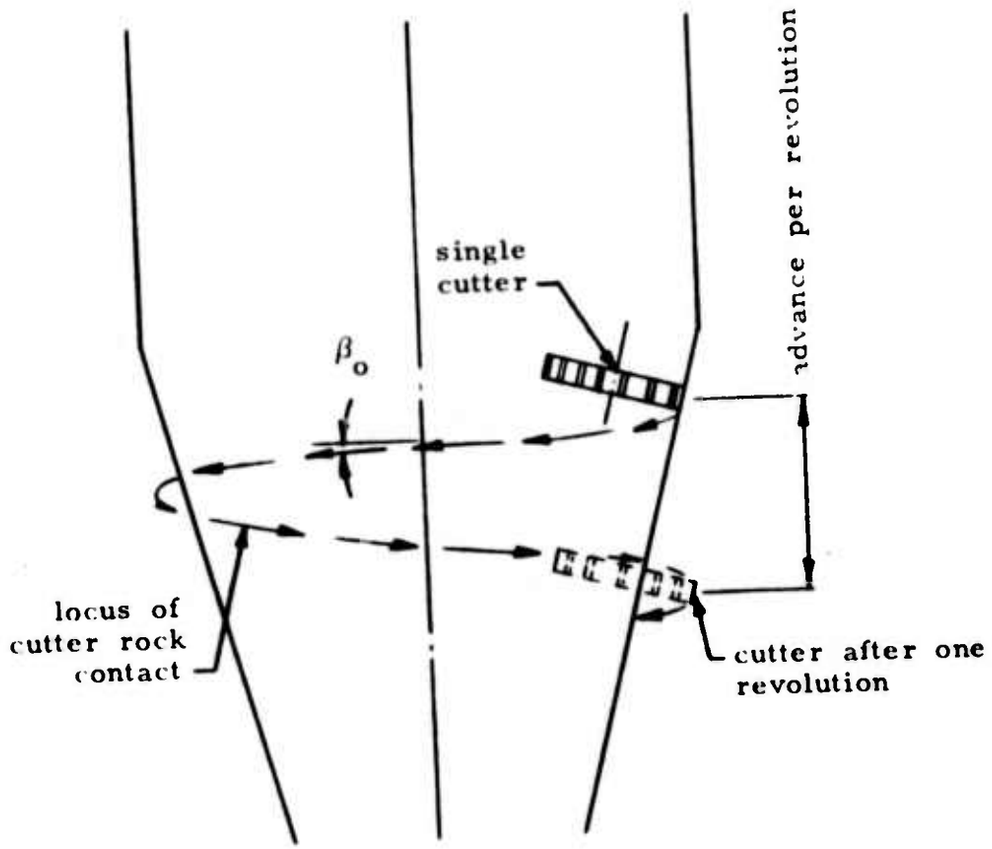

Helical Cutter Element Advance

Figure A-2

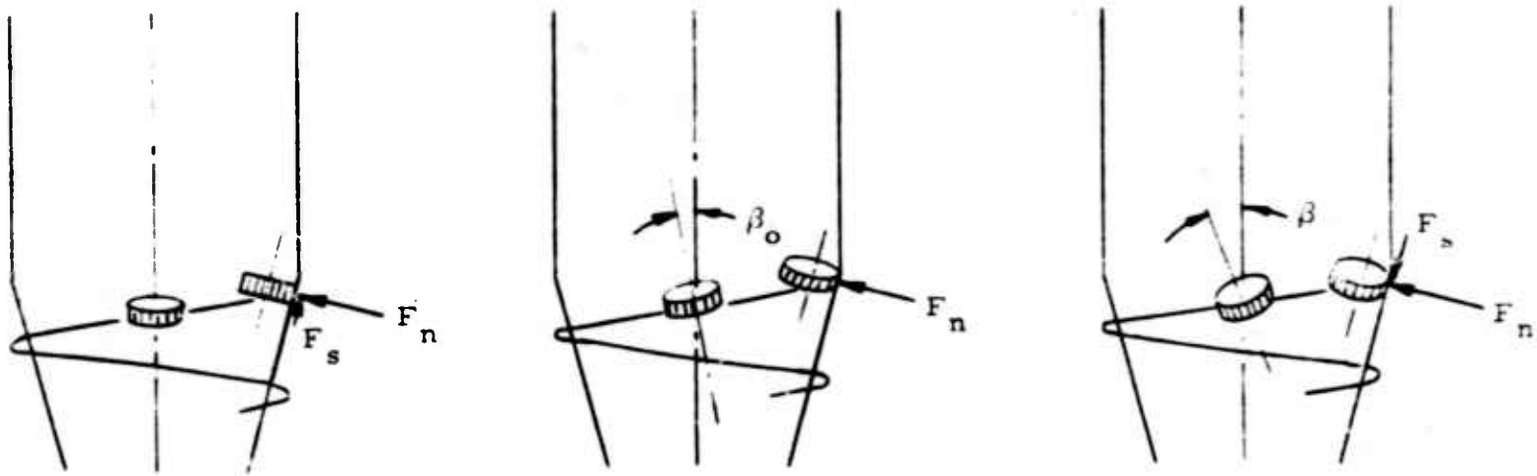

(a) No Skew
$\beta = 0$

(b) Neutral Skew
$\beta = \beta_o$

(c) Forward Skew
$\beta > \beta_o$

Skewed Cutter Geometries and Forces

Figure A-3

Qualitatively, the cutters attempt to roll ahead of the advance helix and, in so doing, they develop a side force which assists, rather than hinders, the advance of the bit. The action is somewhat like that of a screw, but not precisely in that the side force in question is frictional in origin and in no way dependent upon the cutter following a prescribed path.

For any reasonable advance per revolution, the angle β_o is very small except very near the tip of the hole. At the tip, β_o is equal to 90°. However, as stated previously, there are stress considerations which make the tip of the conical hole inaccessible anyway. In addition, a skewed roller of finite length geometrically cannot reach the center of the hole. For a reaming device of moderate advance rate as proposed here, β_o is very small (less than typical machining tolerances). Its variation over the length of the borer is of no consequence because all cutters will be skewed to angles substantially greater than β_o in order to achieve self-advancement.

A.3 Skewed Cutter Forces and Self-Advancement

Skewed cutters have been used on conventional bits for some time, particularly on those for soft and medium rock. In such applications, the teeth are said to display a "gouging and scraping" action which considerably enhances penetration rate. For a conventional bit the existence of a side force on skewed cutters is of no overall consequence, since such forces are radial and self-canceling (although, of course, they do affect individual cutter bearing loads).

The beneficial effect of cutter side force is of major concern in the operation of the proposed conical borer. For, if the side force is large enough, or if the hole-bottom angle is small enough, the borer can be made self-advancing, that is, no external thrust will be required.

The desired condition is very simply shown in Figure A-4. Considering any one cutter-rock contact point, no external axial force will be required if the axial component of the side force, F_s, can be made equal to or greater than the axial component of the much larger normal force F_n. That is,

$$F_s \cos \alpha \geq F_n \sin \alpha \qquad (A-5)$$

or

$$\frac{F_s}{F_n} \geq \tan \alpha \qquad (A-6)$$

In this formulation, as in actual behavior, the action of the self-advancing borer is analogous to that of more conventional devices wherein α is the "friction angle" below which a member will not slip, and F_s/F_n is the coefficient of friction. The conical borer is, however, self-advancing rather than simply self-locking, because the rollers permit rotation even though the borer is axially locked by the side forces on the cutting teeth.

The kinematics of skewed cutter motion and the accompanying forces are best seen in terms of linear rolling over a plane rock

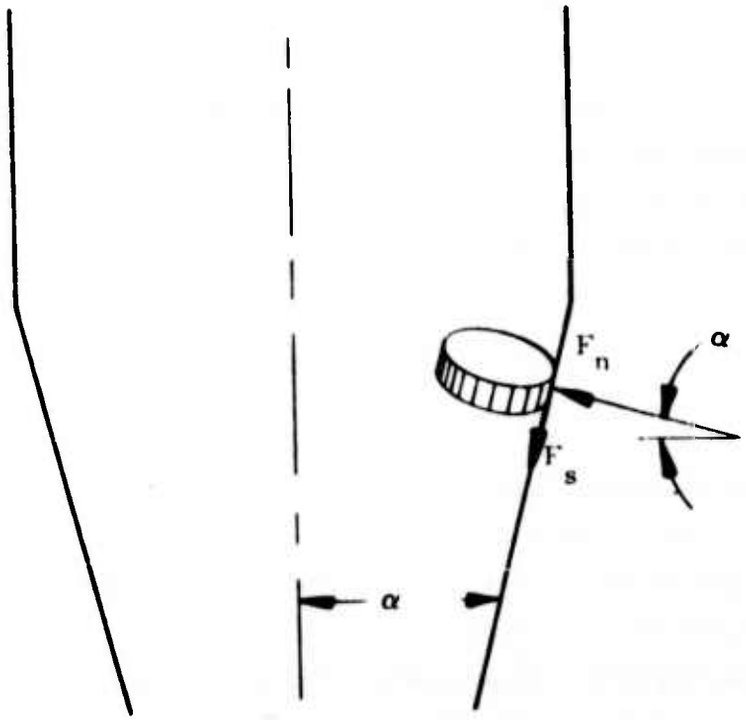

Rock-forces on Skewed Cutter for Self-Advancing Action

Figure A-4

sample. Tests of this type have been performed* and the available data are sufficient to permit the design of a prototype, self-advancing conical borer. Single row cutters of conventional tooth size and shape were rolled over a variety of rock specimens as shown in Figure A-5. Normal force, F_n, side force, F_s, and rolling force, F_r, were measured separately and correlated for a variety of skew angles, cutter penetrations, cutter diameters, and rock types. "Sharp" and "dull" teeth were included in the study. In terms of the important force ratio, F_s/F_n, the data indicate useful side force ratios at moderate (4°) skew angles, with little or no variation with rock type or the "dullness" of the teeth. A slight decrease of F_s/F_n with increasing penetration is noted, which is of benefit in the stable operation of the conical borer (see Section A.4).

The kinematics of individual tooth penetration and the origin of the cutter side force are shown in Figure A-6 for a plane surface. The "footprint" of the tooth is shown for several subsequent positions as seen by an observer riding with the cutter. It can be seen that the tooth initially contacts the rock surface at a position laterally displaced in the direction of the skew from that when the tooth is at maximum penetration. In tests, the side-slip of the tooth appeared to be approximately parallel to the long dimension of the footprint. This motion generates a side force on the tooth, tending to resist the side-slip in a manner which is believed to be frictional. Side-slip continues beyond maximum penetration, of course, but the tooth is unloaded in this region and little side force will result. In transferring these sketches to the

---

* Peterson, C.R., "Rolling Cutter Forces", Paper No. SPE 2393, Society of Petroleum Engineering of AIME, also published in Society of Petroleum Engineering Journal, March, 1970.

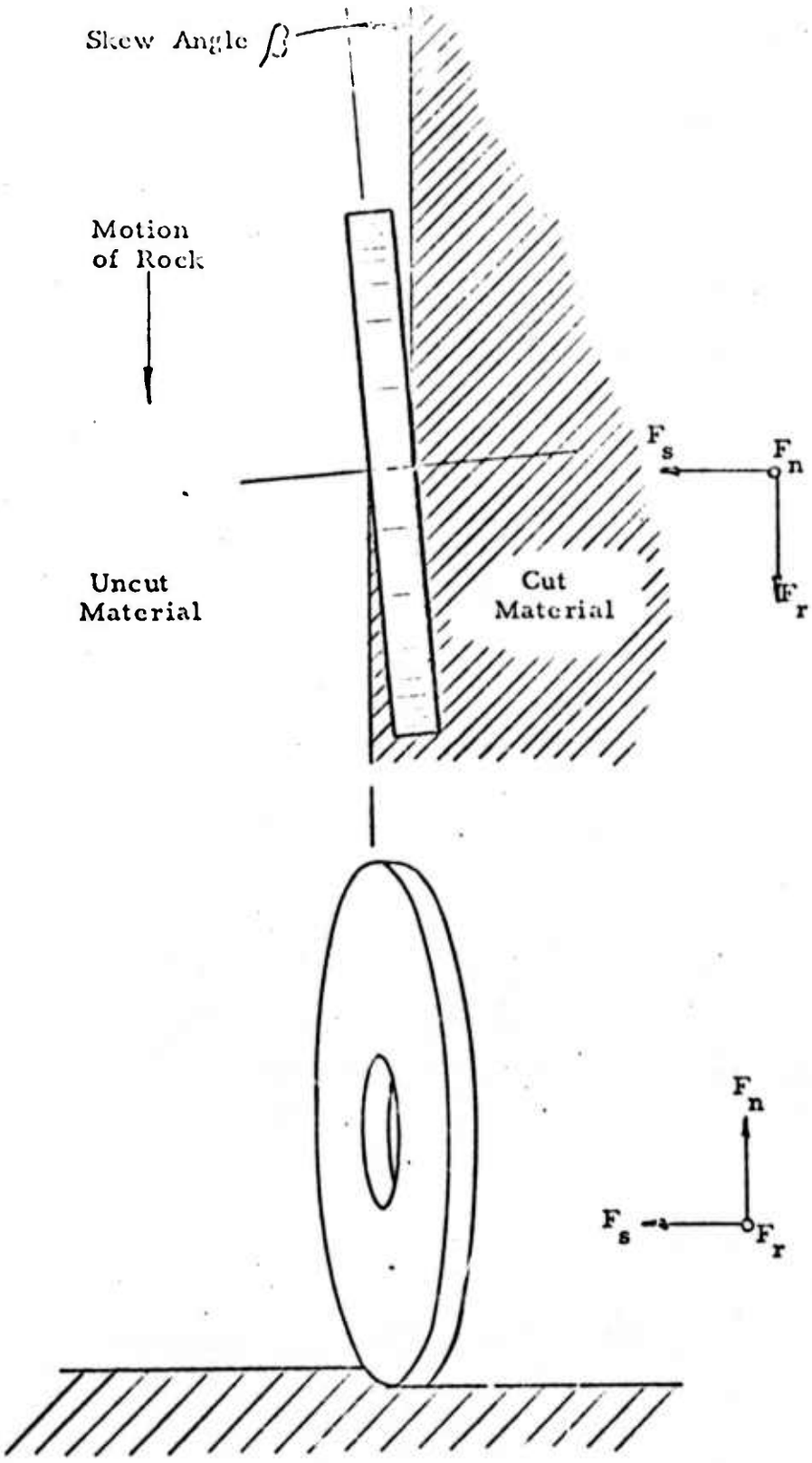

Plan View of Cutter on Rock

(Forces Defined are Forces on Cutter)

Figure A-5

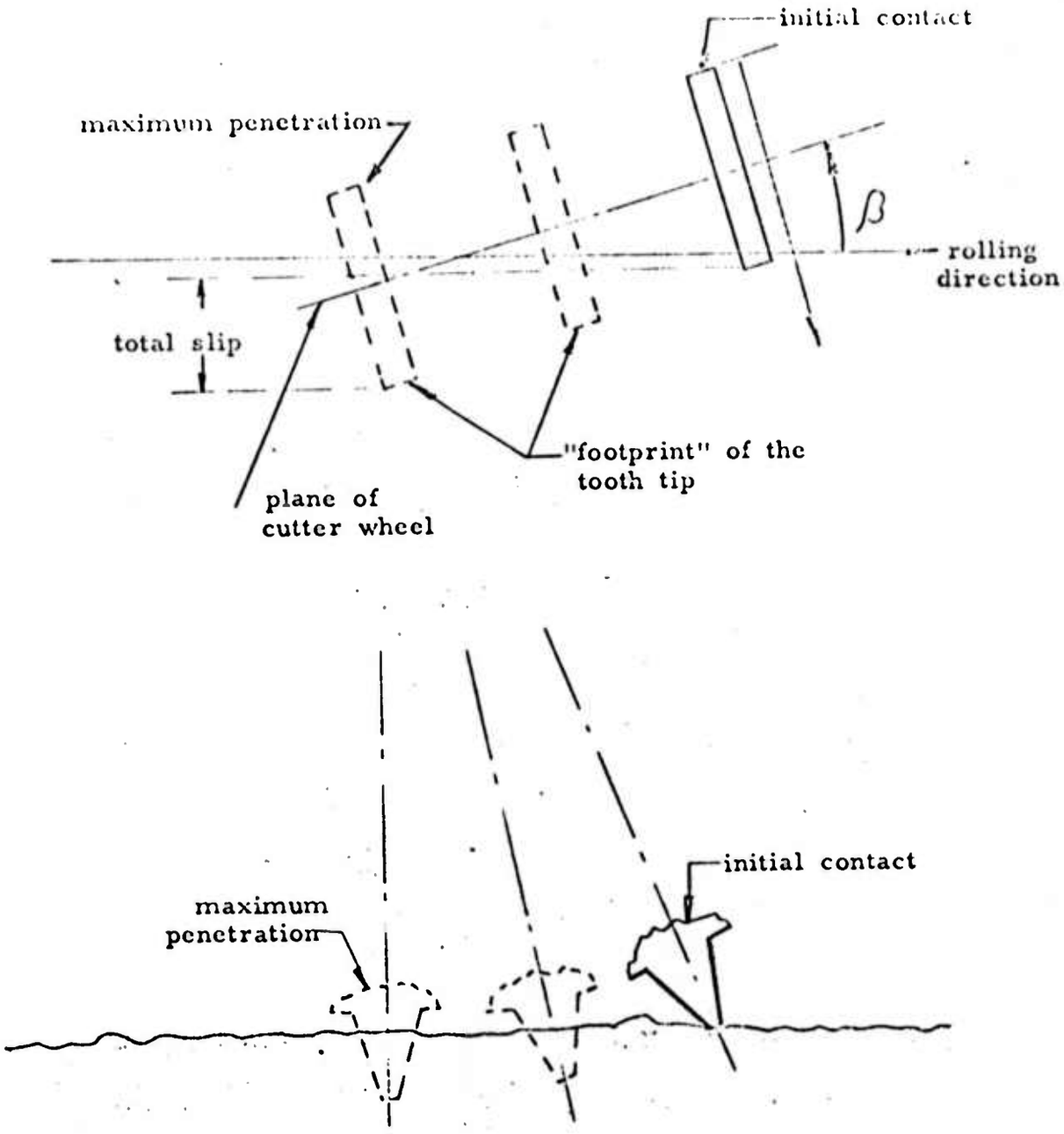

Skewed Cutter Penetration Geometry

Figure A-6

conical geometry, the top of the page corresponds to the apex of the cone; hence the tooth slip is toward the base of the cone. It is important to note that in the performance of these tests and in the operation of a self-advancing borer, the side-slip is actually present at all times. The action is not dependent upon the precarious maintenance of an impending slip.

Typical data indicate a side-to-normal force ratio of approximately 0.2 at a skew of 4°. From Equation A-6, then a self-advancing borer of this skew would require a hole-bottom angle, α, of about 11°.

Greater skew angles generate greater F_s/F_n. This would permit greater hole-bottom angles and, hence, shorter borers. On the other hand, greater skew also contributes to more rapid tooth wear. Commercial applications of the conical borer would necessitate an optimization of the relationship between skew angle and tooth life, probably through rather extensive field testing and design evolution. However, considerable tooth life can be expected at 4° skew and the prototype would be constructed at approximately that angle.

While the cited data provide a preliminary design choice, there remain some uncertainties which suggest that the proposed borer development program should include some testing of simple components before the more complex components are constructed. For example, the ratio F_s/F_n is somewhat dependent on the ratio of cutter diameter to penetration. As can be seen from Figure A-6, a tooth on a larger diameter roller, at a given penetration and skew angle, would experience a greater arc length of contact

and distance of side-slip, and would generate a larger side force. Similarly, if the rock surface were concave, as it would be in the conical borer, each tooth would again experience a greater side-slip. That is, self-advancing conditions in a conical hole will be somewhat easier to realize than the flat surface data would indicate. Finally, in a vertically downward boring application, one can use the weight of the borer to assist penetration.

The self-advancing condition depends on the ratio of side-to-normal force, and not on the magnitude of the side force. Tests to date have shown that this ratio is quite independent of the rock hardness. Hence, each row of cutter teeth, if skewed properly, will provide its own necessary side force regardless of local rock conditions. Therefore, the complete borer will be insensitive to extreme inhomogeneity in rock properties over the length of the borer.

A.4 Stability of Self-Advancement

The observed behavior that F_s/F_n decreases with increasing penetration contributes to the stable operation of the conical borer. Once the borer geometry is is fixed in terms of cone angle, skew angle, and tooth geometry, its advance behavior is fixed. Suppose that the actual F_s/F_n is greater than the designer anticipated at the design penetration (as it may well be on a concave surface). The resultant force on the cutting teeth will then have a forward component, and the borer will pull itself in to greater penetrations. Greater penetration will, of course, generate greater forces and require greater cutter torque. However, provided the borer does not stall or break first, as it cuts deeper the ratio F_s/F_n will decrease. Furthermore, the helix advance angle, β_o, will increase so that the effective skew, $\beta - \beta_o$, will decrease.

Thus, stable operation will be found at some greater penetration. The major design task is clearly to avoid a geometry which stalls or breaks before this stable operation is reached. Design variations to achieve the desired performance are clear cut, but, at present, preliminary testing of borer components is indicated to assure proper performance.

A. 5 Self-Rotating Drive

The conical borer was first conceived to reduce or eliminate the need for external thrust. As an added benefit, the much greater total roller length of the conical borer permits the simultaneous attack of a much greater quantity of rock and, hence, a proportionately greater advance rate. Since the basic rock fragmentation mechanism has not been changed, the power input and torque would also be proportionately greater. The permitted advance rate increase, therefore, would require a torque increase which might be inconvenient or impossible.

An analogy might help to illustrate this point. Consider an ordinary twist drill, as used for metal. The tip of such drills is slightly conical in shape. A more acute tip would permit metal cutting over a larger face and would result in a greater advance rate (thrust and speed being equal). But, even if tip stress problems could be overcome, such operation would not be desirable simply because the drill body cannot transmit the required torque.

Excess torque requirements can be eliminated by simply driving individual rollers. In fact, the need for external torque is completely eliminated by driving rollers from frame-mounted motors. This self-rotating drive is no different from that of any conventional, self-propelled wheeled vehicle in linear motion. The concept is most easily visualized in terms of small, individually-driven rollers on a large frame, such as shown in Figure A-7.

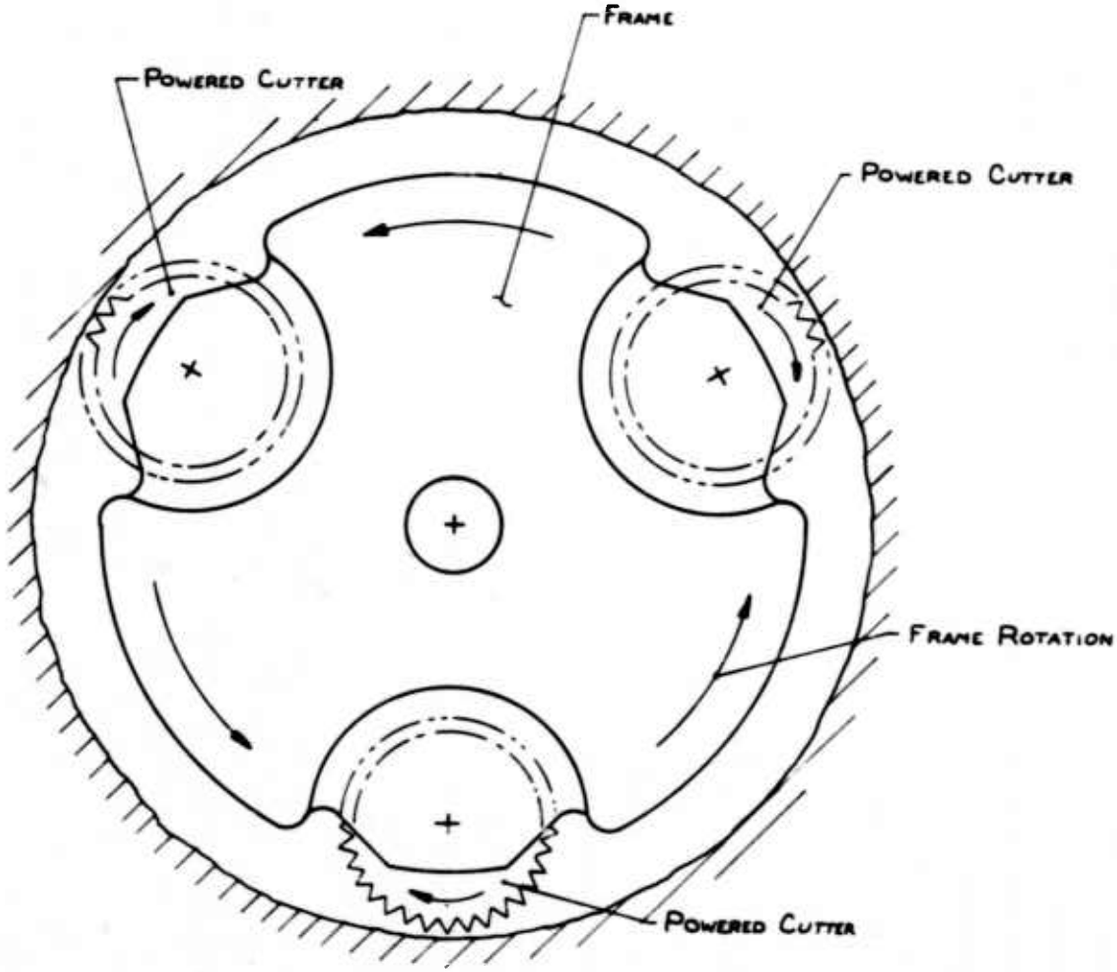

Torqueless Rotary Drive from Frame-Mounted Motors

Figure A-7

The concept of driven rollers is not new, although their use on a conical borer might be. The conical hole shape, in fact, lends itself to driven-roller drive because of the relatively small angle between roller and hole axes.

In addition to avoiding a possibly excessive torque requirement, a self-rotating drive has other advantages. Since neither external thrust nor torque need be provided, the boring unit can be simply suspended in the hole on a cable. Power and cleaning air or liquid can be supplied via flexible lines connected through suitable slip rings or rotary unions. Cuttings return can also be done in a non-rotating flexible line or by a number of other methods. Thus, the entire suspension and communication system can be simply reeled in and out of the hole, with no need for rigid drill pipe, massive surface rotary drive, or excessively high hoist equipment. This, of course, is ideally suited to applications requiring lightweight, highly portable equipment. But beyond this special circumstance, the concept of a boring system without drill pipe has been the dream of practically every deep-hole borer.

A.5 Summary of the Conical Bit Concept

The conical borer operates somewhat like a screw as it rotates and advances into the rock, although this analogy is not entirely correct. The borer uses a "wedging" action to replace the very large axial force requirement of conventional machines by an array of equally large (or even larger) radial forces. Individual roller cutter forces, normal to the conical rock surface, are nearly radial. Considered together the radial components of these forces are self-canceling and, in this sense, "free". The relatively small axial component can be canceled if individual cutters are skewed to develop a frictional side force. This action, which has been successfully demonstrated, is essentially independent of rock properties so that each individual cutter provides its own axial force.

Overall borer behavior is the same for all rock types (all that can be bored by roller cutters) and the device would tolerate extreme variations in rock properties over the length of the borer head.

The most notable, or perhaps even spectacular, characteristic of the conical borer is of course self-advancement. However, further advantages are gained largely because the conical shape provides more room adjacent to the hole bottom. This means more room for cutter teeth, more room for bearings, and more room for cuttings removal. More cutter teeth permit higher power inputs and greater penetration rates (still without thrust) or, conversely, if cutter teeth are not increased, conventional penetration rates are attained at decreased cutter loading. This plus more bearing room means greater bearing life. In fact, the overall machine configuration permits the designer to insert virtually as much bearing capacity as he desires by simply using more rollers of shorter individual length. More room permits freedom to direct cuttings flow as desired or, even without this benefit, decreased cuttings density on bottom. For example, the proposed machine at a given penetration rate and without improved cuttings flow would have only one-quarter the hole-bottom cuttings density of a conventional bit.

In fundamental terms the proposed conical borer promises to eliminate the major obstacles to present mechanical borer advance rate: that is, limited power input as limited in turn by excessive thrust requirement and/or excessive cutter bearing loads; and a limitation imposed by poor cuttings removal.

In specific terms, the following advantages can be cited for the conical borer in comparison to conventional borers:

(1) No external thrust required

(2) No external torque required

(3) High power density, hence high penetration rate. Longer bearing life.

(4) Heavy loads confined to one compact, rugged element

(5) Good cuttings removal. Low total weight

(6) Overall system simplicity

(7) Negligible vertical load on rock

These features add up to a simply, high-speed, lightweight, highly portable, economical boring system.

APPENDIX B

ANALYSIS OF THE BORER MUCKING SYSTEM

The proposed mucking system has been analyzed on the basis of the system model shown in Figure B-1. Air is used as the working fluid in a combination pressure-vacuum system.

The pneumatic transport system has been divided into three discrete areas to facilitate the analysis:

1. air-cuttings flow up the discharge pipe
2. distribution of air in the borer and around the cutting faces
3. down flow of clean air under pressure.

B. 1 Discharge Pipe Analyses

The calculations for pressure loss in the return duct were based on incompressible flow relationships and atmospheric pressure at the inlet to the return duct. From Zenz,* the relationship for pressure drop ΔP, in a vertical pipe is given by

$$\Delta P = \frac{v_a^2 \rho_a}{2g} + \frac{W v_p}{g} + \frac{2f \rho_a v_a^2 L}{gD} \left[1 + \frac{f_p v_p}{f v_a}\right] \frac{W}{v_a \rho_a} + \frac{W L}{v_p} \qquad \text{(B-1)}$$

*Zenz. F. A., et. al., "Fluidization and Fluid-Particle Systems", Reinhold Publishing Corporation, New York, Chapter 11.

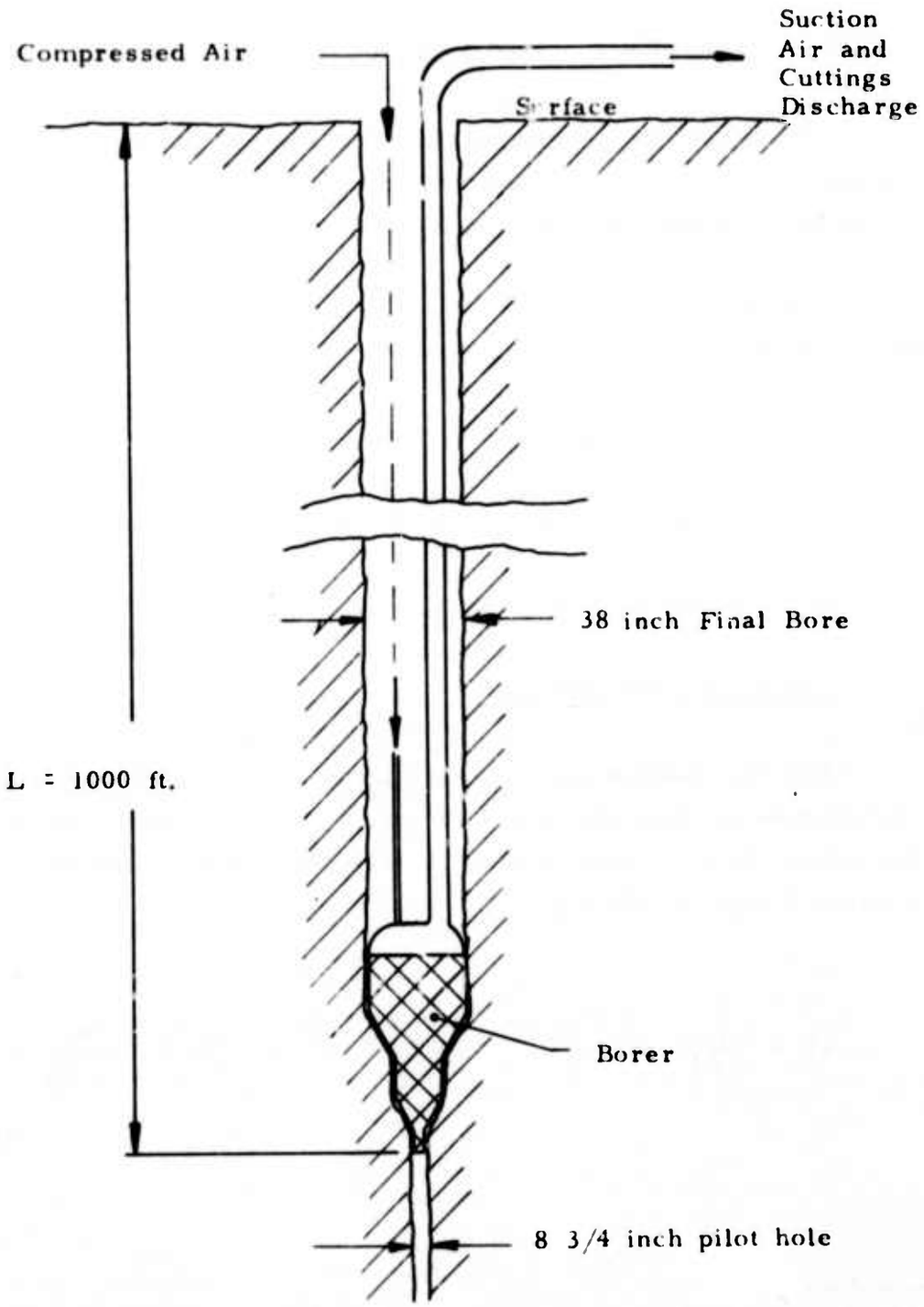

Schematic of Pneumatic Transport System

Figure B-1

where

v_a = velocity of the transporting air

ρ_a = density of the transporting air

g = gravity constant

W = solids mass flow rate

v_p = particle transport velocity

f = Fanning pipe friction factor

L = tube length

D = tube diameter

f_p = fluid to solids friction loss in conveying

Particle transport velocity, v_p, is the difference between the air velocity, v_a, and the particle terminal velocity in air, v_t, where,

$$v_p = v_a - v_t \tag{B-2}$$

Rewriting the pressure drop relation using the above expression yields,

$$\Delta P = \frac{v_a^2 \rho_a}{2g} + \frac{W(v_a - v_t)}{g} + \frac{2f \rho_a v_a^2 L}{gD} \left[1 + \frac{f_p (v_a - v_t) W}{f v_a^2 \rho_a} + \frac{WL}{(v_a - v_t)} \right] \tag{B-3}$$

According to Zenz the fluid to solids friction loss factor may be determined from,

$$f_p = \frac{3 \rho_a C_d D}{2 \rho_p d_p} \left(\frac{v_t}{v_a - v_t} \right)^2 \qquad \text{(B-4)}$$

where:

C_d = drag coefficient

ρ_p = density of the particle

d_p = diameter of the particle.

As recommended by Hinkle*, the factor

$$\frac{f_p (v_a - v_t)}{f v_a} = 1 \qquad \text{(B-5)}$$

was used whenever calculations indicated a value greater than unity.

The terminal velocity, v_t, for the cuttings was determined from Figure B-2, which is based on particles of relatively uniform cross-section. Examination of the cuttings produced during the Phase I tests showed (as expected) that the particles were more like flakes rather than uniform cubes or spheres. However, since the particles tend to tumble during transport, we may assume that the area projected to the flow stream would average out to that of a uniform particle of the same weight. Average particle diameters from .065 to .250 inches were used in the analysis.

Based on the previous relationships, computations were made to predict the total pressure drop in the discharge pipe for the following parametric values,

*Hinkle, B. L., Ph. D. thesis, Atlanta, Georgia Institute of Technology (June 1953).

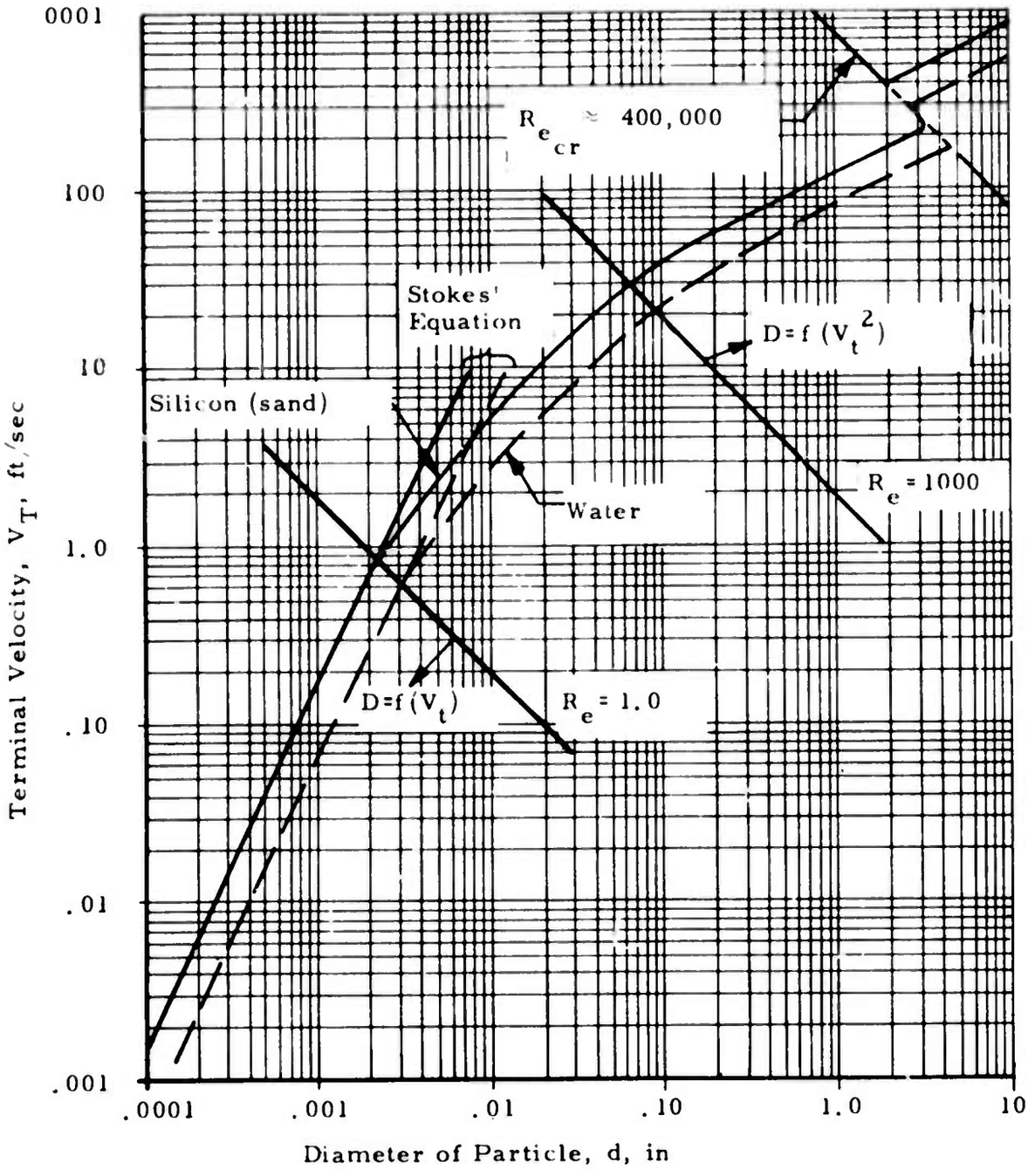

Terminal Velocity of Particles vs. Particle Diameter

Figure B-2

L = 1000 feet

D = 4", 6", 8", 10"

W = lbs/sec = 2.25 lb/sec

f = 0.004, 0.005, 0.006, 0.008, 0.010

v_t = 30, 40, 50, 60 ft/sec

v_a = 50 to 120 ft/sec

ρ_a = 0.075 lb/ft^3

Figure B-3 shows the pressure drop as a function of velocity (based on an 8 inch diameter discharge pipe, 1000 feet long with a friction factor, f = .006) for various particle sizes, i.e., terminal velocities. The curves indicate that the pressure drop would be higher for large particles than for small ones. This is reasonable since the higher terminal velocity means lower transport velocity and hence a larger mass of cuttings in the discharge pipe at any time. For the same reason, the pressure drop for the majority of particle sizes decreases to a minimum at approximately 90 feet per second. Above 90 feet per second the effects of friction predominate and the pressure drop increases.

The proposed transport system will convey a range of particle sizes and the resulting pressure drop will be a function of the net mass loading of the discharge pipe as described above. Assuming an even distribution of particle sizes, by weight, the average terminal velocity would be approximately 45 feet per second. Using V_t = 50 feet per second, the pressure drop vs. air velocity has been plotted for various pipe diameters, as shown in Figure B-4.

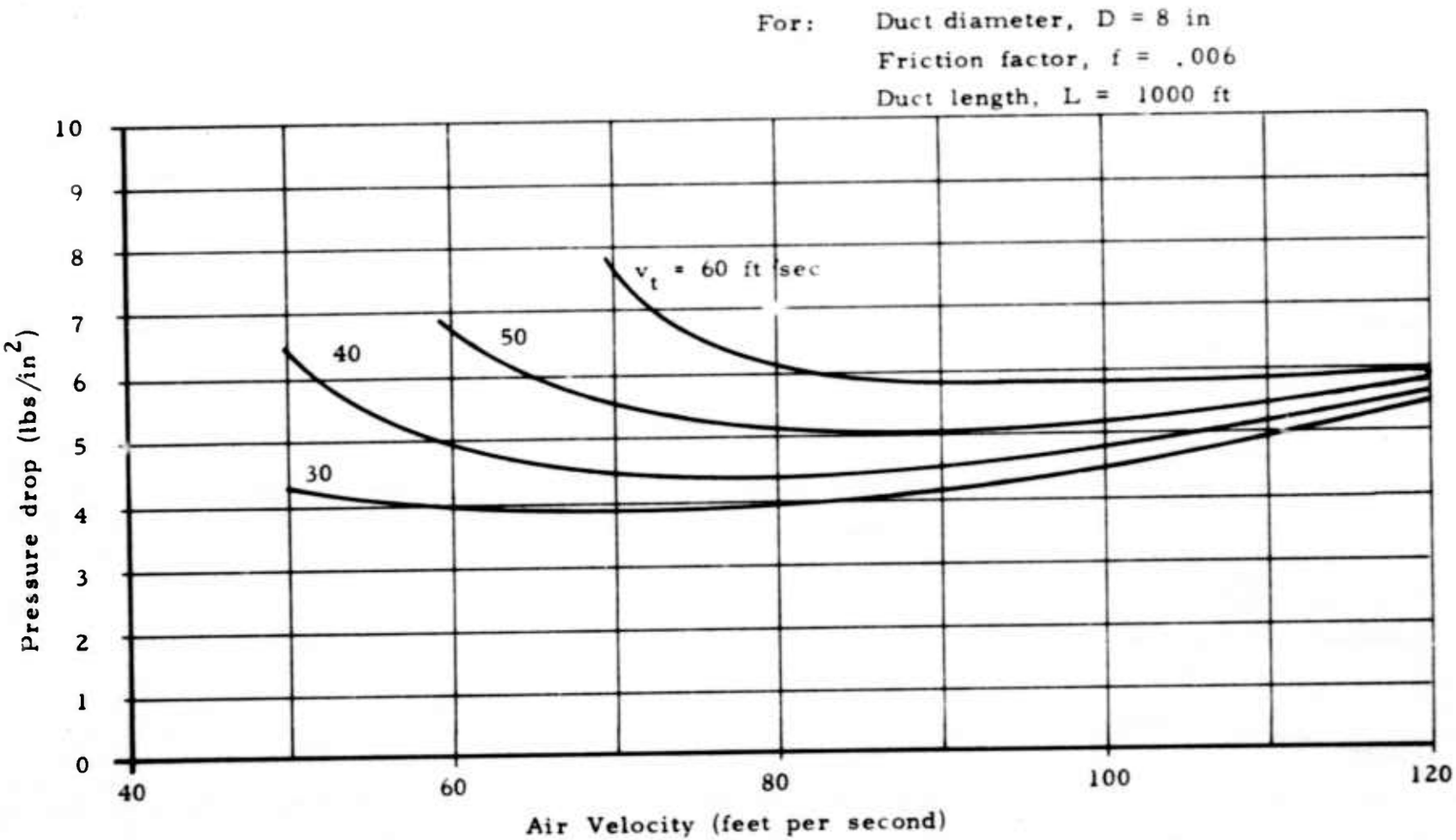

Pressure Drop versus Air Velocity for Various Particle Sizes

Figure B-3

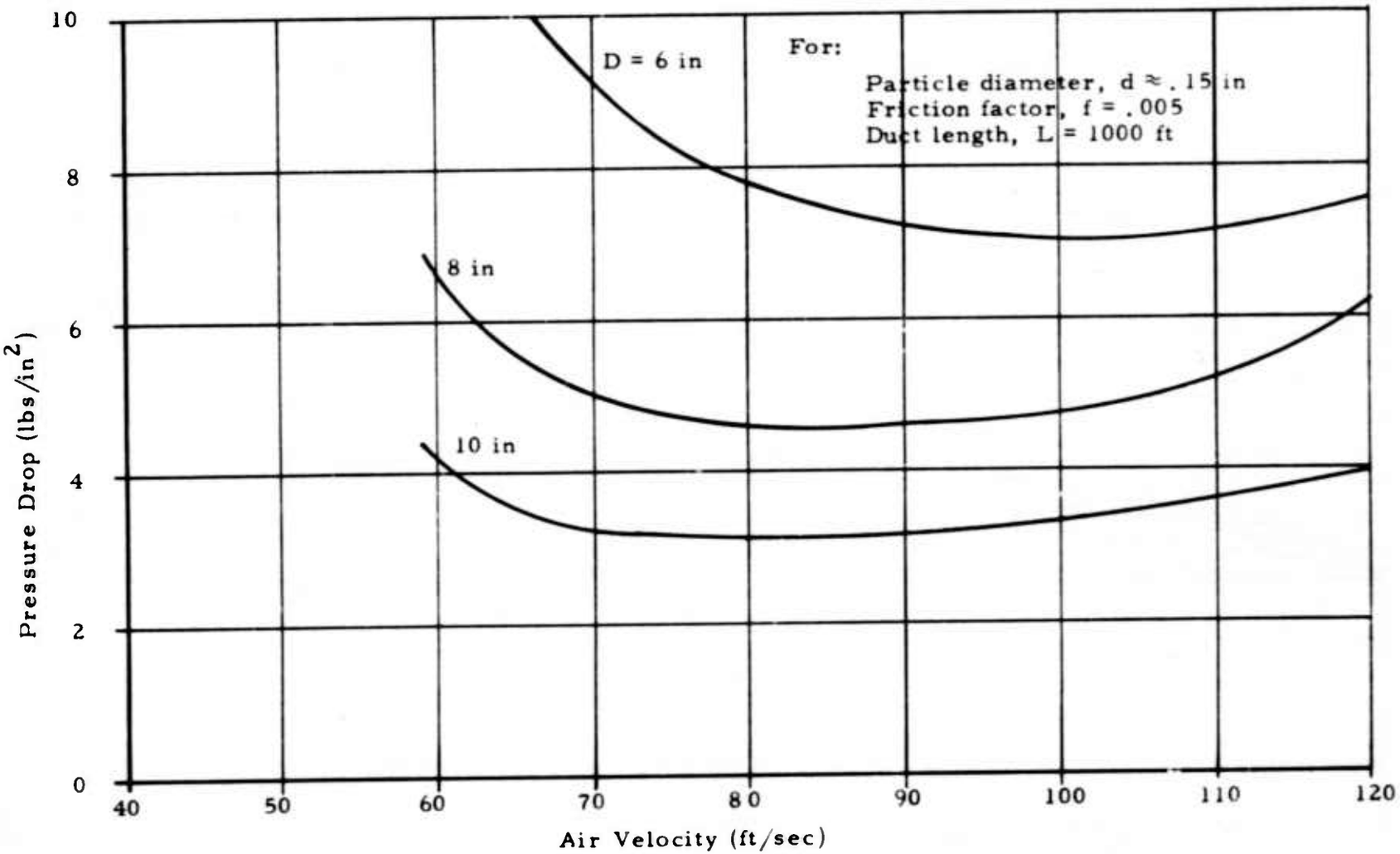

Pressure Drop versus Air Velocity for Various Duct Diameters

Figure B-4

These curves indicate the effect of increasing the diameter of the discharge duct. Since a vacuum system is proposed to supply the required pressure drop, it would be desirable to minimize the pressure drop to whatever extent possible.

The curves of Figure B-4 assume a friction factor typical of standard steel pipe or flexible hose of the type likely to be employed in the application. The inclusion of water in the bore-hole, however, may result in a marked increase in the effective wall roughness due to "cementing" of the cuttings to the duct wall. Figure B-5 shows the variation in pressure drop through the return duct as a function of friction factor. The range of friction factors presented spans the entire range of wall roughnesses which might be encountered. It is not likely for this application, however, that the friction factor will exceed f = 0.008, the value used to compute the intermediate curve.

Among other considerations in sizing the return duct is the power required of the vacuum system. The power requirements have been determined analytically by treating the operating fluid as an ideal gas. The ideal power required to obtain the pressure drops of Figure B-4 was determined using the relationship,

$$P = w\, c_p\, T_1 \left(\frac{T_2}{T_1} - 1 \right) \qquad \text{(B-6)}$$

where,

P = ideal power

w = mass rate of air flow

c_p = specific heat of air at constant pressure

T_1 = temperature of inlet to blower

T_2 = outlet temperature

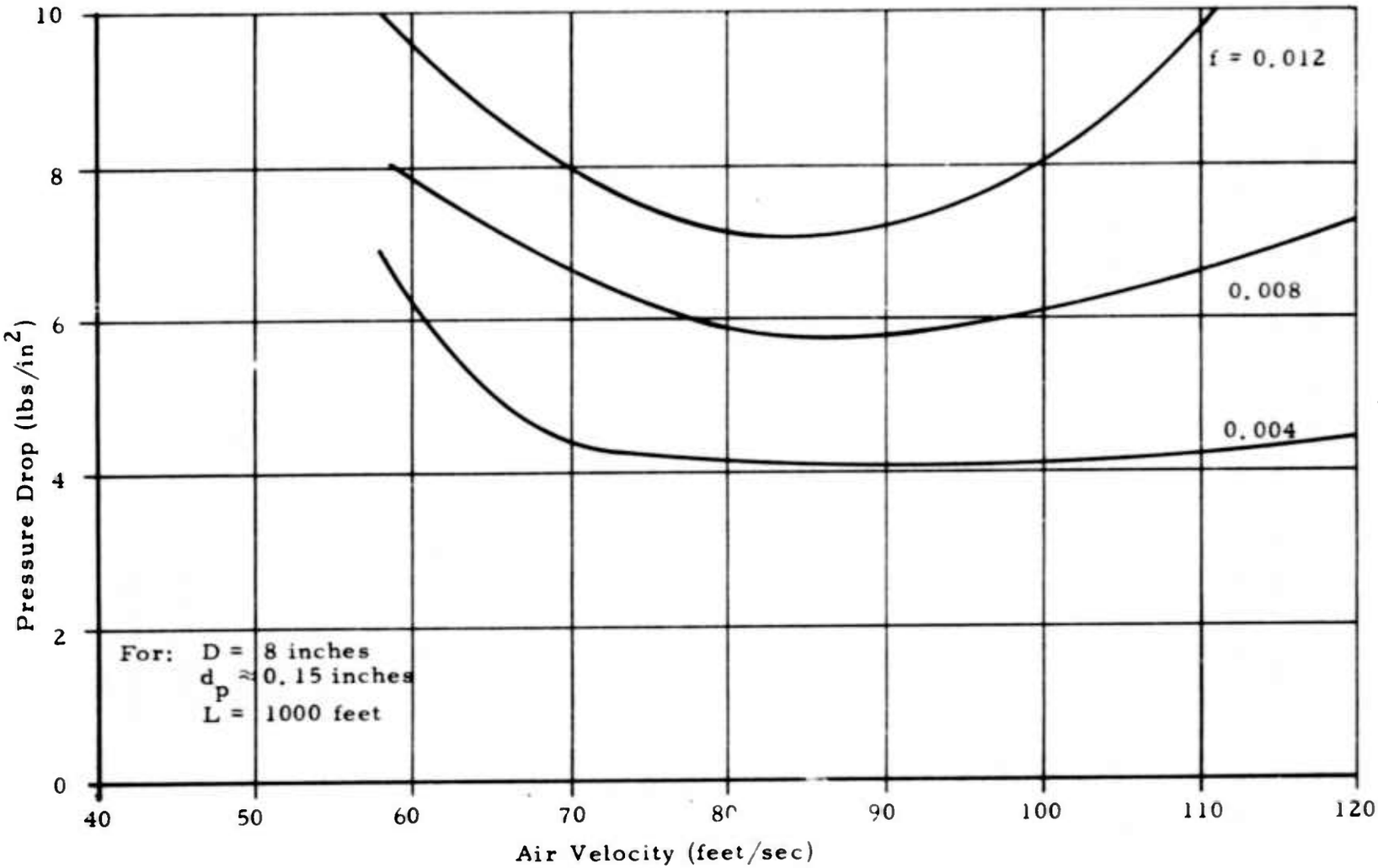

Pressure Drop versus Air Velocity for Various Friction Factors

Figure B-5

To simplify the determination of the temperature at the outlet of the blower we use

$$\frac{T_2}{T_1} = \left(\frac{p_2}{p_1}\right)^{\frac{k-1}{k}} \qquad \text{(B-7)}$$

where

k = ratio of specific heats.

The results of the computation are presented graphically on Figure B-6 where the horsepower required of the vacuum system is presented as a function of air flow rate for several return duct diameters. These curves permit the selection of an optimum return duct size for a particular air flow rate.

The asymptote for low flow rate at each duct size corresponds to an upward gas velocity equal to the terminal velocity of the particles being carried. At this velocity no transport will occur, the duct will load with particles and the pressure head due to these particles will approach infinity. From this lower velocity limit the power decreases with increasing flow rate as the mass loading in the duct drops due to higher transport velocity. The required power passes through a minimum and then increases as frictional losses become the dominant factor.

For the prototype borer, where required flow rates are somewhat indefinite, the relatively flat characteristic of the 8" and 10" ducts present obvious advantages. For these duct sizes variations in flow rate produce less significant changes in required power than for the 6" duct.

These power requirements do not include the effects of inefficiencies of the equipment. To size a suction system it will be necessary to include the efficiency of the particular unit under consideration.

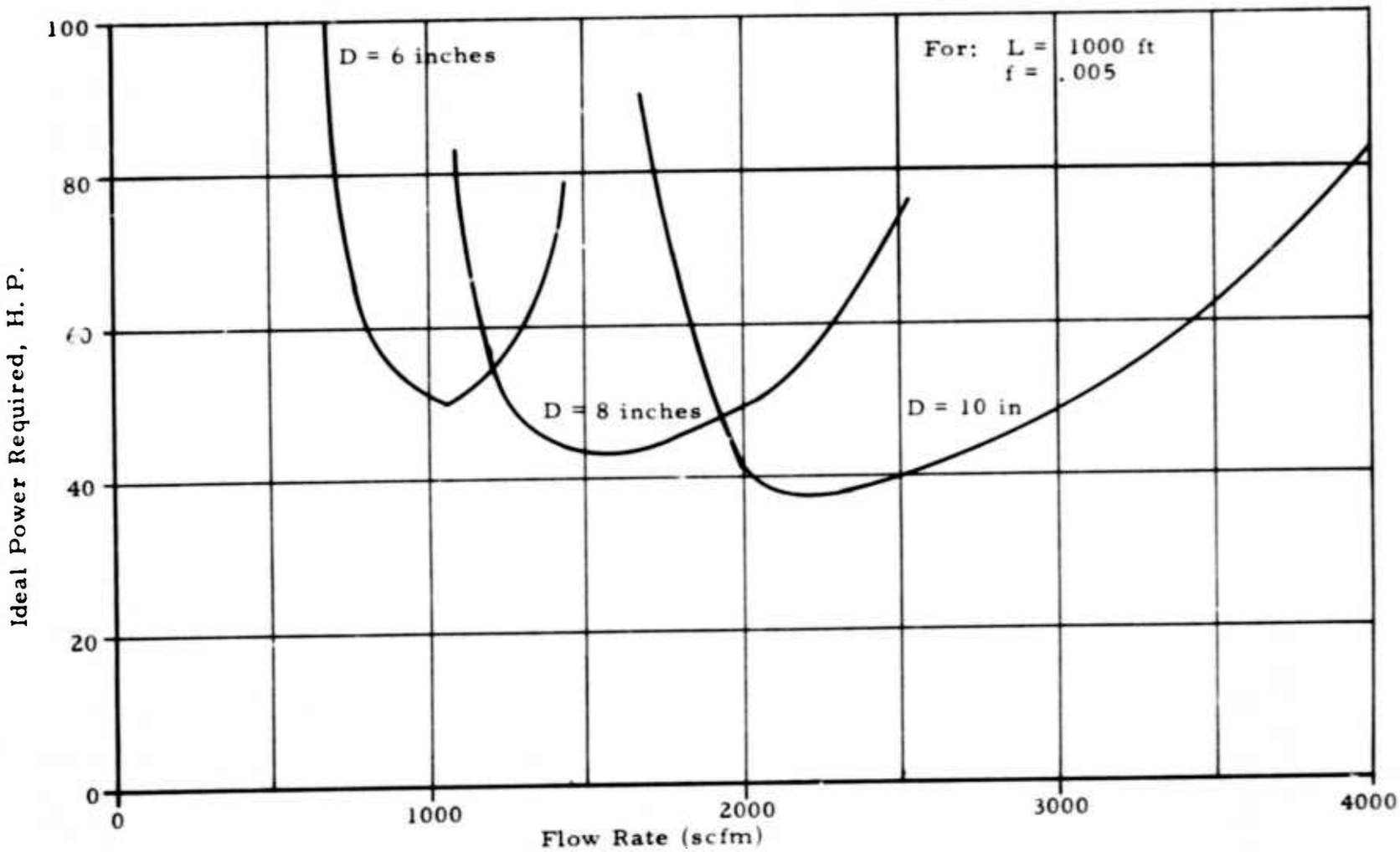

Ideal Suction System Power Required versus Flow Rate for Various Duct Sizes

Figure B-6

It should be noted that the above calculations were based on incompressible flow assumptions. Several data points have been checked by more rigorous and complex compressible flow calculations which indicated pressure drops approximately 10 percent higher than those indicated on the curves.

APPENDIX C

THREE STAGE BORER-BEARING LIFE

Bearing loads were calculated on the basis of a line loading ($F'_{n\alpha}$) of 2000 lbs/in. and a force ratio (μ) of .2. Referring to Figure C-1, from statics

$$T = F_s \cos \beta - F_n \sin \beta \qquad \text{(C-1)}$$

and with $\frac{F_s}{F_n} = \mu$ and $F_n = \ell F'_{n\alpha}$

where F_s = total side force on the cutter (lbs)

F_n = total normal force on the cutter (lbs)

T = axial thrust (lbs)

R_1; R_2 = radial bearing load (lbs)

β = half cone angle

μ = force ratio.

We obtain

$$T = F_n \mu \cos \beta - F_n \sin \beta \qquad \text{(C-2)}$$

or

$$T = \ell F'_{n\alpha} \left[\mu \cos \beta - \sin \beta \right] \qquad \text{(C-3)}$$

and with the assumption $R_1 \quad R_2 = R$

$$R = \frac{\ell F'_{n\alpha} \left[\cos \beta + \mu \sin \beta \right]}{2} \qquad \text{(C-4)}$$

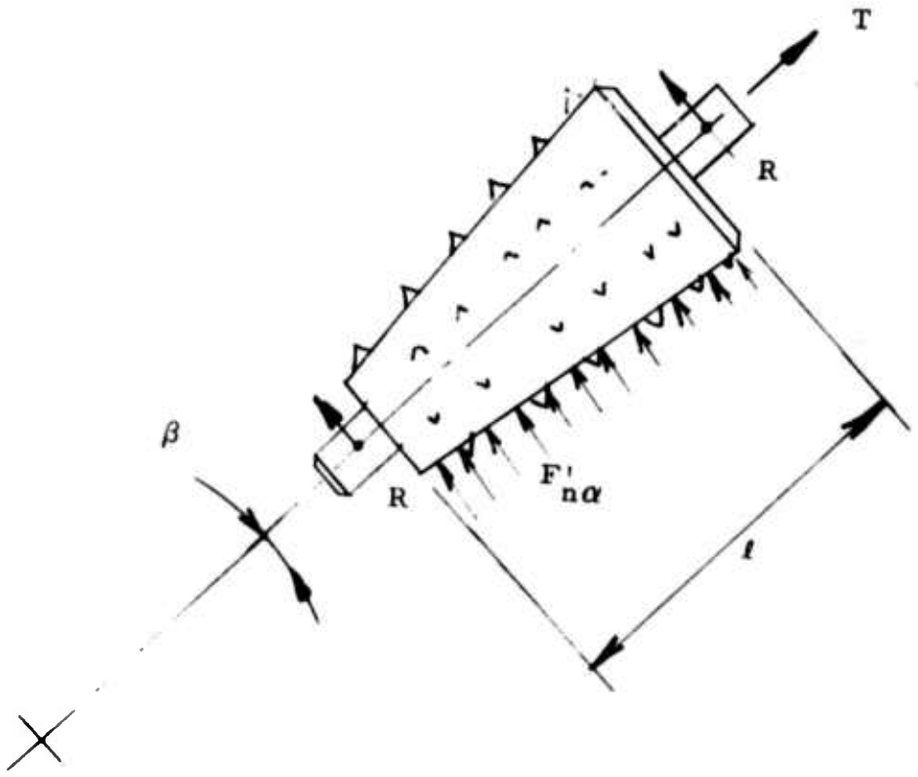

Cutter Configuration

Figure C-1

First Stage Bearing Calculations

$F'_{n\alpha}$ = 2000 lbs/in (from Hughes' Test)

ℓ = 9.0" (as measured)

μ = .2 (assumed)

β = 6.5° (as measured)

From Eq. C-3,

$$T = 9.0 \times 2000 (.2 \times .993 - .113) = \underline{1570 \text{ lbs.}}$$

from Eq. C-4,

$$R = \frac{9.0 \times 2000 (.993 + .2 \times .113)}{2} = \underline{9000 \text{ lbs.}}$$

A. Bearing SKF 22308C (Bottom End of 1st stage cutter)

Assuming R = 9000 lbs, a cone rotational speed of 90 rpm, SKF Engineering Data* predict an estimated life (B_{-10}) of 3000 hours.

B. Bearing SKF 22308C (Top End of 1st stage cutter)

Assuming R = 9000 lbs, T = 1570 lbs, a cone rotational speed of 90 rpm, an estimated life (B_{-10}) of 2500 hrs. is obtained.

Second Stage Bearing Calculations

$F'_{n\alpha}$ = 2000 lbs/in (from Hughes' Test)

ℓ = 22.0 (as measured)

μ = .2 (assumed)

β = 6.5 (as measured)

*Ref. SKF Bearing Manual, SKF Industries, Inc., Philadelphia, Pa.

From Eq. C-3

$$T = 22 \times 2000 (.2 \times .993 - .113) = \underline{3820 \text{ lbs.}}$$

from Eq. C-4,

$$R = \frac{22 \times 2000 (.993 + .2 \times .113)}{2} = \underline{22,500 \text{ lbs.}}$$

C. Bearing SKF 22313C (Bottom End 2nd stage cutter)

Assuming R = 22,500 lbs, a cone rotational speed of 90 rpm, SKF Engineering Data predict an estimated life (B_{-10}) of 2500 hours.

D. Bearing SKF 22317C (Top End 2nd stage cutter)

Assuming R = 22,500 lbs, T = 3820 lbs, a cone rotational speed of 90 rpm, an estimated life (B_{-10}) of 4000 hours is obtained.

Third Stage Bearing Calculations

$F'_{n\alpha}$ = 2000 lbs/in (from Hughes' Test)

ℓ = 34.0 (as measured)

μ = .2 (assumed)

β = 6.5 (as measured)

from Eq. C-3

$$T = 34 \times 2000 (.2 \times .993 - .113) = \underline{5900 \text{ lbs.}}$$

from Eq. C-4

$$R = \frac{34 \times 2000 (.993 + .2 \times .113)}{2} = \underline{35,000 \text{ lbs.}}$$

E. Bearing SKF 22318C (Bottom End 3rd stage cutter)

Assuming R = 35,000 lbs, a cone rotational speed of 90 rpm, SKF Engineering Data predict an estimated life (B_{-10}) of 4500 hours.

F. Bearing SKF 22324C (Top End 3rd stage cutter)

Assuming R = 35,000 lbs, T = 5900 lbs, a cone rotational speed of 90 rpm, an estimated life (B_{-10}) of 10,000 hours is obtained.

APPENDIX D

STRESS EVALUATION OF FIXED-END TAPER BEAM USED IN CONICAL BORER

GIVEN:

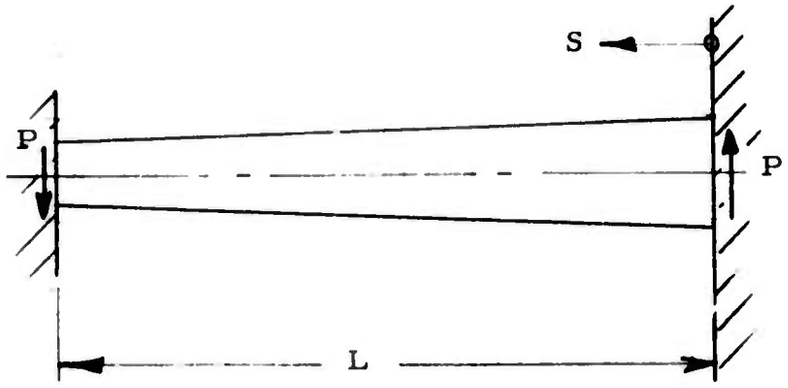

SOLUTION:

A. General

Using the energy approach, and Castigliano's theorem, we take the free body as

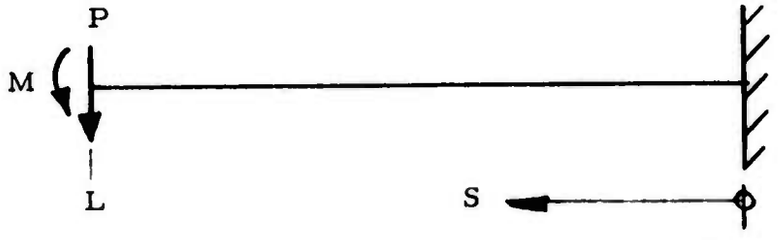

where M is the unknown moment, and the strain energy U is

$$U = \int_0^L \frac{M(s)^2 ds}{2EI(s)} \qquad \text{(D-1)}$$

Further, the necessary boundary condition on the left-hand end is

$$\theta = \frac{\partial U}{\partial M} = 0 \qquad \text{(D-2)}$$

Writing the equation for moment, M(S)

$$M(S) = M + P(L-S) \qquad \text{(D-3)}$$

Substituting equation (3) into (1) and satisfying the boundary condition (2) results in,

$$M = PL \left[\frac{\int_0^L \frac{S\,dS}{I(S)}}{L \int_0^L \frac{dS}{I(S)}} - 1 \right] \qquad \text{(D-4)}$$

and

$$M(S) = -PL \left[\frac{S}{L} - \frac{\int_0^L \frac{S\,dS}{I(S)}}{L \int_0^L \frac{dS}{I(S)}} \right] \qquad \text{(D-5)}$$

or in dimensionless terms

$$s = \frac{S}{L} \qquad 0 \leq s \leq 1 \qquad \text{(D-6)}$$

there results,

$$M(s) = -PL \left[s - \frac{\int_0^1 \frac{sds}{I(s)}}{\int_0^1 \frac{ds}{I(s)}} \right] \qquad \text{(D-7)}$$

From equation (7) the bending moment, and stress are evaluated. This solution is valid for a general cross-section beam wherein the geometric section properties vary arbitrarily with position(s).

The "general solution" can be carried out by computer or graphical integration, i.e.,

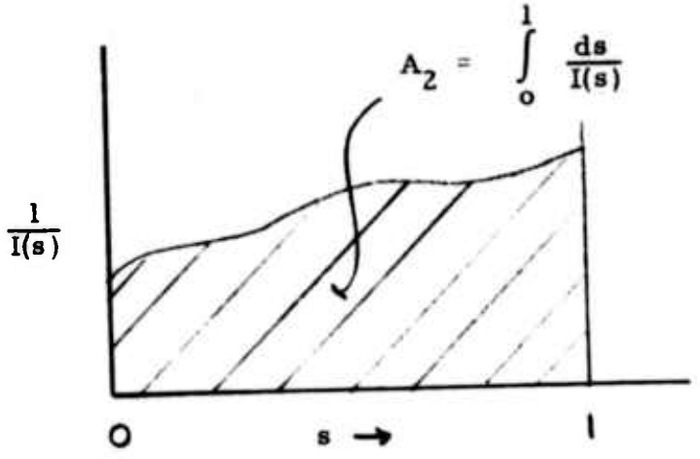

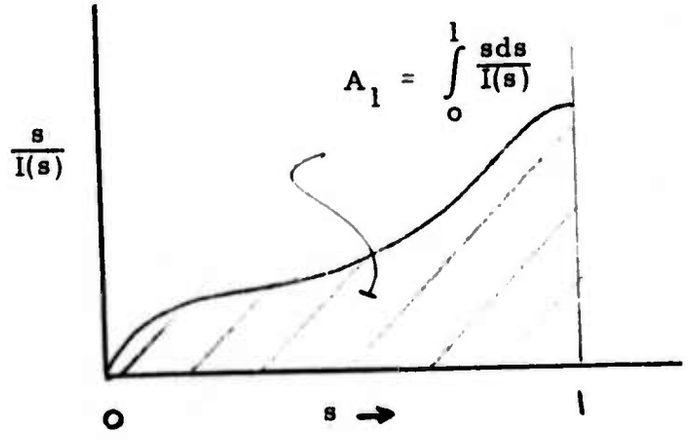

The functions $\frac{1}{I(s)}$, $\frac{s}{I(s)}$ are plotted for $0 \longrightarrow 1$, and the areas under these curves represent the integrals; from which

$$M(s) = - PL \left[s - \frac{A_1}{A_2} \right] \qquad \text{(D-8)}$$

B. Triangular Cross-Section

(1) General

Specializing to the specific case in hand, we have

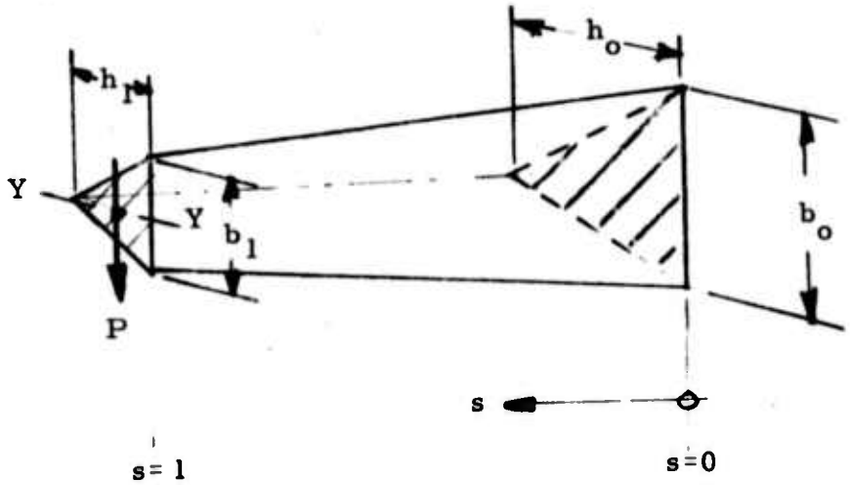

For this cross-section

$$I_{yy}(s) = \frac{b^3(s)\, h(s)}{48}$$

Assuming a linear variation in b(s), h(s) there results:

$$\left.\begin{aligned} b(s) &= b_o(1 - sB) \\ h(s) &= h_o(1 - sH) \end{aligned}\right\} \qquad \text{(D-9)}$$

$$\text{where} \quad B = \frac{b_o - b_1}{b_o}$$

$$H = \frac{h_o - h_1}{h_o}$$

From which

$$I(s) = \frac{b_o^3 h_o}{48} (1 - sB)^3 (1 - sH) \qquad \text{(D-10)}$$

and in general, equation (9) can be introduced into equation (7), the integrals obtained and M(s) evaluated.

If few results are required, the graphical solution described earlier is the preferred method. For repeated solutions an integration or computer solution could be more economical.

(2) Special Case

In the special case where the triangular cross-section is geometrically similar throughout the entire beam length, a simplification results.

In this case it is shown that

$$B = H \qquad \text{(D-11)}$$

since

$$\frac{b_o - b_1}{b_o} = 1 - \frac{b_1}{b_o}$$

$$\frac{h_o - h_1}{h_o} = 1 - \frac{h_1}{h_o}$$

so that B = H requires only that $\frac{b_1}{b_o} = \frac{h_1}{h_o}$, which follows from geometric similarity

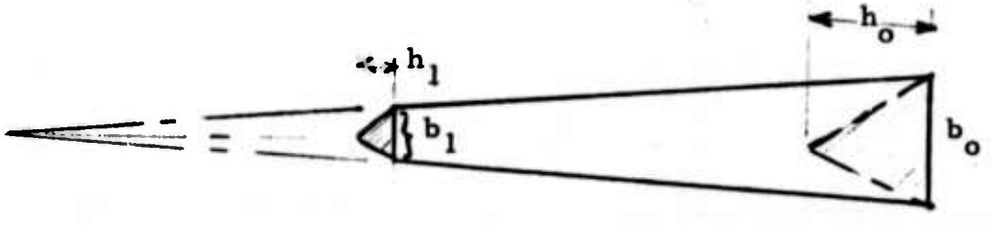

Thus

$$I(s) = \frac{b_o^3 h_o}{48} (1 - sB)^4 \qquad \text{(D-12)}$$

and it follows that,

$$\int_o^1 \frac{ds}{I(s)} = \frac{48}{b_o^3 h_o} \left(\frac{1-(1-B)^3}{3B(1-B)^3} \right)$$

$$\int_o^1 \frac{sds}{I(s)} = \frac{48}{b_o^3 h_o} \left(\frac{3-B}{6(1-B)^3} \right)$$

Substituting in equation (7)

$$M(s) = - P L \left[s - \frac{3-B}{2(3-3B+B^2)} \right] \qquad \text{(D-13)}$$

$$0 \leq s \leq 1$$

Further, since

$$\sigma(s) = \frac{M(s)\, b(s)}{2I(s)}$$

Combining equations (9), (12), (13) there results

$$\sigma(s) = \mp \frac{24\, P L}{b_o^2 h_o} \left[\frac{s - \frac{3-B}{2(3-3B+B^2)}}{(1-Bs)^3} \right] \qquad \text{(D-14)}$$

We should note the maximum bending stress distribution along the beam appears as,

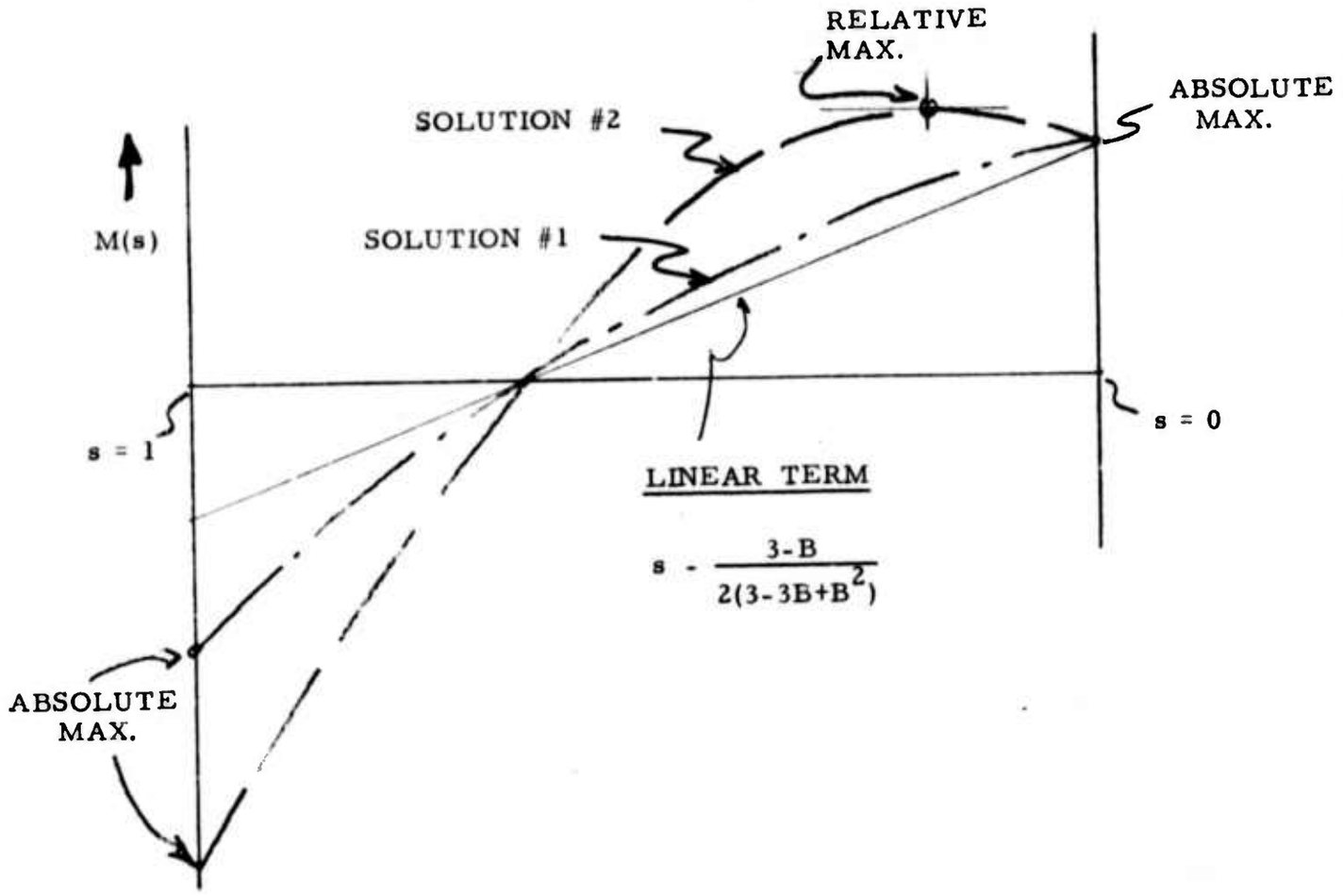

The maximum stress should always be examined at the end points (s = 1, 0) and at a possible relative max. obtained by $\frac{d\sigma}{ds} = 0$. The latter is obtained from

$$\frac{d\sigma}{ds} = 0$$

which leads to

$$s^* = \frac{-5B^2 + 15B - 6}{4B(3-3B+B^2)} \qquad \text{(D-15)}$$

and is only meaningful for values $0 \leq s^* \leq 1$. So that three values of stress should be examined for maximums,

$$\sigma(0),\ \sigma(s^*),\ \sigma(1).$$

C. Total Combined Stress

In addition to the bending stresses there may be axial thrust loads, so that

$$\sigma_{axial}(s) = \frac{P_{TOT}}{nA(s)} \qquad \text{(D-16)}$$

where $A(s)$ = cross-section area of each strut

n = number of struts

P_{TOT} = total axial thrust load

Since the bending stress is maximum on the outer fibers, the axial stress constant, and the bending shear related to (P) is maximum at the neutral axis (and not large), only the outer fiber stresses need be considered. Thus,

$$\sigma_{total} = \sigma_{bend}(s) + \sigma_{axial}(s) \qquad \text{(D-17)}$$

D. Specific Calculation

GIVEN:

From drawings it is found,

$b_o = 6.5''$ $\quad b_1 = 5.5''$

$h_o = 4.25''$ $\quad h_1 = 3.5''$

$L = 6.0''$ $\quad r = 4\ 1/8''$ (effective torque radius)

$n = 3$ struts

Also,

TORQUE = 48,000 in lbs

P_{AXIAL} = 90,000 lbs

Calculations:

1) Bending Stress

From the above the bending force on each strut is,

$$P = \frac{T}{(n)(r)} = \frac{48,000}{(3)(4\ \frac{1}{8})} = 3875\ \# \qquad \text{(D-18)}$$

It is next necessary to evaluate the dimensionless geometric values, B, H. Substituting into equation (11)

$$B = \frac{6.5 - 5.5}{6.5} = .154$$

$$H = \frac{4.25 - 3.6}{4.25} = .154 \qquad \text{(D-19)}$$

which satisfies the special requirement, B = H, so that the special integrated stress solution of equation (14) can be utilized.

Thus, from equation (14) the outer fiber bending stress is given as,

$$\sigma_b(s) = \mp \frac{(24)(3875)(6)}{(6.5)^2(4.25)} \left[\frac{s - \frac{3 - .154}{2(3-3(.154) + (.154)^2)}}{(1 - .154s)^2} \right]$$

which reduces to,

$$\sigma_b(s) = (\mp)\ 3.1 \times 10^3 \left[\frac{s - .54}{(1 - .154s)^2} \right] \qquad \text{(D-20)}$$

$$0 \leq s \leq 1$$

To further search for a relative maximum, equation (15) is utilized. from which

$$s^* = \frac{-(5)(.154)^2 + 15(.154) - 6}{4(.154)(3 - 3(.154) + .154^2)}$$

leading to

$$s^* < 0$$

which is outside the "real" strut length of

$$0 \leq s \leq 1$$

and no relative maximum exists. It is now sufficient to first evaluate the end position bending stresses, $\sigma(0)$, $\sigma(1)$, to ascertain whether the maximum occurs at the smaller end and then to combine with the maximum axial stress, which does occur at the small strut end.

From equation (20), it is found that

$\sigma_b(0) = 1670$ psi (larger end)

$\sigma_b(1) = 2000$ psi (smaller end)

and the full outer fiber stress plot is as shown below.

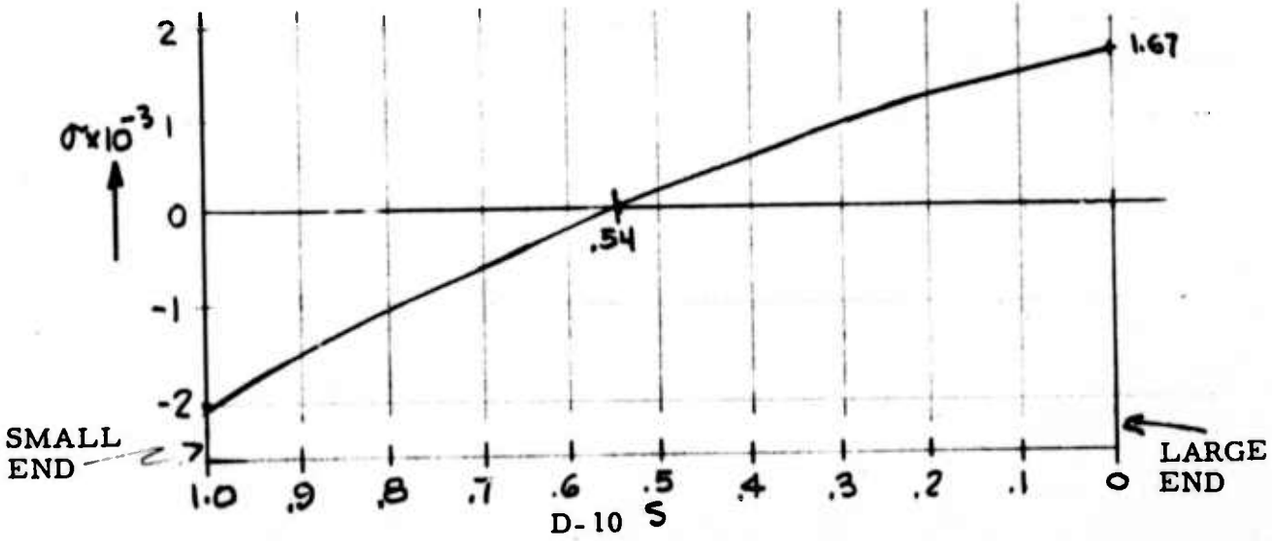

(2) Axial Stress

Since the maximum fiber stress occurs at the smaller end it is only necessary to evaluate end position axial stresses. From equation (16)

$$\sigma_{axial}(s) = \frac{90,000}{3A(s)} = \frac{30,000}{A(s)}$$

from which

$$\sigma_A(0) = \frac{30,000}{(\frac{1}{2})(6.5)(4.25)} = 2160 \text{ psi}$$

$$\sigma_A(1) = \frac{30,000}{(\frac{1}{2})(5.5)(3.6)} = 3400 \text{ psi}$$

(3) Maximum Combined Stress

From equation (17), there results

$$\sigma_{TOT}(0) = 1670 + 2160 = 3830 \text{ psi}$$

$$\sigma_{TOT}(1) = 2000 + 3400 = 5400 \text{ psi}$$

which is maximum at the smaller end (s = 1).

UNCLASSIFIED

SECURITY CLASSIFICATION OF THIS PAGE (When Data Entered)

REPORT DOCUMENTATION PAGE

READ INSTRUCTIONS BEFORE COMPLETING FORM

1. REPORT NUMBER

2. GOVT ACCESSION NO.

3. RECIPIENT'S CATALOG NUMBER

Final

4. TITLE (and Subtitle)

DESIGN AND DEVELOPMENT OF A CONICAL BORING DEVICE TO ENLARGE A PILOT HOLE THROUGH ROCK.

5. TYPE OF REPORT & PERIOD COVERED

Annual Technical Report
1 May 1972 through 1 June 73

6. PERFORMING ORG. REPORT NUMBER

7. AUTHOR(s)

Hans A. Hug
Paul R. Wurlitzer

8. CONTRACT OR GRANT NUMBER(s)

H0220076
ARPA Order-1579

9. PERFORMING ORGANIZATION NAME AND ADDRESS

Foster-Miller Associates, Inc.
135 Second Avenue
Waltham, Massachusetts 02154

10. PROGRAM ELEMENT, PROJECT, TASK AREA & WORK UNIT NUMBERS

ARPA Order No. 1579,
Amend 3, Code Number
3F10

11. CONTROLLING OFFICE NAME AND ADDRESS

Advanced Research Projects Agency
1400 Wilson Boulevard
Arlington, Virginia 22209

12. REPORT DATE

5 December 1973

13. NUMBER OF PAGES

116 pages

14. MONITORING AGENCY NAME & ADDRESS (if different from Controlling Office)

115 p.

15. SECURITY CLASS. (of this report)

Unclassified

15a. DECLASSIFICATION/DOWNGRADING SCHEDULE

16. DISTRIBUTION STATEMENT (of this Report)

Distribution of this document is unlimited

17. DISTRIBUTION STATEMENT (of the abstract entered in Block 20, if different from Report)

18. SUPPLEMENTARY NOTES

19. KEY WORDS (Continue on reverse side if necessary and identify by block number)

Rock Mechanics -- Mechanical Rock Fragmentation
Roller Cutters
Vertical Hard Rock Boring Devices
Pilot Hole Reamer
Conical Borer -- Rapid Excavation

20. ABSTRACT (Continue on reverse side if necessary and identify by block number)

This report summarizes Foster-Miller Associates effort completed during the second year of a multi-year program to design and develop a conical, self-advancing and self-rotating boring machine. The conical borer will use a proven and energy effective mechanical fragmentation system - roller cutters - and will operate as a reaming device to enlarge an existing 8 3/4 inch pilot hole to a final 39 inch bore.

(Continued)

DD FORM 1 JAN 73 1473 EDITION OF 1 NOV 65 IS OBSOLETE

UNCLASSIFIED

SECURITY CLASSIFICATION OF THIS PAGE (When Data Entered)

142 400 LB

20. ABSTRACT (Continued)

The general research approach has been to continue the development efforts begun under Contract H021044 during which a prototype single stage conical borer was fabricated and "proof" tested.

In the current program detailed testing and refinement of the cutting structure of the prototype borer was completed. As a result of this research a marked reduction in the values of the thrust loads which were obtained during the first year proof tests was achieved. Thrust loads of approximately 10 percent of that required for conventional tri-cone bit were observed. The specific energy required (inch-pounds per cubic inch of rock removed) was only 13 percent higher than that of a comparable tri-cone bit. This is considered very good in view of the extensive development history of tri-cone cutters.

The detailed design of the borer (Phase II) was completed. Design layouts are presented in this report.

The transport of the cuttings is critical. Solutions to overcome potential transport problems were generated and tested experimentally to determine the most efficient system. A mucking test unit, consisting of a half-scale, two stage model of the borer encased in a plexiglass shell was built and used.

Investigation and determination of the auxiliary equipment that will be required for full scale field testing of the borer was completed during the last part of the year.